CR 114373
AVAILABLE TO THE PUBLIC

ME-TR-033-4

HEAT TRANSFER BETWEEN SURFACES IN CONTACT:

AN ANALYTICAL AND EXPERIMENTAL STUDY OF
THERMAL CONTACT RESISTANCE OF METALLIC INTERFACES

by

L.S. Fletcher and D.A. Gyorog

FACILITY FORM 602

N71-38748
(ACCESSION NUMBER)

192
(PAGES)

CR-114373
(NASA CR OR TMX OR AD NUMBER)

G3 (THRU)

(CODE)

33
(CATEGORY)

Mechanical Engineering Department
Arizona State University
Tempe, Arizona

JULY. 1968
Revised May, 1971

HEAT TRANSFER BETWEEN SURFACES IN CONTACT:

AN ANALYTICAL AND EXPERIMENTAL STUDY OF

THERMAL CONTACT RESISTANCE OF METALLIC INTERFACES

by

L. S. Fletcher
Rutgers University

and

D. A. Gyorog
University of Missouri-Rolla

ABSTRACT

A new dimensionless correlation for the prediction of thermal contact resistance between similar metal surfaces in a vacuum environment has been developed in terms of known engineering measurements. This expression was formulated from the results of an experimental investigation using aluminum, brass, stainless steel, and magnesium, with a wide range of test variables.

The dimensionless parameters for this expression correlated the experimental data of this investigation and published data within an average overall rms error of 24 percent or less for most of the data. These experimental data included mean junction temperatures of -250°F to 500°F, apparent interface pressures of 10 to 7,000 psi, surface flatness deviations of 15 to 4,500 microinches, and surface roughnesses of 3 to 120 microinches.

ACKNOWLEDGMENTS

TABLE OF CONTENTS

LIST OF TABLES

LIST OF FIGURES

NOMENCLATURE

A	Constant; Area, sq ft
a	Contact spot radius, in
B	Constant; Fluid Thickness Number, $\dfrac{\delta}{b}$
b	Elementary cylinder or specimen radius, ft
C	Constriction Number, $\dfrac{a}{b}$
D	Constant; Diameter, in
d	Constant; Surface Parameter
E	Modulus of Elasticity, psi
F	Shape Factor; Force, lbs
FD	Flatness Deviation, microinches
f	Alleviation factor; Function
g	Function
H	Hardness
h_c	Contact Conductance, Btu/hr sq ft °F
I	Current, amps
K	Thermal Conductivity Number, k_j/k_s
k	Thermal Conductivity, Btu/hr ft °F
L	Equivalent length, ft
m	Constant
n	Constant; Number of contact spots
P	Pressure, psi
P*	Dimensionless pressure, $\dfrac{P_a}{E}$

q	Heat flux, Btu/hr
R	Resistance
R_c	Contact Resistance, hr °F/Btu
RD	Roughness Deviation, microinches
r	radius
s	Sum of peak-to-mean surface distances
T	Temperature, °F
T*	Dimensionless temperature, βT_m
ΔT	Temperature difference, °F
t	Film thickness, ft
U	Conductance Number, $h_c \delta / k_f$
V	Voltage
w	Uncertainty increment
x	axial length along specimen
Δx	increment of length

α	Contact area ratio, $\dfrac{A_c}{A_a}$, $\dfrac{a^2}{b^2}$
β	Coefficient of Thermal Expansion, $\dfrac{1}{°F}$
Γ	Gamma function
δ	Equivalent gap thickness or surface parameter, in
ϵ	Emissivity
η	Surface interference parameter, ft^{-1}
θ	Angle of surface ridging, deg
λ	Surface profile wavelength
ξ	Accommodation coefficient

ρ	Electrical resistance
σ	Stefan Boltzmann Constant
ψ	Thermal Conductance number, $\dfrac{h_c \delta}{k_m}$

SUPERSCRIPTS and SUBSCRIPTS

a	Apparent
B	Brinnell
CC	Clausing and Chao
CF	Centinkale and Fishenden
c	Contact
d	Dividing flowline
D	Diamond Pyramid
FR	Fenech and Rohsenow
f	Fluid
g	Gas
h	Harmonic Mean
j	Junction
ℓ	Length correction factor
m	Mean
ma	macroscopis
mi	microscopic
M	Meyer
n	exponent
r	Radiation
s	Solid
T	Tachibana

t	Total
λ	Geometrical modification factor
0	Ambient condition
1	Specimen 1; Surface 1
2	Specimen 2; Surface 2

CHAPTER I

INTRODUCTION

Energy transfer in solid materials has been studied both theoretically and experimentally for many years. These studies have resulted in the development of techniques for the prediction of heat transfer in solids. In contrast, however, similar studies have produced few established techniques for the prediction of energy transfer between contacting solid materials.

That resistance to heat transfer exists between contacting solids has long been acknowledged. This thermal resistance varies considerably, depending upon the mechanical and thermophysical properties of the materials composing the contact, the surface conditions, and the interstitial fluid or filler. In addition to these variables, the mechanics of the contact also effect the heat transfer. When two surfaces are held together under pressure, the effective contact area is composed of many small points which constitute only a fraction of the total surface area. Considering a microscopic section of this contact area, the modes of heat transfer across the interface would be:

(1) Solid conduction through the effective contact area;

(2) Gaseous, molecular, or other conduction through the interstitial fluid or filler; and

(3) Thermal radiation.

The thermal contact conductance is defined as:

$$h_c = \frac{q/A}{T_1 - T_2} \qquad (1-1)$$

where T_1 and T_2 are the temperatures of the bounding surfaces of the contact gap, and q/A is the heat flux per unit area. The contact resistance would then be defined as:

$$R_c = \frac{1}{h_c A} = \frac{T_1 - T_2}{q} \qquad (1-2)$$

where

$$R_c = \frac{1}{\frac{1}{R_s} + \frac{1}{R_f} + \frac{1}{R_r}} \qquad (1-3)$$

and

R_s = resistance due to solid conduction,

R_f = resistance due to interstitial substance

conduction or convection,

R_f = resistance due to radiation.

In order to make a complete theoretical study of the problem of contact conductance, each mode of energy transfer should be considered. A vacuum environment minimizes the resistance due to energy transfer by the interstitial fluid. Since the conductance due to radiation between the contacting surfaces is usually negligible, the primary contribution to the contact resistance would be due to solid conduction. Hence, an investigation conducted in a vacuum environment would permit the experimental contact resistance results to be analyzed in terms of conduction through the contact region alone.

The need for thermal contact conductance values has led to a number of analytical and experimental investigations, as evidence by

the bibliographies of Atkins [9]*, Gex [40], and Vidoni [80]. In addition, critical reviews of the status of experimental and analytical developments in the area of heat transfer across interfaces in contact have been presented by Hudack [47], Minges [58], and Thomas and Probert [76]. In spite of all the published work, however, there have been relatively few attempts at correlation of the existing experimental data or at prediction of contact conductance.

The few investigators who have attempted such prediction have had to resort to mathematical and physical models combined with experimental procedures to determine actual conductance values. The analyses of Clausing and Chao [19, 20] and Fenech and Rohsenow [31, 32] have met with some success, yet their equations, using specific constants, have a very limited range of validity. These and other theories will be analyzed and compared with experimental data in a later section of this work.

The objective of the present study was to develop a generalized expression for the prediction of contact conductance values in a vacuum. This relationship was developed in terms of known or easily determined physical properties for similar metallic surfaces in contact. Experimental data were obtained in a vacuum environment for several test materials over a wide range of junction temperatures and loads. These data were analyzed and used to determine the necessary

---

* Numbers in brackets designate references cited in the bibliography.

empirical constants for the generalized equation. Previously pub-
lished experimental data were also analyzed and compared with the
predicted results.

The newly developed equation was then compared with two of the
more recent analyses of contact conductance. It appears that the
present expression more accurately predicts contact conductance over
a wider range of conditions. Furthermore, the dimensionless para-
meters developed herein permit good correlation of a large amount of
published conductance data.

CHAPTER II

REVIEW OF PUBLISHED THEORETICAL ANALYSES AND

EXPERIMENTAL INVESTIGATIONS

One of the first expressions for the thermal conductance between

contacting surfaces was developed by Kottler [52] in 1927. He drew

upon the electrical analogy of the constriction resistance for a

single contact and extended this for multiple contacts. Simplified

empirical correlations have been developed for contact conductance

as a function of applied load [6, 16, 44, 46]; other correlations

are slightly more complex and include material properties and surface

conditions. Although there have been many attempts to correlate

experimental contact conductance data with theory, very few of these

theories have been found suitable for prediction of conductance values

at conditions other than those on which they are based. The theories

which resulted in some successful correlations between analytical

studies and experimental data are presented and analyzed here. Pub-

lished experimental data are also analyzed for comparison with the

more successful theories. The results of these comparisons are used

to establish criteria for an equation to predict thermal contact

conductance.

I. PRESENTATION OF THEORIES

A majority of the analytical studies of contact resistance

originate with heat flow through a single idealized contact. These
analyses are then expanded in a number of ways to include real contact
situations with multiple contacts. The contact resistance solutions
associated with the basic single contact model are presented here for
comparison. The mathematical models and assumptions employed in some
of the more important experimental-analytical investigations are then
developed in a consistent nomenclature with discussion of their appli-
cations and restrictions.

Resistance of a Single Contact

The contact or constriction resistance induced in an electrical
conductor exhibiting a discontinuous reduction in cross section was
originally solved by Kottler [52] using the classical electrical
analogy. The flux lines were approximated by hyperbolic curves in
the contacting samples, thus defining eliptical isotherms. The
resulting constriction resistance was given as:

$$R_c = \frac{1}{2ka} \tag{2-1}$$

Clark and Powell [18] derived the constriction resistance
equation by considering heat flow between two semi-infinite regions
in contact at a point of radius a. Their solution, obtained by
applying transform techniques to the Laplacian, resulted in a temp-
erature field that could be used in the basic contact resistance
definition, equation (1-1). The resulting equation was given as:

$$R_c = \frac{1}{2 k_h a} \tag{2-2}$$

Their results were then reduced to the form of the constriction

resistance given in equation (2-1), by assuming that the electrical

resistivity can be rep. iced by the reciprocal thermal conductivity.

Holm [46] extended the work of Kottler and proved that equation

(2-1) may be derived for a constant heat flux condition. That is:

$$R_c = \frac{1}{\pi k_h a} \qquad (2-3)$$

This solution was coupled with the assumption that the maximum

centerline temperatures best represented the axial temperature

profile.

The total constriction resistance for a singular isothermal

contact spot at the center of the apparent contact area was found

by Roess [64] to be:

$$R_c = \frac{g(C)}{2a k_h} \qquad (2-4a)$$

where

$$g(C) = 1 - 1.40925C + 0.?95910C^3 + 0.0525419C^5$$
$$+ 0.0210497C^7 + 0.0110752C^9 + \ldots \ldots \qquad (2-4b)$$

and C is the constriction number. This solution was developed cn

the basis of a constant potential for either finite or infinite

length cylinders with an isothermal interface area.

The total constriction resistance of Roess was modified by

Jeng [51] to include the number of contact spots. The constriction

resistance was then written as:

$$R_c = \frac{g(C)}{2a k_h Cn^\lambda} \qquad (2-5)$$

where λ is a geometrical modification factor dependent upon the physical geometry of the contacting surfaces. For fixed values of C, the constant λ was determined as 0.47 by simulating the contact geometry with an electrolytic tank.

For the limiting case of a single contact, all of the above resistance expressions reduce to:

$$R_c = \frac{1}{B \, k_h \, a} \qquad (2\text{-}6)$$

where B is a function of C. This single contact model served as a basis for the metallic conduction component of the contact resistance in most of the following experimental-analytical theories.

Cetinkale and Fishenden

One of the first analytical studies of thermal contact conductance was presented by Cetinkale and Fishenden [17] in their extension of the single contact model using Southwell's relaxation technique. The authors assumed that if two parallel, relatively smooth surfaces were held together under pressure, the points of actual physical contact would be uniformly distributed over the contact interface. They also assumed that at some distance from the interface, the lines of heat flux would be parallel, converging toward the contact points as the interface was approached. This would occur because the thermal conductivity of the surrounding fluid would be much less than the metallic specimens. The lines of heat flux converging to one contact spot would form an imaginary elementary cylinder as shown in Figure 2-1. The ratio of the fluid thickness to the elementary cylinder

diameter is quite small, hence radial heat flow through the fluid may be neglected.

The model for analytical study, then, was assumed to be a cylindrical column of radius b, with a centrally placed circular spot of radius a surrounded by a fluid of thickness δ_{CF}, as shown in Figure 2-2. In order to assume an isothermal contact surface with radial symmetry, the protuberances of the contact spots were assumed proportional to the thermal conductivity ratios $k_2/(k_1 + k_2)$ and $k_1/(k_1 + k_2)$. With these boundary conditions, it was possible to use relaxation techniques to determine a steady state temperature solution to the Laplace equation. The heat transfer through the contact spot was determined by subtracting the heat transfer through the fluid from the total heat transfer, which was calculated by using the temperature gradient at some distance from the interface. The dividing flow line in Figure 2-3 represents the separation point for heat flow through the contact and heat flow through the fluid.

Cetinkale and Fishenden specify one of the isotherms found by the relaxation technique, the no-contact isotherm, to be coincident with the plane of the interface if no gap exists between the solids. The difference between this isotherm and the plane of the interface, as shown in Figure 2-3, would yield the temperature drop caused by the contact. The thermal contact resistance was then calculated from the heat flux through the interface spot and fluid, and the temperature drop caused by the contact.

As a result of their analysis of this simplified contact model,
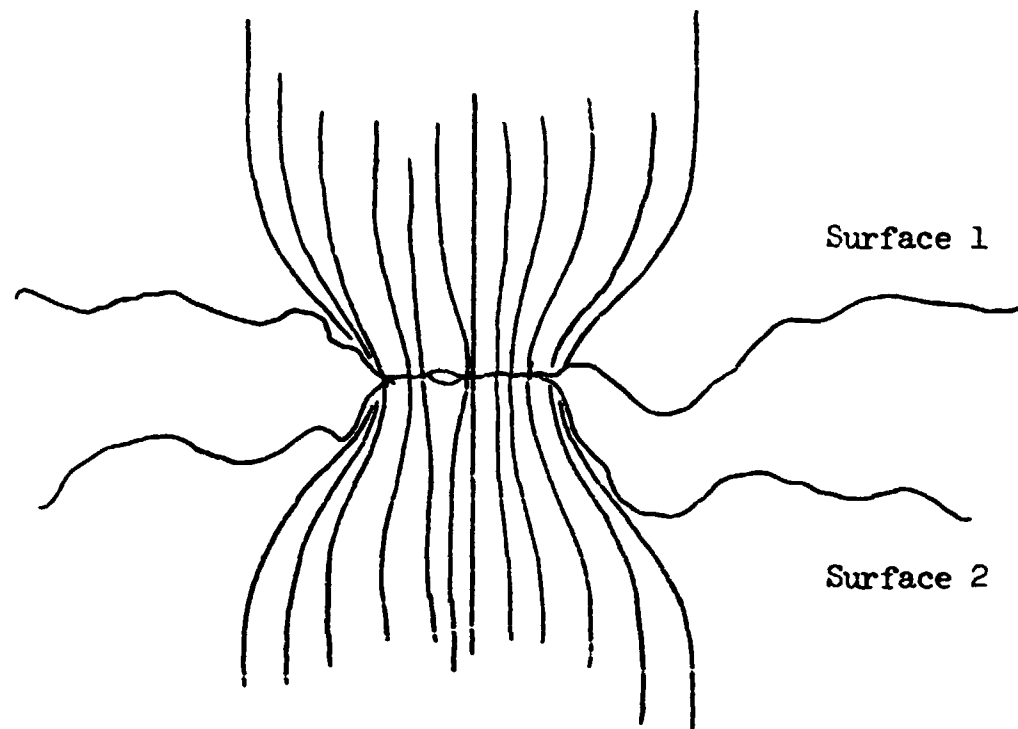
Figure 2-1. Flux Field Distribution at an Interface.
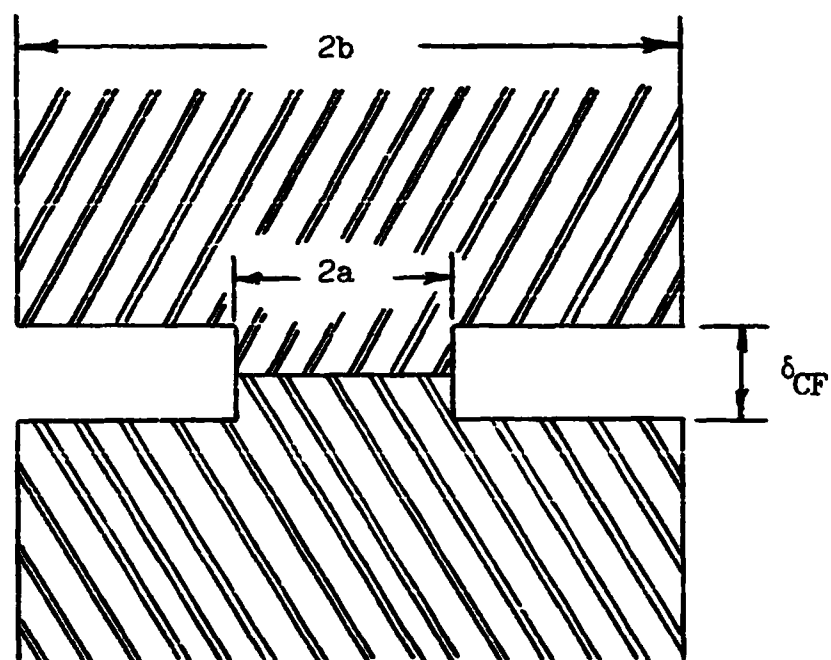
Figure 2-?. Elementary Contact Element.
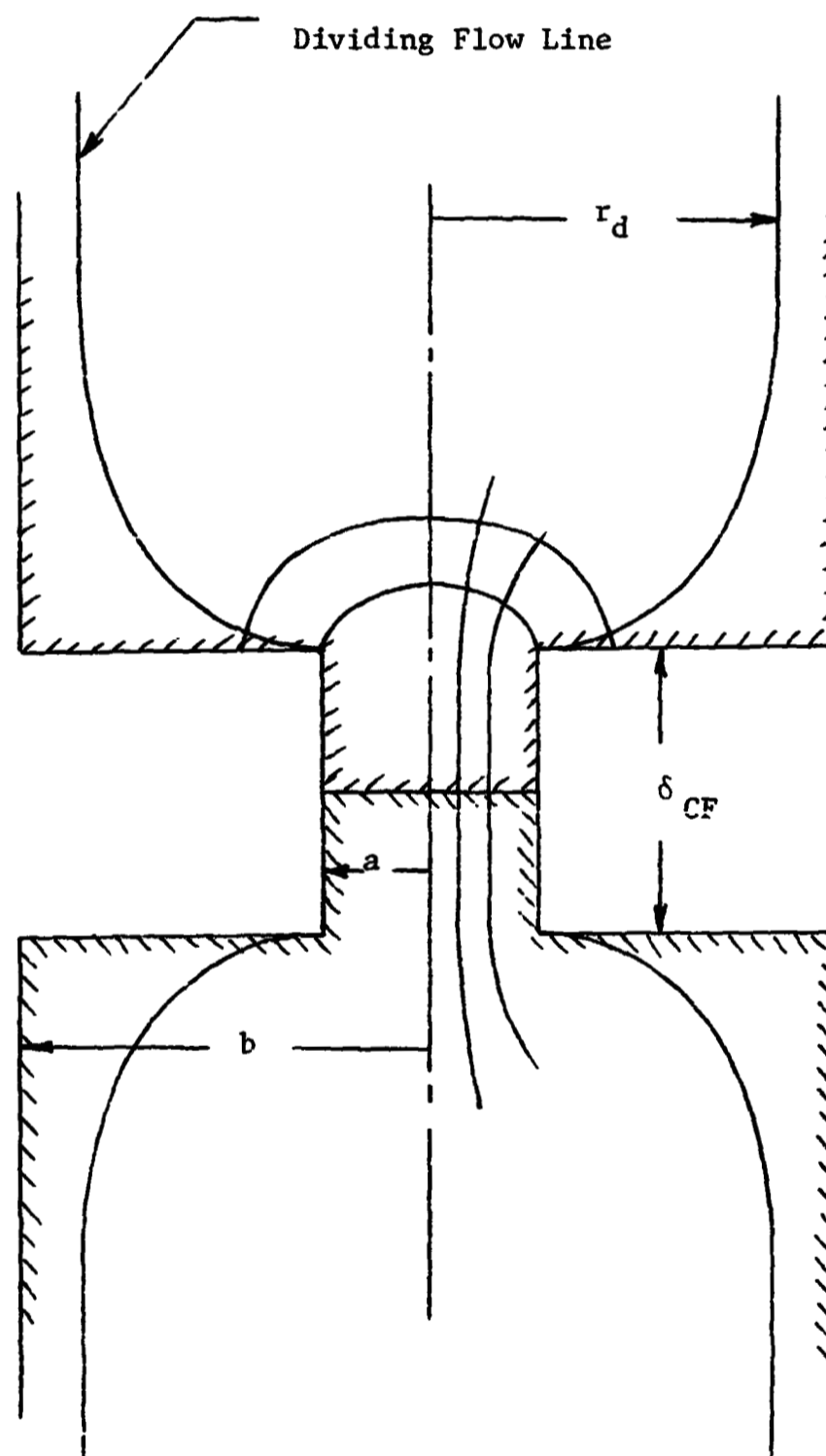
Figure 2-3.   Flux-Potential Distribution for a
Single Contact.

the thermal contact conductance is given as the sum of the conduct-
ance for the interstitial fluid and the conductance through the
metallic contact points. Treating the resistances in parallel, the
total contact conductance was given as;

$$h_c = \frac{k_f}{\delta_{CF}} + \frac{a\,k_h}{b^2 \, Tan^{-1}\,(\frac{r_d - a}{a})} \qquad (2-7)$$

where r_d is the radius of the dividing heat flow line. The results
for the solid resistance would then be:

$$R_c = \frac{1}{\pi\,a\,k_h}\,Tan^{-1}\,(\frac{r_d - a}{a})$$

By permitting $(r_d - a)$ to approach infinity, the equation reduces to
the basic constriction resistance as follows:

$$R_c = \lim_{(r_d - a)\to\infty}\,\{\frac{1}{\pi\,a\,k_h}\,Tan^{-1}\,(\frac{r_d - a}{a})\} \cong \frac{1}{2\,k_h\,a}$$

This result is identical with the contact resistance for a single
contact with constant heat flux boundary conditions developed by
Clark & Powell, i.e. equation (2-2).

A more useful relationship for the conductance may be developed
by eliminating r_d from equation (2-7). The resulting conductance
expression includes the conductivity of the interstitial fluid:

$$r_d = b\,\sqrt{1 - \frac{\pi b^2\,k_f}{\delta_{CF}\,h_c}}$$

$$h_c = \frac{k_f}{\delta_{CF}} + \frac{a\,k_h}{b^2\,Tan^{-1}\{\frac{b}{a}\,\sqrt{1 - \frac{k_f}{h_c\,\delta_{CF}}} - 1\}} \qquad (2-8)$$

This same relation in non-dimensional terms is given as:

$$U = 1 + \frac{BC}{K \, \text{Tan}^{-1} \{ \frac{1}{C} \sqrt{(1 - \frac{1}{U})} - 1}$$ (2-9)

where U = Conductance Number = $\dfrac{h_c \delta_{CF}}{k_f}$

C = Constriction Number = $\dfrac{a}{b}$

K = Conductivity Number = $\dfrac{k_f}{k_h}$

B = Fluid Thickness Number = $\dfrac{\delta_{CF}}{b}$

An experimental investigation was conducted by Cetinkale and Fishenden at atmospheric conditions using steel, brass, and aluminum specimens with ground surfaces and varying degrees of roughness. Air, spindle oil, and glycerol were used as interstitial fluids. The authors stated that the conductance for smooth contacts can be estimated with sufficient accuracy for practical purposes using their equation. They also indicate that in order to use their equation for contacts of surfaces with other types of finish, it would be necessary to determine the appropriate constants either experimentally or otherwise.

Determination of the equivalent fluid conductivity for the Conductance Number proves to be quite difficult. For an interstitial gas, if the gap height is large compared to the mean free path of the gas particles, and the temperature is low enough, there will be no lack of accommodation at the surfaces. The conductivity

of the equivalent fluid may then be considered as the normal temperature-dependent conductivity. At low vacuum pressures, on the order of 10^{-5} Torr, the conductivity of the interstitial gas would be extremely small and may be considered negligible.

For contacting surfaces of the same material, the harmonic mean thermal conductivity of the solid would be:

$$k_h = \frac{2 \, k_1 \, k_2}{(k_1 + k_2)} = k_1 = k_2$$

Hence, the Conductivity Number would range from a very small number to a negligible term for vacuum conditions.

The Constriction Number, a/b, is equivalent to the square root of the contact area ratio. That is:

$$C = \frac{a}{b} = \sqrt{\alpha}$$

The Constriction Number may also be related to the pressure at the interface and the Meyer hardness, which is the average resistance per unit area against indentation. Since the softer of the two metals will flow plastically as pressure is applied, until the mean solid spot pressure is equal to the Meyer hardness, the resulting substitution is:

$$C = \sqrt{\frac{P_a}{H_M}} \qquad \text{for plastic flow.}$$

For smaller pressures, the metallic flow would be elastic and the area of the solid spots would be given by Hertz's equation [77]. The resulting substitution would then be:

$$C = \sqrt{\frac{(P_{max}^{1/3}\ P^{2/3})}{H_M}} \qquad \text{for elastic flow.}$$

It was found that the hardness of a metal would decrease with the time of application of the test load, although at a continually decreasing rate until a new limit is reached. It was also noted that the temperature would effect the rate of hardness change; thus detailed information would be required for each type of metal tested.

The Fluid Thickness Number, $\dfrac{\delta_{CF}}{b}$, is composed of two variables not readily available. Cetinkale and Fishenden specify δ as a constant independent of pressure up to 800 psi. At further increased pressure, the effects of any change in δ_{CF} on the contact conductance would be very small. The radius of the elementary cylinder was r_d for the case of no heat transfer across the interstitial fluid and b for the case including heat transfer through the interstitial fluid. These radii were assumed to depend upon the Constriction Number and the wave length of the roughness deviation of both surfaces. Cetin-kale stated that dimensional analysis and results of their experimental investigation led to the following relationship for b:

$$b = 0.0048\ (FD_1 + FD_2)C$$

At zero pressure, the equivalent gap dimension was then determined by assuming:

$$\delta_{CF} = \frac{k_f}{h_c}$$

This δ_{CF} would be equivalent to the distance between geometrically

smooth parallel planes. For their experimental results, δ_{CF} could

be approximated by the relationship:

$$\delta_{CF} = 0.61 \ (RD_1 + RD_2)$$

The values for both b and δ_{CF} were found to be independent of the

nature of the metallic specimens and the inteistitial fluids.

The Conductance Number, U, varies widely depending upon the

interstitial fluid thickness and conductivity. It also depends upon

the radius of the elementary cylinder and the contact area ratio.

Thus the Conductance Number, or the dimensionless contact conductance,

is more complex than the basic equation for contact conductance.

In order to ascertain the practical usefulness of the empirical

relation presented by Cetinkale and Fishenden, an attempt was made to

correlate currently available experimental data and determine the

appropriate constants to predict contact conductance values. This

analysis met with little success for experimental data at vacuum

conditions.

It is difficult to assess the validity of an empirical relation-

ship without access to the experimental data from which it was form-

ulated. There seems to be little foundation for the assumption that

the film thickness is independent of pressure. For experimental

tests at atmospheric conditions with interstitial fluids, a film

thickness independent of pressure may have been satisfactory; how-

ever, when extended to a vacuum environment, the film thickness or

surface gap parameter appears to be pressure dependent. Furthermore,

as will be shown later, the no-load conductance is not necessarily the

true fluid conductance, and this assumption could result in sub-
stantial errors. A finite solid contact may still remain at no-load
conditions, which would contribute to the no-load conductance along
with the radiation transfer. Only when the contacting surfaces are
slightly separated can the true fluid conductance be determined.

Tachibana

Another analytical-experimental treatment was advanced by
Tachibana [74], in which the combined thermal contact resistance of
the solid contact and interstitial fluid was expressed as an equi-
valent length of material. Although different contact conditions
would be created every time a contact of two surfaces was made, the
author assumed that the surface could be represented by a regularly
oriented series of peaks and valleys. More peaks were allowed to
come into contact as the interface pressure was increased, limited
to the point at which plastic flow would occur. Secondly, he assumed
that the heat flux lines across the gaps caused by the valleys were
parallel, permitting the analysis to treat the resistance as inde-
pendent of the shapes of the irregularities.

These preceding assumptions allowed development of a multiple
contact model similar to the single contact model, as shown in
Figures 2-4 and 2-5. Several different surface length parameters
are defined as a result of this model, assuming a sufficient number
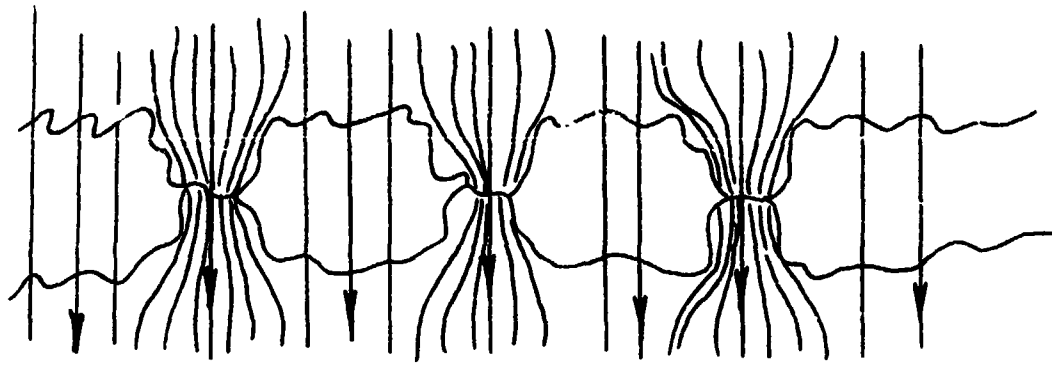
Figure 2-4. Microscopic View of Contact Interface.
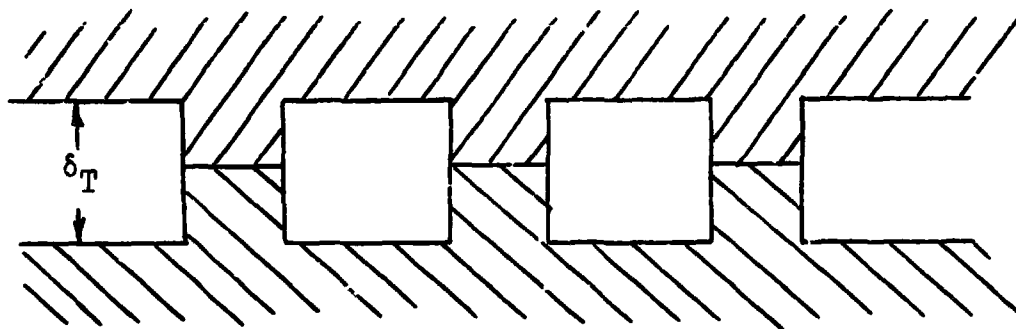
Figure 2-5. Multiple Contact Model

of protrusions exist in a unit length of surface. The gaseous con-
duction was assumed to be proportional to the ratio of the effective
gap width and the gas conductivity.

Tachibana suggested that the thermal contact resistance could be
represented by an equivalent length of material. This equivalent
length, when soldered between the interface surfaces, would result
in the same resistance at the original contact. The contact resist-
ance multiplied by a harmonic mean thermal conductivity of the
metallic specimens and by the apparent contact area would be the
equivalent length; that is:

$$L = A_a R_c k_h = \frac{k_h}{h_c}$$

Thus, the resulting expression for equivalent length in terms of
material properties and test conditions would be:

$$\frac{1}{L} = \frac{1}{\delta_T + \delta_\ell} - \frac{1}{\delta} \frac{k_f}{k_s} \frac{A_c}{A} + \frac{1}{\delta T} \frac{k_g}{k_s} \qquad (2\text{-}10)$$

where δ_T is the average of δ_1 and δ_2, and δ_ℓ is a small length
correction for any additional resistance which might occur due to
oxides on the metallic contact surface.

The principle purpose of Tachibana's research program was to
determine the effects of surface finishes. Tests were conducted at
atmospheric conditions with gun-metal specimens for three different
degrees of surface finish. Air, oil, and paraffin were used as
interstitial fluids. Results of the experimental investigation
allowed simplification of equation (2-10), since the conductivity

ratio for oil and air-filled gaps ranged from 10^{-4} to 10^{-3}. The resulting expression for equivalent length would be:

$$\frac{1}{L} = \left(\frac{1}{\delta_T + \delta_\ell} \right) \frac{A_c}{A} + \frac{1}{\delta_T} \frac{k_f}{k_s} \qquad (2-11)$$

The resistance to solid conduction may then be written in the form:

$$R_c = \frac{\delta_T + \delta_\ell}{k_h \pi a^2}$$

As the surfaces become smoother, $(\delta_T + \delta_\ell)$ will approach the magnitude of the contact radius, and the expression reduces to equation (2-3); that is:

$$R_c = \lim_{(\delta_T + \delta_\ell) \to a} \left\{ \frac{\delta_T + \delta_\ell}{k_h \pi a^2} \right\} \simeq \frac{1}{\pi k_h a}$$

Thus, in the limiting case, the multiple contact approach used by Tachibana yields the same constriction resistance as the single contact model.

The process of contact was assumed to be similar to the action of a Brinell hardness test, hence the contact area ratio could be related to a function of the apparent pressure and hardness. This approximation was assumed by Tachibana to be suitable for surface regions of plastic flow, and the contact area ratio was:

$$\frac{A_c}{A_a} = \frac{P_a}{\xi H_B}$$

The value of ξ was not known but was assumed to be independent of P_a and dependent on the shape of the irregularities of the surfaces in contact.

Equation (2-10) may be revised to include the relationship for contact area ratio. The resulting conductance is:

$$h_c = \frac{k_h \, P_a}{(\delta_T + \delta_\ell) \, \xi \, H_B} + \frac{k_f}{\delta_T} \tag{2-12}$$

For a material of Brinell hardness 115, the contact area ratio ranged from 1/11,500 at fifteen psi to 1/115 at 1,500 psi, assuming ξ was selected as 1.0. As a result of the range of the contact area ratio, Tachibana assumed that δ_T could be considered almost a constant for the range of pressures investigated. The final experimental results indicated that the relation between P_a and L was hyperbolic, and that between P_a and 1/L was linear. It was also noted that a more realistic value for ξ would have been 2.5 At zero pressure L was not infinite but finite due to heat conduction through the interstitial fluid. Although it was not possible to predict contact conductance using equations (2-10), (2-11), or (2-12), the author stated that these relationships did give quantitative agreement with his experimental results in general.

Tachibana found that smoother surfaces usually reduced the resistance. This was due to the fact that a smaller gap thickness was associated with a smoother finish, while the area of direct contact remained approximately the same. Poor agreement was found when comparing theory and conductance results from smooth surfaces. The agreement improved, however, as the surfaces became rougher.

The lack of agreement for the smooth surface data may be accounted for in several ways. As the surface becomes smoother,

the effective gap parameter becomes small and convection by the interstitial fluid is minimized. Large deviations often occur in experimental conductance data for smooth surfaces. Further, Tachibana indicated that the manner in which the surface parameter was defined could be in error by factors of two or more for smooth surface finishes.

An attempt was made to apply the analytical-empirical relations of Tachibana to recent published experimental data. In this analysis, several questions arose as to the interpretation and use of the unknown factors. The preliminary assumptions made to determine the physical contact model are in themselves satisfactory for the purpose of the experimental investigation. The general determination of the factors δ_ℓ and ξ is difficult, since they were found from the experimental data and may only apply to one particular set of data.

The values for the surface parameter δ_T were determined from a regularly machined model a⁻¹ would not be entirely suitable for a surface with randomly oriented contact spots of different heights. Tachibana also assumed that δ_T was constant over the range of interface pressures investigated. As in the case of Cetinkale and Fishenden [17], this assumption of a film thickness independent of pressure may be satisfactory when using interstitial fluids; however, it would not be accurate when extended to vacuum conditions. Clearly the experimental-empirical relation was developed for experimental data obtained at atmospheric conditions. When it is

used for data determined at vacuum conditions, the results vary by several orders of magnitude.

Tachibana used the results of Weills and Ryder [81] to show that his equation predicted the increase in equivalent length with an increase in material hardness. It was also shown that a soft mater ' with a low thermal conductivity would have a larger resistance than a hard material. Further, when the hardness was extremely high, the area corresponding to direct contact would be very small.

For his experimental investigation, Tachibana used machined surfaces with three different degrees of roughness. He has shown that the surface parameter, δ_T, for these surfaces can be calculated if the radius of the cutting tool and the feeding speed are known. No consideration of flatness deviation as opposed to roughness deviation was involved in the determination of δ_T. The value of ξ was found on the basis of experimental results which were not consistent, yielding a constant which was rather unreliable.

The equivalent length representation for thermal contact resistance developed by Tachibana may be useful; however, his expression in the present form is unsuitable for the prediction of contact conductance at vacuum conditions. Further analysis of the equation and comparison with experimental data might yield an expression for the prediction of conductance values at higher interface pressures. At pressures approaching zero, however, the form of the equation would prevent accurate prediction of contact conductance.

Fenech and Rohsenow

The most basic method of analyzing the heat transport in the simplified one-contact model involves rewriting the Laplacian equation in cylindrical coordinates and solving the resultant zero order Bessel equation with appropriate boundary conditions. The problem of determining the heat transfer across a single contact was solved by Clark and Powell [18] using the assumption of no heat flow across the void area. The case of allowed heat transfer across the void was solved by Fenech and Rohsenow [31, 32] after making several simplifying approximations.

Fenech and Rohsenow divided the simple one-contact model into several regions, as shown in Figure 2-6, and the Laplacian equation was set up for each region. Average boundary conditions were determined based on the following assumptions:

1) Only axial conduction was permitted across the interstitial fluid;

2) The thermal conductivity of the metal was much greater than the conductivity of the interstitial fluid, thus permitting heat flow to channel through the points of metal-to-metal contact;

3) The points of metallic contact would increase in both size and number as the interface pressure was increased;

4) The void space height was small compared to the distances between contact points;

5) Radiation and convection in the interstitial fluid were negligible;
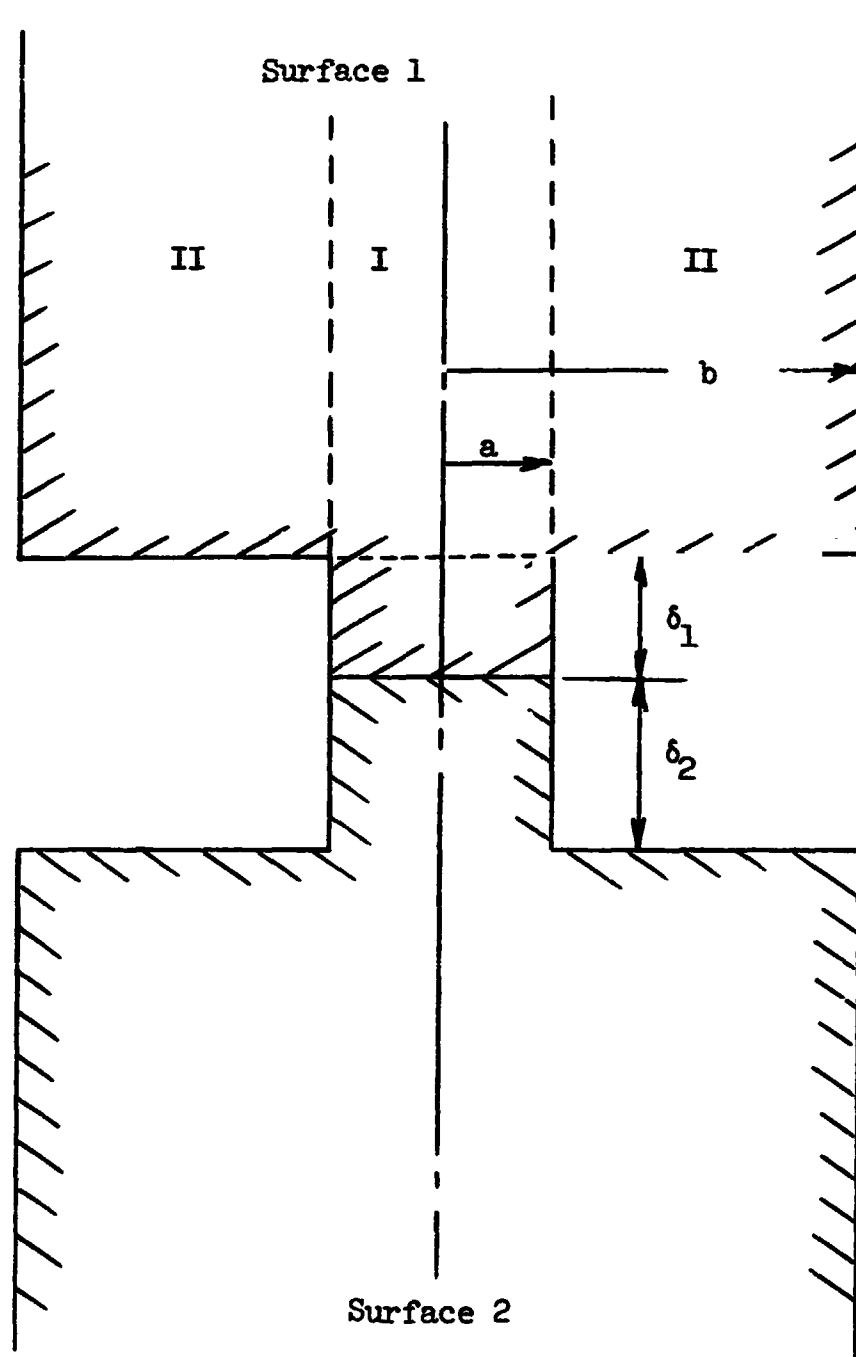
Figure 2-6. Idealized Multi-zone Contact.

6) The contact geometry was idealized such that the true number of contact spots were of equal size and uniformly distributed;

7) Each contacting specimen could be divided into a number of imaginary elementary cylinders which transfer no heat to one another and "feed" one solid contact spot apiece.

Solution to the Laplacian equation resulted in an expression which incorporated the physical parameters of the contact (i.e. number of contact points, real area of contact, average thickness of the voids) and the physical properties of the materials in contact. Fenech stated that his expression would provide a method "for calculating the thermal conductance of a metallic contact for any combination of metals, surface states, and fluid in the voids at the temperature and pressure considered."

The assumed approximations permitted a solution to the Laplacian equation in the form:

$$h_c = \frac{\frac{k_f}{(\delta_1 + \delta_2)}\left[(1-\alpha)G + 1.1\ C\ g(C)\ (\frac{1}{k_1} + \frac{1}{k_2})\right] + 4.26\ C\ h^{1/2}}{(1-\alpha)\left[1 - \frac{k_f}{\delta_1+\delta_2}\ (\frac{\delta_1}{k_1} + \frac{\delta_2}{k_2})\right]\ G} \qquad (2\text{-}13)$$

where

$$G = \left(\frac{4.26\ n^{1/2}\ \frac{\delta_1}{C} + 1}{k_1} + \frac{4.26\ n^{1/2}\ \frac{\delta_2}{C} + 1}{k_2}\right)$$

and

  n = number of contact spots

$$C = \sqrt{\frac{A_c}{A_a}} = \frac{a}{b} = \sqrt{\alpha}$$

  f(C) = function of C, generally taken as 1.0 for C
     greater than 0.1.

In equation (2-13), the first term in the brackets of the numerator accounts for the heat flow across the fluid at the interface. The second term in the numerator accounts for the heat flow through the metallic contact spots.

Since the film thicknesses associated with actual surfaces are not constant, the authors developed a weighted average film thickness:

$$\delta_i = \frac{\beta_i}{1 - \dfrac{k_f}{k_i}} \qquad i = 1, 2; \; k_f \neq k_i$$

where β_i is the volume average thickness associated with each surface, determined as a surface function in cylindrical coordinates.

The authors conducted an experimental investigation to verify their analytical results. A single contact cylinder was tested using air, water, and mercury as the interstitial fluids. Contact conductance measurements were then made on an interface of roughly milled armco iron and aluminum.

The practical application of equation (2-13) is dependent on the evaluation of several unknown parameters. Fenech and Rohsenow developed a technique whereby they could evaluate the unknown surface parameters graphically. Profiles of the contacting surfaces were measured along two perpendicular directions. These profiles were transferred to transparent paper and superimposed upon one another to simulate pressure conditions. The volume average thickness was determined by planimeter measurements of the void space profile. The number of contact points was found by counting the

contact points along the profile and dividing their product by the area. The actual contact area was found by the product of the widths of the contacts along the profile.

According to the authors, experimental results agreed with the predicted conductance values within about 5 percent over a load range from 100 to 2,600 psi for the iron-aluminum contact. When the conductance values were plotted as a function of apparent pressure on log-log paper, they exhibited a linear increase with pressures above 100 psi. The hysteresis observed on cycling the compressive load was not accounted for quantitatively since neither elastic deformation nor plastic flow was considered in the analysis. The assumptions made by Fenech and Rohsenow seem to be reasonable considering the results of their experimental investigation.

Physically, the difference between the results of this model and analysis and that of Cetinkale and Fishenden [17] is shown in Figure 2-7, as given by Minges [58]. The coupling boundary conditions cause the heat flux lines to have a steeper slope near the constriction. Thus the heat flux through the solid and void areas at the interface plane is directly proportional to k_s and k_f, respectively. This implies that the plane of the contact is isothermal, and that the isotherms some distance from the junction seem to be flatter and less distorted than those given by the Cetinkale and Fishenden model. Some flattening should be expected due to heat flow through the voids, but not to the extent shown by the Fenech analysis. Experimental results of Fenech and Rohsenow, however,

Fenech and Rohsenow

Cetinkale and Fishenden

a

b
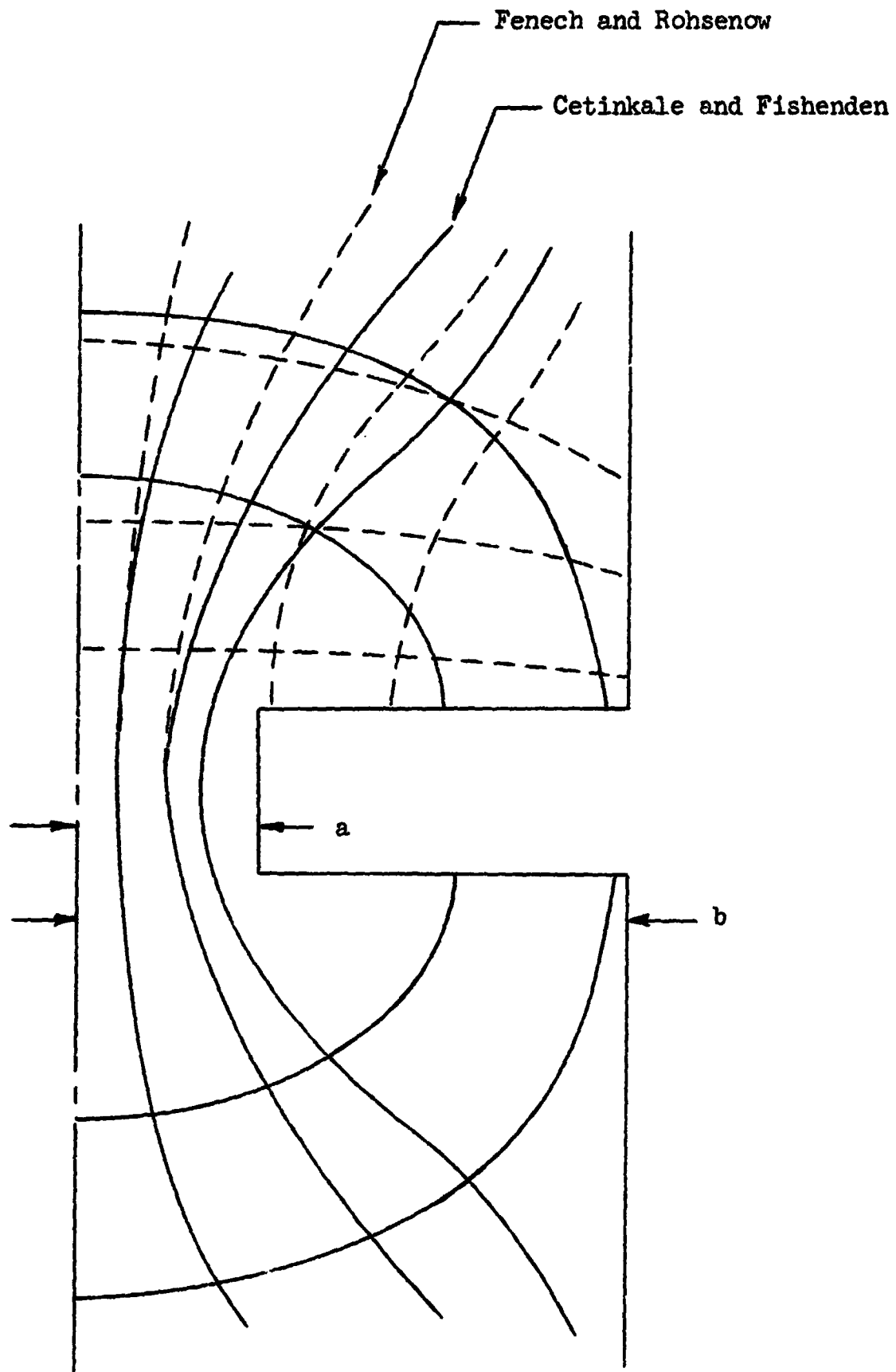
Figure 2-7. Distortion of Temperature and Heat Flux Field
as a Result of Assumed Boundary Conditions [58].

indicate that the initial approximations are of no serious consequence.

An analog computer program for the evaluation of surface profile parameters was developed by Henry and Fenech [45] in an attempt to further the work of Fenech and Rohsenow. An experimental investigation was conducted with stainless steel specimens at three interface temperatures over a pressure range of 300 to 20,000 psi. Surface measurements were made and the profilometer traces, in terms of analog voltages, were placed on magnetic tapes. The traces of the two surfaces were then simultaneously fed into the computer in order to determine the interface parameters. Using surface parameters for similar surface finishes determined in this manner, Henry states that the maximum deviation observed in the calculation of contact conductance with equation (2-13) was thirty percent. This large deviation occurred at the higher loads where interface temperature differences were on the order of one to three degrees Fahrenheit. This approach yields good results. It is not feasible for the actual prediction of conductance data, however, since each surface under consideration must be completely analyzed and surface parameters placed on tape.

Equation (2-13) may be simplified in a number of different ways. At low environmental pressures, i.e. pressures less than 10^{-3} Torr, the thermal conductivity of an interstitial gas or fluid is much smaller than at atmospheric pressure. The ratio of fluid conductivity to solid conductivity would become extremely small, permitting the

assumption of negligible heat transfer through the interstitial fluid. Hence, for vacuum conditions, equation (2-13) may be reduced to:

$$h_c = \cfrac{\cfrac{4.26}{(1-\alpha)\,b\sqrt{\pi}}}{\cfrac{1}{k_1}\left(\cfrac{4.26\,\delta_1}{\alpha b\sqrt{\pi}}+1\right) + \cfrac{1}{k_2}\left(\cfrac{4.26\,\delta_2}{\alpha b\sqrt{\pi}}+1\right)} \qquad (2\text{-}14)$$

This equation also may be used for dissimilar materials with different surface conditions.

The resistance due to the metallic conduction part of the generalized solution for the one contact model may be written:

$$R_c = \cfrac{\cfrac{\delta_1}{R_1}+\cfrac{\delta_2}{R_2}+\left(\cfrac{1}{k_1}+\cfrac{1}{k_2}\right)\cfrac{\sqrt{\alpha}\,b}{2.4}}{\cfrac{\alpha}{1-\alpha}\,\pi\,b^2}\;.$$

This expression was simplified [83] by permitting $\delta_1 = \delta_2 = \delta_{FR}$ and including the mean harmonic thermal conductivity:

$$R_c = \cfrac{2.4\,\dfrac{\delta_{FR}}{a}+2}{^\circ.4\;\pi a\;k_m} \;\approx\; \left.\cfrac{1}{1.7\;a\;k_m}\right)\;\delta \approx a$$

Thus, for the case of $\delta \sim a$, the constriction resistance is slightly greater than that found by Clark and Powell in equation (2-2).

The analysis presented by Fenech and Rohsenow is by far the most detailed analytical study of thermal contact resistance. However, the resulting equations, (2-13) and (2-14), are not readily usable for the correlation of experimental data of most investigations due to the lack of required information for the determination of n, β, and C. The graphical technique used to determine these parameters

is satisfactory only for the particular surfaces investigated. The attempt by Henry to provide these parameters by means of an analog treatment has only led to a more complex procedure for the prediction of thermal contact conductance. An extension of the basic theory presented by Fenech and Rohsenow will be presented in a later chapter. The results of this extension simplify the prediction of thermal contact conductance for apparent interface pressures of 200-800 psi.

Laming

It is interesting to note that Laming studied under Dr. Margaret Fishenden at Imperial College in London, and his analysis is basically an extension of the work presented by Cetinkale and Fishenden. Laming [55] chose to analyze the single contact model and determine the conduction through the metallic contact spot and the conduction through the interstitial fluid. He used contacting specimens with machined parallel grooves to obtain contact conductance data for the development of a semi-empirical equation.

On the basis of work by Bowden and Tabor [16] and Holm [46], Laming assumed that since loads which can be supported by elastic deformation are extremely small, the pressure on each contact spot is equal to the indentation yield pressure, or the Meyer hardness. In addition, he considered a "constriction alleviation effect" which would account for the cases of extremely high loads and/or comparable solid and fluid conductivities.

The conductance per unit area for the metallic spots, in terms of the constriction alleviation factor, f, was then given as:

$$h_s = \frac{2\ k_s}{1 - f} \left(\frac{n}{\pi}\ \frac{P}{H_M}\right)^{1/2}$$

The thermal conductivity is the harmonic mean value.

The constriction alleviation factor was calculated from the results of the analytical study by Roess [64]. He found that the constriction resistance, R, associated with a contact spot of radius a and an elementary cylinder having the radius of the dividing flow line, could be determined from equation (2-4) with $C = \frac{a}{r_d}$. Laming assumed that for most cases the ratio $\frac{a}{r_d}$ would be small, and the constriction alleviat on factor could be approximated by the first term of the series, i.e.,

$$f = 1.4093\ \frac{a}{r_d} \qquad\qquad \frac{a}{r_d} < 0.3.$$

Since many machined surfaces may have a regularly pitched ridging or waviness in one direction, the number of potential contact points would be the number of ridge-intersections available. Assuming that the ridges would be situated at some angle, the number of contact points at the interface was specified as $n = \sin \alpha/\lambda_1\lambda_2$ and the metallic conductance became:

$$h_s = \frac{2\ k_s}{(1 - f)} \left(\frac{\sin\ \theta}{\pi\ \lambda_1\lambda_2}\ \frac{P}{H_M}\right)^{1/2}$$

Heat transfer across the interstitial fluid occurred only by conduction, since radiation and convection were considered to be negligible. Defining an effective film thickness parameter, t, the

fluid conductance per unit area was given as:

$$h_f = \frac{k_f}{t}$$

The resulting equation for the total contact conductance was:

$$h_c = h_s + h_f = \frac{k_f}{t} + \frac{2 k_h}{(1 - f)} \left(\frac{\sin \theta}{\pi \lambda_1 \lambda_2} \quad \frac{P}{H_M} \right)^{1/2} \quad (2\text{-}15)$$

The resistance for the solid conduction may then be written as:

$$R_c = \frac{(1 - f)}{2 k_h \pi b^2} \left(\frac{\pi \lambda_1 \lambda_2}{\sin\theta \, P_a} \right)^{1/2}$$

The above resistance equation may be reduced to equation (2-2), the expression from which Laming started his analysis, by making several simplifying assumptions. The maximum number of contacts will occur when $\theta = 90°$, and the term in the parentheses may be replaced by the appropriate contact area ratio. The resulting equation is:

$$R_c = \frac{(1 - f)}{2 k_m n a}$$

Allowing the constriction alleviation factor to approach zero, and treating the single contact case, n = 1, the expression simplifies to equation (2-2).

An experimental facility operating in an atmospheric environment was used to obtain contact conductance data. This facility was the same as that used by Cetinkale and Fishenden. Steel, brass, and aluminum specimens with peak-to-mean surface roughness ranging from 170 to 2,000 microinches were tested with interstitial fluids of air, glycerol, and water

Results of the experimental investigation were used to determine a semi-empirical relationship for the heat transfer through the interstitial fluid. This relationship,

$$h_f = 1.5 \frac{k_f}{s} = 0.667 \frac{k_f}{t}$$

is usually expressed as a function of the gap dimension, δ_{CF}. Since δ_{CF} is difficult to ascertain, Laming chose as the gap parameter the sum of the peak-to-mean distances for the two surfaces. In his analysis, Laming assumed that the conductance of the fluid was independent of the pressure, and that s/t was constant. It should be pointed out here that although the contribution to heat transfer by radiation and convection were neglected in the initial analysis, the effects may very well be included in the factor of 1.5 in the preceding equation.

After further investigation of his experimental conductance data on log-log plots, Laming decided that the contact conductance could be represented by:

$$h_c = h_f + J(P_a)^n \qquad (2\text{-}16)$$

where J is a constant. The value for n resulting from analysis of the solid conductance was 0.50; however, a value of 0.667 best fits the experimental data. The fluid conduction component was determined by subtracting a constant from the total conductance. These values of fluid conduction agreed favorably with the direct experimental data of the conduction components obtained by varying the interstitial fluids at constant load.

Several deficiencies have been found in the use of equation (2-15). In the region of most engineering applications, the predicted values were somewhat higher than actual experimental data obtained at atmospheric conditions. For pressures on the order of 200 psi, the conductance was over-predicted by factors of 100 percent or more. At pressures near 6,000 psi, however, the predicted conductances compare favorably with experimental data. Further, contact conductance values for interfaces with fine finishes had proportionately lower conductances than the coarse finishes. These deviations were accounted for by the increased apparent hardness of the finer contact points, and the fact that the hardness is quite dependent upon the load. It should be pointed out that the experimental data were obtained on machine-grooved surfaces rather than surfaces with randomly distributed contact spots. It appears that the expression presented by Laming would be suitable for prediction of contact conductance only at atmospheric conditions when surface parameters and orientation are known, and even then, only in the pressure range of 2,000 to 10,000 psi.

Since a majority of the surfaces exhibiting contact conductance are smooth with no specific orientation, it is not possible to determine a surface wavelength. Thus the original problem of determining the contact area is unresolved. Secondly, the relationship of Laming is not suited for correlation of published experimental data since very few, if any, authors give surface orientation. The simplified form of the conductance, equation (2-16), has been proposed several times [7, 16, 44] and has been found to fit available

experimental data only over a small range of pressure.

Clausing and Chao

A more recent theory for the prediction of thermal contact con-
ductance has been presented by Clausing and Chao [19, 20]. This
experimental-analytical relationship was derived for the one-contact
model as an extension of the constriction resistance theory of Holm
[46]. Like other investigators, Clausing assumed that the contribu-
tion to the heat transferred across a joint by convection and radia-
tion would be negligible in a vacuum, thus permitting the metal-to-
metal conduction to be the dominant mechanism. In a model such as
that shown in Figures 2-2 and 2-5, the constriction of the flow of
heat to the small areas manifested itself as a contact resistance at
the macroscopic level.

The interface area was divided into two regions: the contact
region and the non-contact region. The contact region or macro-
scopic contact area was defined as that portion of the surface
where the density of the micro-contact areas was high. The non-
contact region, then, contained few if any microscopic contact
areas. The size of the regions was governed by elastic deformation
at the contact, since relatively low pressures are exerted in prac-
tical joints.

On the basis of these surface divisions, Clausing felt that the
constriction of heat flow at an interface could be represented by
two resistances in series: the macroscopic constriction resistance
and the microscopic constriction resistance. Analysis of the

microscopic resistance was based on the following assumptions:

1) Surfaces were free from films;

2) Microscopic contact areas were all circular and of identical radius;

3) Contact areas were uniformly distributed over the region.

Clausing initiated the analysis by writing the microscopic resistance in the form of equation (2-2) and extending this expression to include the number of contacts. Clausing also suggested that this expression should be analyzed with a variable radial temperature in the axial direction rather than the maximum center-line temperatures used by Holm. Clausing combined this premise with the solution of Roess, equation (2-4), and evaluated the constriction resistance. The resulting expression was:

$$R = \frac{g(C)}{2\ a\ k_h\ n}$$

Assuming that the asperities carried the load and deformed plastically, the area of contact was represented as a function of the load and hardness. This assumption* was also made by Cetinkale and Fishenden [17], Tachibana [74], and others [44, 71]. The resulting relationship for the microscopic interface conductance was:

$$h_{mi} = \frac{2}{\pi}\ \frac{P_a}{\xi H_D}\ \frac{k_h}{a\ g(C)} \quad ; \quad C = \frac{a}{b} \qquad (2\text{-}18a)$$

or in dimensionless form:

$$\frac{h_{mi}\ a}{k_h} = \frac{2}{\pi}\ \frac{P_a}{\xi H_D}\ \frac{1}{g(C)} \qquad (2\text{-}18b)$$

---

* See discussion of the validity of this substitution on pages 64-65.

This relationship is similar to that of Boeschoten and van der Held
[15].

Clausing made some simplifying approximations in order to
estimate the microscopic constriction ˙ ˙istance. To account for
the decrease in resistance due to non-circular areas and the increase
in contact area due to microscopic elastic deformation, a value
$\xi = 0.3$ was chosen. The parameter $g(C)$ was selected as unity, except
in cases of very smooth surfaces and extremely high interface pres-
sures. Microscopic contact areas were considered to be independent
of load. Simplifying equation (2-18b), the dimensionless microscopic
conductance became:

$$\frac{h_{mi}a}{k_h} = \frac{2P_a}{H_D}$$

The principle model considered for analysis of the macroscopic
constriction resistance was again the single contact model. Heat
was permitted to flow in a cylindrical column of fixed radius and
constrained to flow through a smaller circular contact spot, as
shown in Figure 2-2. The Laplacian equation in cylindrical coordin-
ates, solved with appropriate boundary conditions, was combined with
equation (2-18a). The thermal resistance of a constriction for both
the case of a uniform temperature contact and the case of a uniform
heat flux contact were solved numerically and found to be essentially
identical. Clausing stated that this result indicated that the
macroscopic constriction resistance was independent of the magnitude
and radial distribution of the microscopic constriction resistance.

The actual physical model used by Clausing and Chao consisted

of two cylinders in contact, with the contacting surfaces finished
to a convex spherical radius of curvature. For this model, the
total macroscopic conductance was given as:

$$h_{ma} = \frac{2 \; k_h \; X}{\pi \; b \; g(X)}$$
(2-19)

In order to determine the macroscopic area, Clausing chose to
use the radius of a circular contact between two spherical bodies
in elastic contact, solved by Hertz [77]. This relationship pro-
vides a radius variation as a function of load. With some simplify-
ing approximations, the constriction ratio became:

$$X = 1.285 \; \left[\left(\frac{P_a}{E} \right) \left(\frac{b}{\delta_{CC}} \right) \right]^{1/3}$$
(2-20)

where $\left(\frac{P_a}{E} \right) \left(\frac{b}{\delta_{CC}} \right)$ was defined as the elastic conformity modulus.
Hence the macroscopic conductance was determined by combining equa-
tions (2-19), (2-4b), and (2-20).

Experimental values of contact conductance were determined for
stainless steel, brass, aluminum, and magnesium, in a vacuum, with
varying surface conditions. It was stated that good agreement was
found between the measured and predicted values for thermal contact
resistance for values of X less than 0.65. Beyond this point, the
macroscopic areas of the contact may be plastically deformed, and
the Hertz equation would no longer be valid. Good correlation was
found for fairly rough (200-400 microinches) surfaces; however, very
poor correlation was found for smoother surfaces. It should be noted
here that the agreement was with the dimensionless parameters of
contact conductance and elastic conformity modulus given in equations
(2-19) and (2-20).

Film resistanc can be a significant factor. Tests by the authors indicated that the interface conductance was reduced by a factor of four or five as a result of surface films. Since it was not possible to correlate or estimate with any certainty the surface film resistance, the relative importance of the macroscopic and microscopic constriction resistances was examined. The ratio of these resistances was determined to be:

$$\frac{R_{ma}}{R_{mi}} = \pi \ (\frac{P_a}{\xi \ H_D}) \ (\frac{b}{a}) \ (\frac{g(X)}{X}) \tag{2-21}$$

Perhaps the major contribution of Clausing and Chao to thermal contact resistance was to predict and show experimentally the predominance of the macroscopic constriction resistance over the microscopic constriction resistance. The ratio of macroscopic-to-microscopic resistance ranged from a low of 29 for aluminum to a high of 176 for magnesium.

Although the analysis of Clausing and Chao is useful for the correlation of contact resistance data, it is not very reliable for magnitude predictions, particularly for smooth surfaces. This theory will be discussed in more detail in a later chapter, where comparisons will be made with available experimental data.

II. SUMMARY OF PUBLISHED EXPERIMENTAL DATA

In order to establish the correct magnitudes and trends for thermal contact conductance values, the experimental data available in the literature must be analyzed and compared to select the more

reliable data. There are a number of different ways in which this analysis might be carried out. Comparison of magnitudes, slopes at different pressures and surface finishes, and effects of mean junction temperature are a few of the characteristics considered in this section. In many cases, investigators have not given all of the information necessary for analysis. In some instances, assumptions have been made in order to complete the data for this analysis. Since the objective of the present work has been to predict conductance values in a vacuum environment, only the data of investigations conducted at vacuum conditions will be treated. Table 2-1 lists the experimental work reviewed with some of the pertinent characteristics for each investigation. The corresponding experimental data used for comparison with prediction equations are tabulated in Appendix A.

Preliminary Analysis

Study of available published data indicates that there is not a simple form or manner of describing the surface or gap depth. A number of investigators have presented various expressions, and for the most part, these expressions include some function of flatness deviation and rms roughness. In order to compare the published data a common expression must be used.

A model for surfaces in contact w. . chosen to represent surfaces with similar finishes as well as dissimilar finishes. These surface combinations are shown in Figures 2-8 and 2-9. It was desired that the smooth-to-rough surface combination (Figure 2-8) should yield the

TABLE 2-1

EXPERIMENTAL INVESTIGATIONS REVIEWED

(Vacuum Lower than 10^{-3} Torr)

Investigator	Metallic Specimens	Temp. Range (°F)	Pressure Range (psi)
Bloom [13]	Aluminum 7075	-270 to 300	50 to 950
Clausing & Chao [20]	Aluminum 2024	220 to 240	10 to 990
	Stainless Steel 303	230 to 245	10 to 990
	Brass Alloy 271	160 to 340	10 to 955
	Magnesium AZ31B	___ to 215	10 to 990
Cunnington [22]	Aluminum 6061	60 to 250	15 to 95
	Magnesium AZ31B	60 to 150	15 to 95
Fletcher, et al [33]	Aluminum 2024	-50 to 300	100 to 385
Fried [35,36,37]	Aluminum 2024	90 to 220	50 to 1130
	Stainless Steel 304	90 to 390	30 to 1170
	Magnesium AZ31B	75 to 105	140 to 3270
Hargadon [43]	Stainless Steel 304	250 to 260	15 to 810
Smuda, et al [69,70]	Aluminum 2024	-255 to 300	10 to 1040
Yavonovich [84]	Aluminum 2024	450 to 515	250 to 5900
	Stainless Steel 303	500 to 540	250 to 4400
	Magnesium AZ31B	470 to 500	250 to 3600

largest value of the surface parameter[*], and surface combinations more similar in nature (Figure 2-9) would result in smaller values of the surface parameter. For convenience, it was also desired that this surface parameter be a function of flatness deviation and roughness.

The total profile height of the surface roughness (peak-to-valley height) was specified by Oberg [60] to be four times the rms value. The flatness deviation is measured to the centerline of the roughness profile, or to the mean surface [60, 75]. Hence, the total peak-to-valley height of a surface could be represented as the measured value of the flatness deviation plus one half of the total roughness height, or FD + 2RD. Combining flatness deviation and roughness in an additive manner has been suggested by several investigators [17,55,75].

Two similar surfaces placed together under load will overlap to some extent (Figure 2-9). However, dissimilar surface combinations such as a smooth surface against a rough surface (Figure 2-8) will overlap very little if at all.[*] In either case, it is assumed that the contact occurs at the mean surface interface of the smoother surface. This mean surface is located at one half of the total peak-to-valley height [60,75]. Hence, a surface parameter for a contact or an effective gap between surfaces may be defined as:

$$d = (FD + 2RD)_{\substack{rough \\ surface}} \quad -1/2(FD + 2RD)_{\substack{smooth \\ surface}} \qquad (2-22)$$

For a contact of similar surfaces, the surface parameter or effective gap is shown in Figure 2-9. For the combination of a smooth and

---

[*] Experimental data presented in Chapter III have shown that conductance data for smooth-to-rough surfaces are lower than conductance data for similar rough surfaces.

Rough Surface
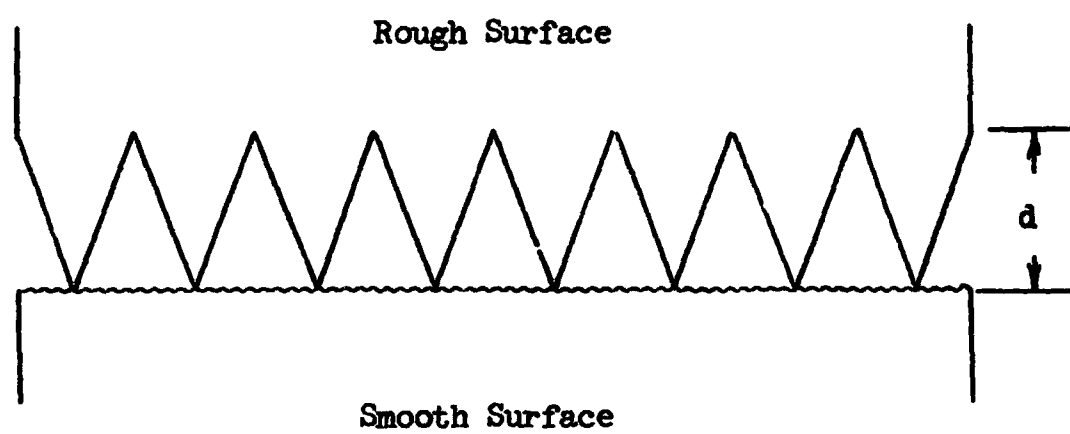
Smooth Surface

Figure 2-8. Diagram of a Smooth-to-Rough Surface Combination.

Rough Surface
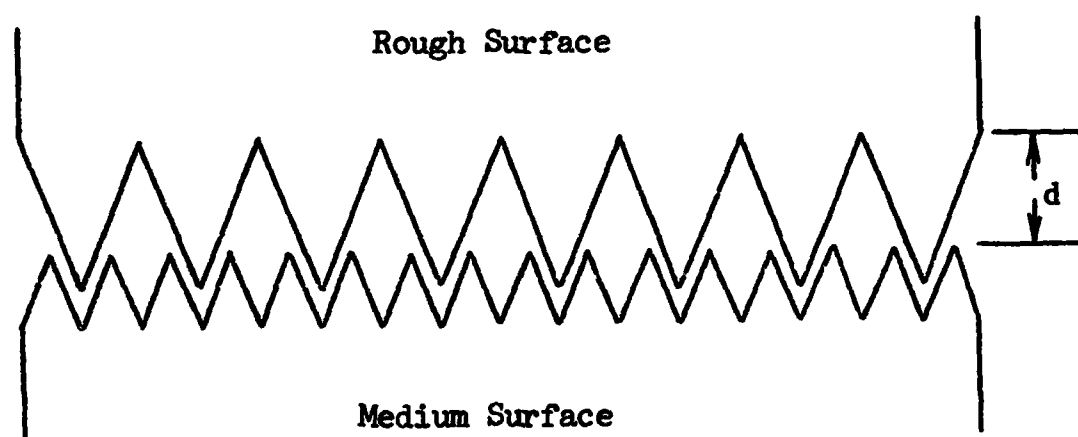
Medium Surface

Figure 2-9. Diagram of a Medium-to-Rough Surface Combination.

rough surface, the resulting surface parameter would be approximately the value of the rough surface, as shown in Figure 2-8.

This expression, then, is suitable for contacts composed of smooth surface finishes against rough surface finishes, as well as for surfaces with similar finishes. Also important is the fact that it is formulated in terms of defined surface characteristics usually measured and published.

In the published work on experimental contact conductance, a discussion was presented by each investigator regarding the validity of his data. Each author suggested that some data were questionable, although the majority should be acceptable for further analysis. In some cases in which deviations existed, it was possible to explain these discrepancies as due to transient rather than steady state conditions. Typographical errors were also present in some of the published works. Several sets of data were in error due to the change in physical properties of the specimen during the course of the experimental investigation. This change caused erroneous heat flux calculations, and as a result, the conductance values were too small. Several investigators have experienced and reported these changes [19, 36, 69]. Other sets of data were stated to have visible oxidized surfaces due to prolonged storage before testing [20]. These data were considered in this analysis; however, they showed marked differences from what would be expected for clean surfaces. Finally, some contact conductance data included an interstitial grease or flux. These runs were not considered as they were not pertinent to the objective of this study. As a result of this preliminary analysis

of the available data, some data were eliminated. A larger amount

of data, however, were still suitable for further analysis.

Comparative Analysis

The magnitude of contact conductance varies considerably depend-

ing upon the various characteristics and test conditions of the

contacting surfaces. The contact pressure, mean junction temperature,

and surface parameter play extremely important roles. Thus, compari-

sons of the conductance values can only be in terms of order of

magnitude since it is highly unlikely that any two investigators

would have used all of the same test conditions. Experimental data

might be consistent, however, with other data of the same investiga-

tion. It has been found that better agreement exists between differ-

ent investigators for the rougher surfaces; however, smooth surfaces

exhibit a sometimes unexplainable variation in magnitude. Curves

for contact conductance as a function of pressure were plotted for

magnitude and trend comparisons. Certain data points exhibiting

large deviations were eliminated as questionable data, since they

were not consistent with the other data of the same investigation.

A large amount of the published experimental data at vacuum

conditions has been obtained with aluminum test specimens. A re-

presentative sample of aluminum data with different surface condi-

tions and mean junction temperatures is shown in Figure 2-10*, which

---

* The codes for the data shown in the figures of this Chapter are
  listed by the first letter of the authors last name and his
  respective run number. These codes are also listed in Table 2-2.
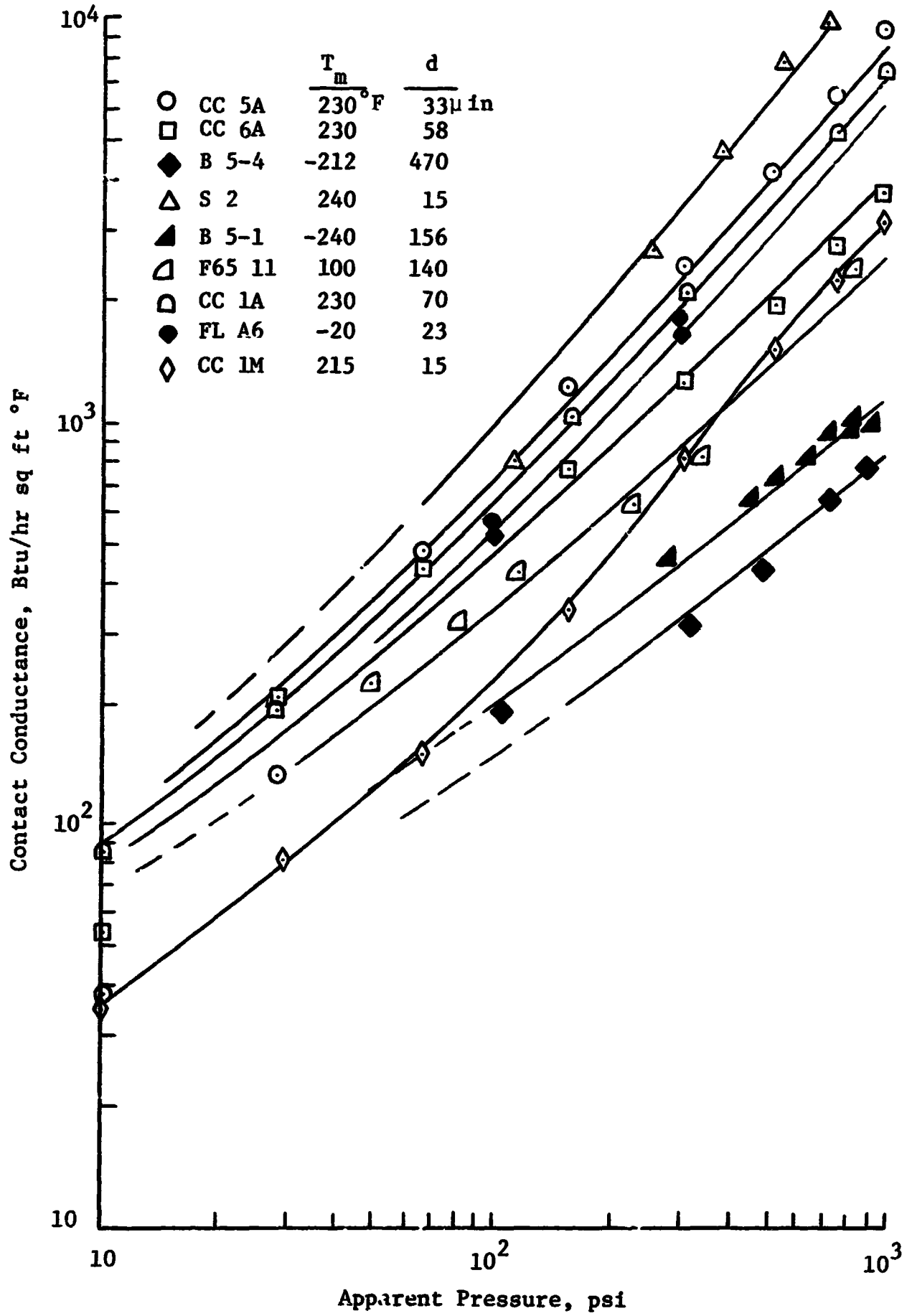
Figure 2-10. Variation of Contact Conductance with
Apparent Interface Pressure for Selected
Aluminum Data.

gives the magnitude of the conductance as a function of pressure. One oxidized magnesium run is also included for comparison [20]. It may be noted that as the surface finish becomes smoother (i.e., roughness and flatness deviation become smaller) the slope increases more rapidly. The curves suggest that the conductance will become extremely large in the limit as pressure increases; however, as the pressure becomes very small, it is difficult to determine whether the conductance remains finite or approaches zero.

The curve of the derivative of conductance with respect to pressure (for the data of Figure 2-10) is shown in Figure 2-11. Analysis of these graphically obtained derivatives suggests that the slopes of some data approach zero as the pressure becomes large while the slopes of other data appear to increase as pressure becomes large. It is difficult to determine which of the data exhibit the correct trend.

That both the contact conductance and its derivative should approach infinity as pressure increases can be illustrated using an expression for a single contact developed by Roess [64]. This relationship, given in equation (2-4), may be simplified by using the first two terms of the series expansion, $g(C)$. The resulting conductance may be written as:

$$h_c = \frac{2\, k_h}{\pi\, b\, (1-\frac{a}{b})}$$

In the limiting case, as pressure becomes large, the contact radius a approaches b, and the constriction ratio approaches one. Hence:
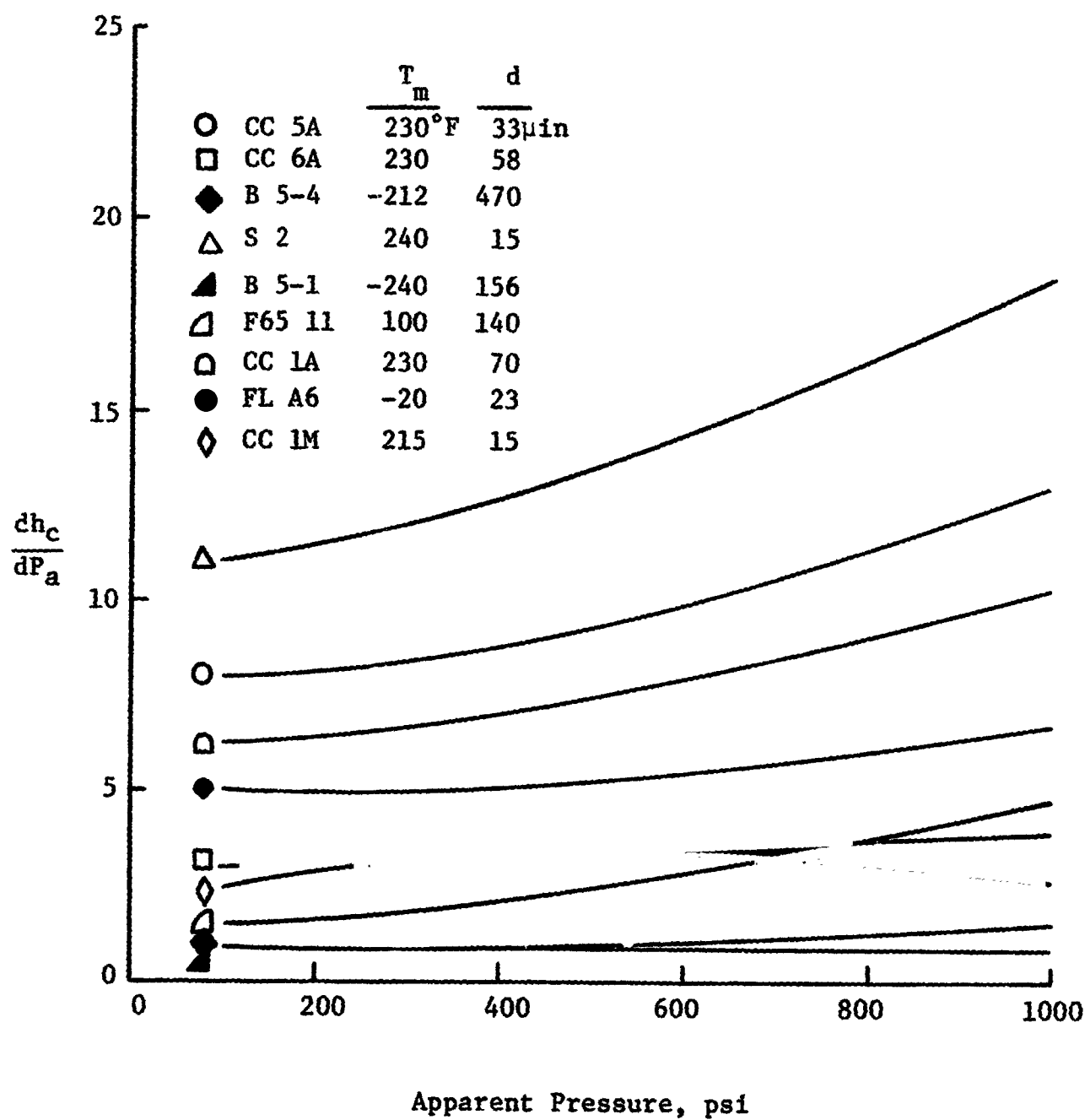
Figure 2-11. Variation of dh_c/dP_a with Apparent Interface Pressure for Selected Aluminum Data.

$$\underset{\substack{P \to \infty \\ a \to b}}{\text{Lim}} \quad h_c = \underset{a \to b}{\text{Lim}} \quad \frac{2\,k_h}{\pi b(1-\frac{a}{b})} = \infty$$

In a similar manner, it can be shown that the derivative of the conductance with respect to pressure must also become infinite. The derivative of the conductance with respect to contact radius is:

$$\frac{dh_c}{da} = \frac{2\,k_h}{b^2(1-\frac{a}{b})^2}$$

Again, as pressure becomes large, a approaches the size of b, and $\frac{dh_c}{dP_a}$ becomes large, or:

$$\underset{\substack{P_a \to \infty \\ a \to b}}{\text{Lim}} \quad \frac{dh_c}{da} = \underset{a \to b}{\text{Lim}} \quad \frac{2\,k_h}{\pi b^2(1-\frac{a}{b})^2} = \infty$$

For good data, then, both the conductance and its slope should increase as pressure becomes large.

It should be pointed out that at least one of the curves in Figure 2-10 which exhibits a tendency toward a zero slope as pressure increases was oxidized [20]. Oxide films are almost always present on metallic surfaces [21, 27, 35, 82]. Fenech and Rohsenow [31] state that the surface film does not appreciably affect the thermal resistance. Clausing and Chao [20], on the other hand, suggest that for the relatively small areas of actual contact, the film effects may no longer be negligible. It appears from the present analysis that the effects of surface films may alter the slope of the conductance pressure curve, depending upon the degree to which the surfaces are oxidized.

It is not possible to accurately extrapolate the slope to the

region of the origin. A few curves suggest a zero value for the

slope, yet others indicate a finite value. It would appear, however,

that a majority of the data in Figure 2-11 indicate a finite value

for the slope at zero pressure.

The mean junction temperature is also a major factor to consider

in analysis of published data. It appears that the conductance is

directly a function of temperature, as exhibited in Figure 2-12. Note

that as the temperature decreases, so does the magnitude of the con-

ductance. Although there has been little experimental work done in

this area, available data do suggest a marked change in the deriva-

tive of conductance with temperature as the temperature increases

from low temperatures to values near 300°F. In addition, the effect

of mean junction temperature appears when comparing the derivative

of conductance with respect to pressure at various mean junction temp-

eratures, as shown in Figure 2-13.

Although a surface parameter has been defined [equation (2-22)],

it is difficult to make direct comparisons with all data since the

surface characteristics of roughness and flatness have been measured

in different manners. An attempt has been made, however, to show

the trends that the data seem to suggest. The change in conductance

as a function of surface parameter at various pressures may be seen

in Figure 2-10. Note that at similar mean junction temperatures

and constant pressure, the change in conductance seems to follow a

logrithmic pattern. The smoother surfaces exhibit extremely high

conductances while changes in the surface parameter for rougher
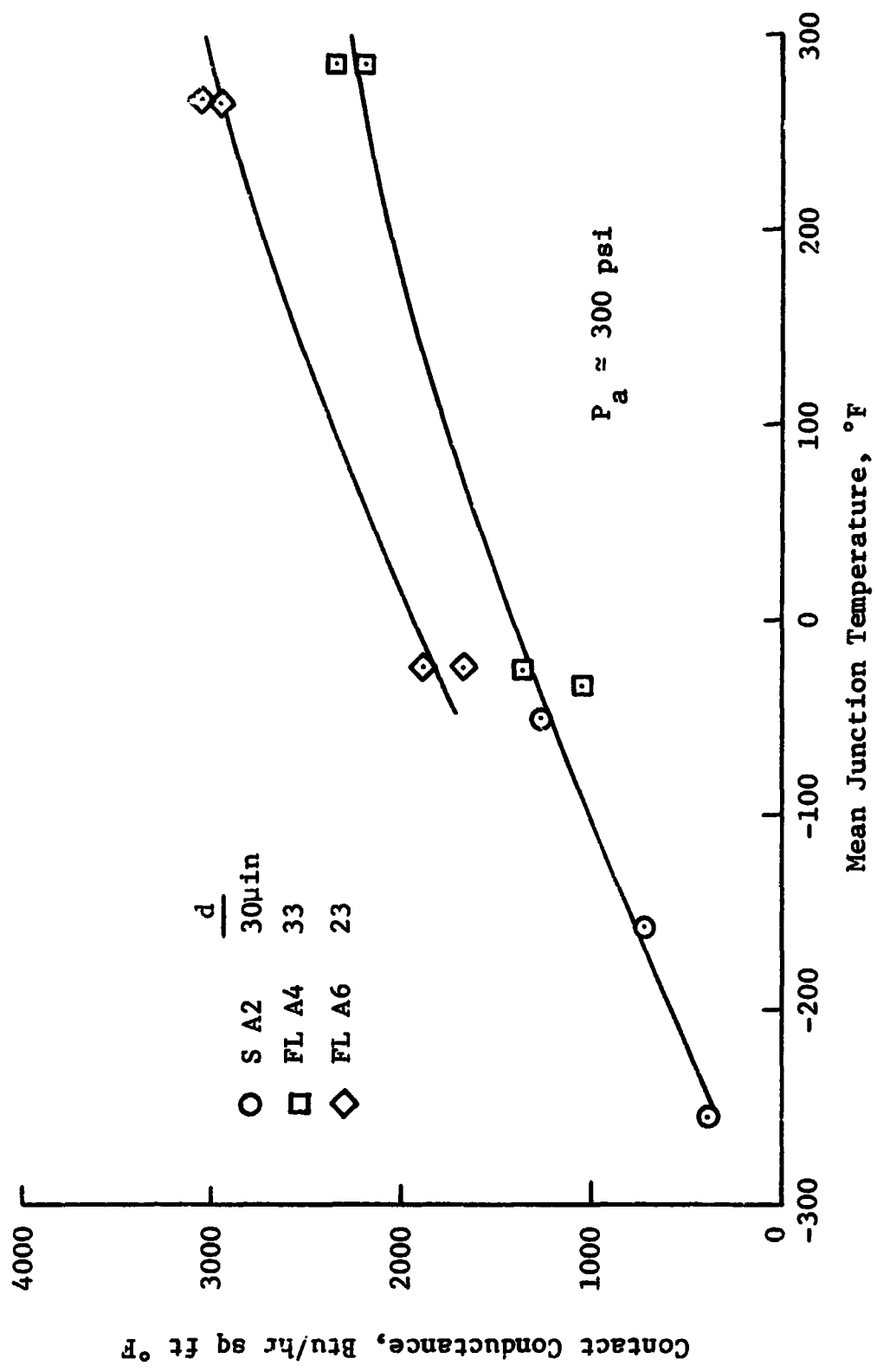
Figure 2-12. Variation of Contact Conductance with Mean Junction
Temperature at Constant Interface Pressure.
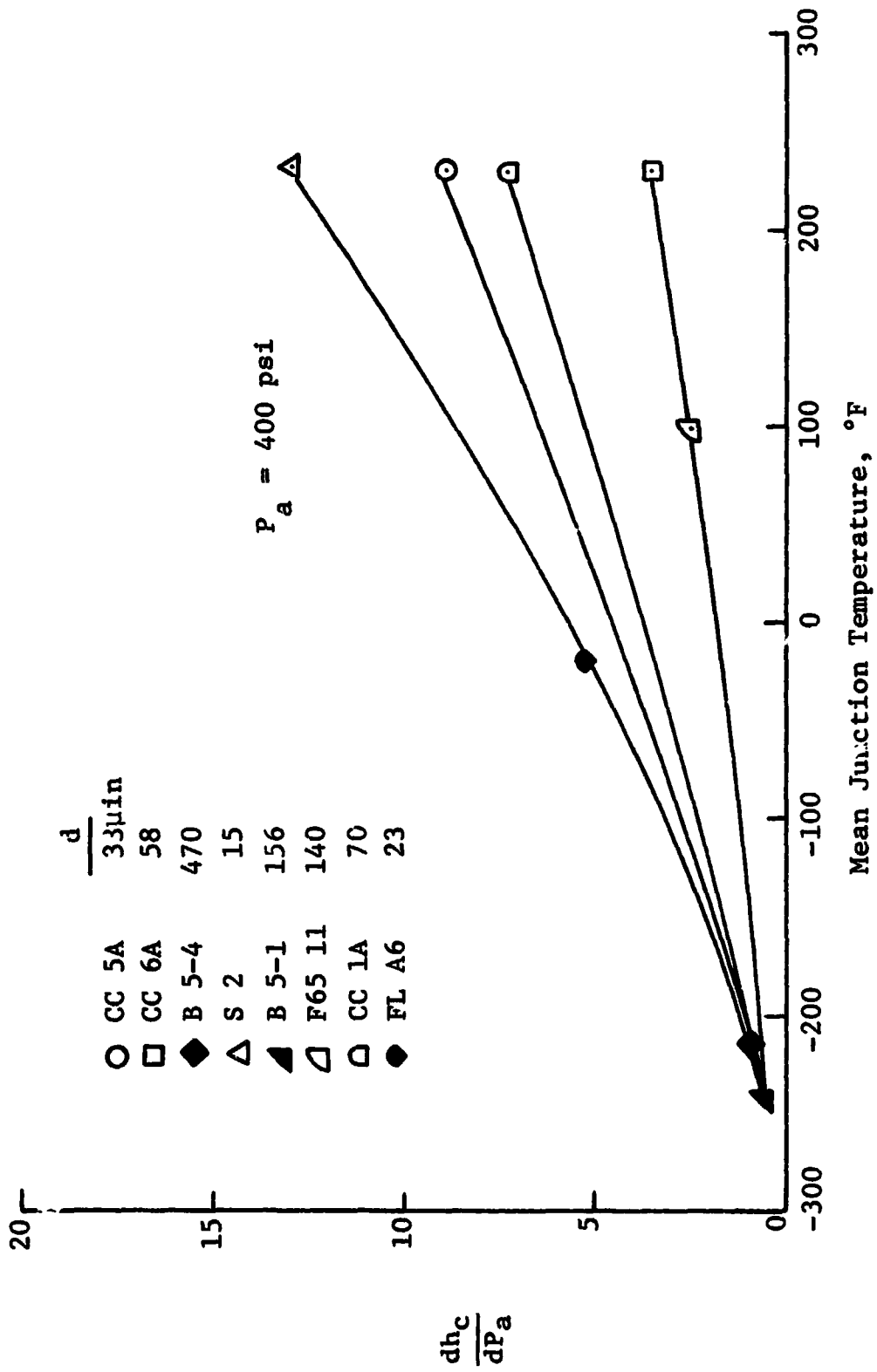
Figure 2-13. Variation of dh_c/dP_a with Mean Junction Temperature at Constant Pressure.

surfaces yield a very small change in conductance, as shown in

Figure 2-14. The derivative of conductance with respect to pressure,

compared with the surface parameter, is shown in Figure 2-15 for

several sets of data. As the surfaces become smooth, the slope

approaches infinity, and as the surfaces become rough, the slope

approaches zero.

Acceptable Published Experimental Data

The experimental data of the investigators listed in Table 2-1

have been reviewed. Of the data presented by these investigators,

only the bare junction results of aluminum, stainless steel, brass,

and magnesium were analyzed. In this section, the experimental data

are discussed, indicating the reasons for eliminating certain runs

and the values selected to complete the analysis of other runs. The

run numbers of the data that were selected are given in Table 2-2,

and the data are listed in Appendix A.

Bloom [13] has done extensive work at low temperatures using

aluminum 7075 test specimens. Only data obtained in ascending order

of pressure with at least four points in series were used in this

analysis, since some scatter existed in the data obtained at random

pressures. Data are listed by figure number in Bloom's report. The

thermal conductivity, coefficient of thermal expansion, and modulus

of elasticity were not specified; therefore, suitable values were

selected from the literature [2, 12, 30]. The data of runs 5-3 and

5-6 were not used because they were not consistent with other data

given by Bloom. The data on 5-3 were obtained using oil
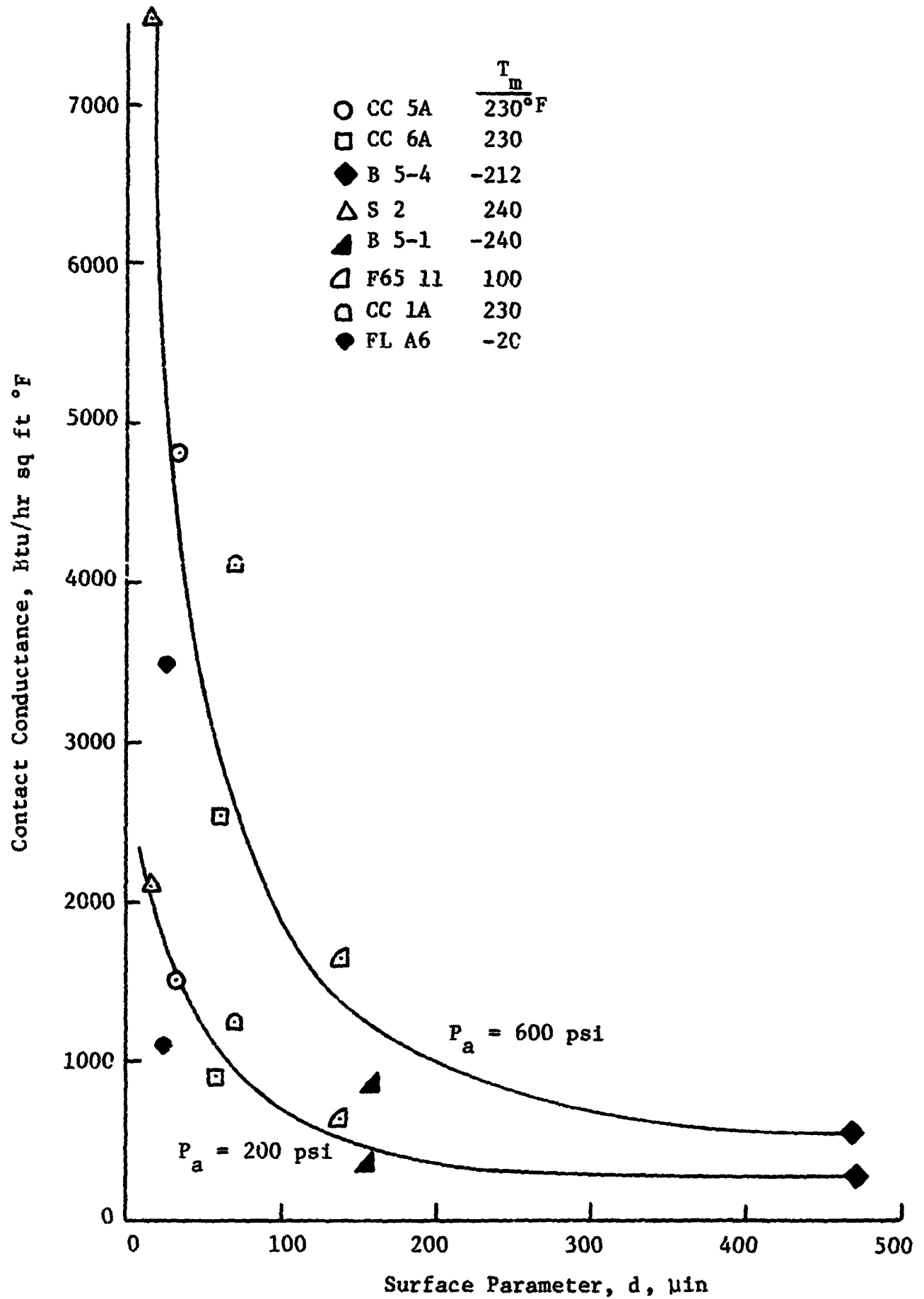
Figure 2-14. Variation of Contact Conductance with the Surface Parameter at Constant Pressure.
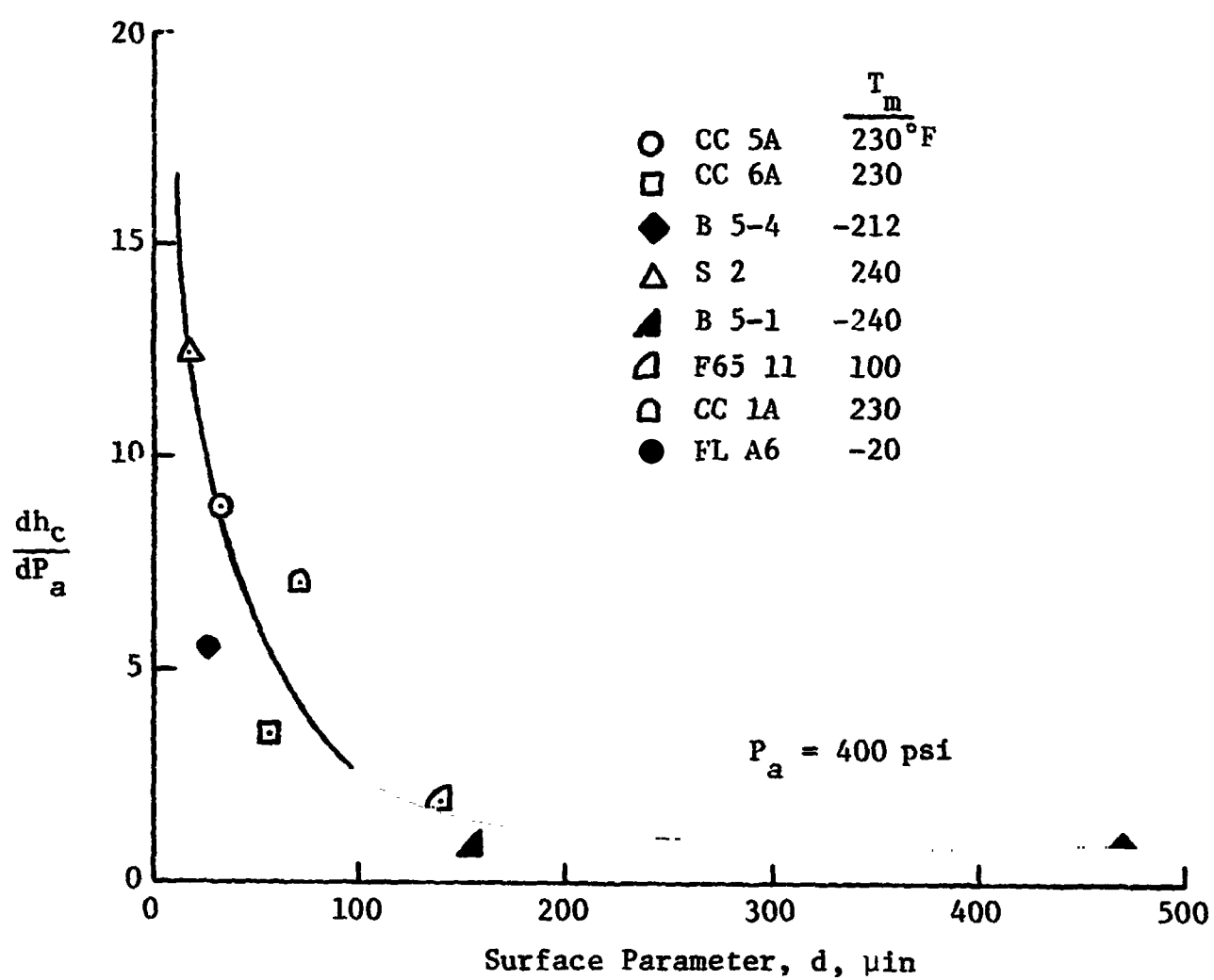
Figure 2-15. Variation of dh_c/dP_a with the Surface Parameter.

TABLE 2-2

PUBLISHED EXPERIMENTAL DATA

USED IN THE PRESENT ANALYSIS

Investigator	Code	Data Runs
Bloom [13]	B	5-1, 5-2, 5-4, 5-5, 5-7
Clausing & Chao [20]	CC	1A, 2A, 5A, 6A, 7A; 3S; 1B, 2B, 3B, 4B; 1M, 2M, 3M
Cunnington [22]	CN	5, 6, 7
Fletcher, et al [33]	FL	A2, A4, A6, A8
Fried [35, 36, 37]	FR	65:1-6, 11-17, 134-41; 66:4-12, 31-6, 57-66, 88-92
Hargadon [43]	H	2
Smuda, et al [69, 70]	S	2, 3, 4; A2

as an interstitial fluid. The surfaces for the bare junction test, then, may have been slightly contaminated, causing larger conductance magnitudes than other data at similar conditions. In the case of run 5-6, it was stated that air was entrapped between the surfaces. The remainder of the aluminum data were consistent with each other as well as with the published data of other investigators.

Clausing and Chao [20] have presented experimental conductance data for brass, aluminum, stainless steel, and magnesium and have included most of the pertinent material properties and test conditions. Values for the coefficient of thermal expansion were selected from the literature [2, 5, 26, 79]. With a few exceptions, the experimental data were consistent with each other. Aluminum runs 3A and 4A exhibited considerably lower conductance magnitudes than their stated surface parameters would suggest. Clausing indicated, however, that numerous large surface scratches often present were overlooked when measuring the surface parameters. The conductance curves for runs 1S and 2S indicated larger slopes than data of other investigators. Run 3S, however, was consistent with other published data. The magnesium data included one run with surfaces which were visibly oxidized (run 1M).

Cunnington [22] has presented limited data for aluminum and magnesium. These data were not tabulated, so conductance values had to be extracted from curves and are approximate at best. Modulus of elasticity and coefficient of thermal expansion were not given; hence values were selected from the literature [2, 26]. The surface characteristics given resulted in conductance magnitudes which were

not consistent with other published data. These data could be adjusted, however, by changing the surface parameter to allow better correlation with the published data.

Fletcher, et al [33] have given experimental data for aluminum 2024. All of the necessary properties and test conditions were available for data analysis. These data are satisfactory, except for a few isolated data points.

Fried [35, 36, 37] has published a large amount of experimental data with a wide variation in test materials. The results presented in his first report [35] were not treated since insufficient surface characteristics were given. The data considered are referred to by year and run number. The mean junction temperature, modulus of elasticity, and coefficient of thermal expansion were not included in any of the reports. It was possible, however, to deduce a value for the mean junction temperature, since the average temperature of each specimen was given. Based on this information, the material properties could be obtained from the literature [2, 5, 26, 79].

Data obtained using an aluminum specimen that was annealed during testing were not considered since the exact value of conductivity was not known (runs 65:31-36, 66-70). Some data runs were not consistent with other data of the same investigation nor with other published data (runs 65:103-0, 149-52; 66:231-9). Other data runs contained isolated points which deviated from the curve by factors of two or more. These data points were discarded as questionable; however, the remainder of the data in those runs were used (runs

65:134-41; 66:31-6, 57-66). Surface characteristics for several surfaces were given as measured by an optical flat, which increases the possibility of error. Some of these data, however, could be corrected by adjusting the surface parameter for one data point to a value comparable to other published data, and noting that the remainder of the data would then be consistent.

Hargadon [43] presented a limited amount of data for stainless steel. These data were extracted from a curve and are therefore only approximate. Thermal conductivity and modulus of elasticity values were not given; therefore, the values were selected from the literature [79].

Smuda, et al [69, 70] presents experimental data for aluminum 2024. All of the material properties and test conditions for these data were available for analysis. These data are consistent except for a few isolated data points.

Yavanovich [84] presented data for aluminum, stainless steel, and magnesium. These data were obtained for surface finishes with a machined geometric pattern, hence, are not applicable to this analysis.

Of the investigators reviewed, the experimental techniques and results of some investigations appear to be more thorough or better than others. The works of Bloom, Clausing and Chao, Fletcher, et al, Fried, and Smuda, et al have generally resulted in consistent, usable data.

Results of Data Analysis

The trends suggested by this analysis may be enumerated as follows:

1) The conductance should increase toward infinity in the limit as pressure becomes large, and toward zero or a small finite value as pressure tends toward zero (Figure 2-10). When dh/dP_a curves are extrapolated to zero pressure (Figure 2-11) and graphically integrated, the resultant value of conductance generally approaches some finite value as pressure becomes small. This may be partially explained as the result of the more pronounced effects of radiation as the energy transfer due to conduction is decreased.

2) The derivative of conductance with respect to pressure should increase toward infinity in the limit as pressure becomes large, and toward a small finite value as pressure becomes zero (Figure 2-11).

3) The conductance should increase as the mean junction temperature increases (Figure 2-12).

4) The derivative of conductance with respect to pressure should increase as temperature increases (Figure 2-13).

5) The conductance, as well as the derivative of conductance with respect to pressure, should be greater for smoother surfaces than for rougher surfaces (Figures 2-14 and 2-15).

III. COMPARISON OF THEORIES

The theories presented in the first section of this chapter were analyzed in several ways. Some assumptions were first made to reduce the equations to similar conditions. In this section, the theories

are compared with each other and with published data obtained at vacuum conditions. Finally, the results of this analysis and comparison with experimental data are used to show what trends and characteristics should be expected of a theory for the prediction of contact conductance.

Application in Vacuum Environments

Considerable interest has been focused on contact resistance problems occurring in aerospace applications. Most of the recent thermal contact conductance experimental investigations have been conducted at vacuum conditions. The usefulness of the foregoing theoretical analyses, therefore, will be examined at these conditions. The effect of convection is avoided in a vacuum environment, thereby enabling a more thorough experimental study of the contact problem. Thus, in the discussion which follows, the gas or fluid conduction terms will be eliminated from the conductance equations and a comparison made between the solid conductance expressions.

The expressions for the solid conductance taken from each author are given as follows:

Cetinkale and Fishenden [equation (2-7)]:

$$h_c = \frac{a \, k_h}{b^2 \, \text{Tan}^{-1} \, [\frac{r_d - a}{a}]}$$

Tachibana [equation (2-11)]:

$$h_c = \frac{a^2 k_h}{b^2 \, (\delta_T + \delta_\ell)}$$

Fenech and Rohsenow [equation (2-13)]:

$$h_c = \frac{\dfrac{\alpha}{1 - \alpha}}{\dfrac{\delta_1}{k_1} + \dfrac{\delta_2}{k_2} + (\dfrac{1}{k_1} + \dfrac{1}{k_2})\dfrac{\sqrt{\alpha\,b}}{2.4}}$$

Laming [equation (2-15)]:

$$h_c = \frac{2\,k_h}{(1 - f)}\left(\frac{\sin\theta\,P}{\pi\,\lambda_1\lambda_2\,H_M}\right)^{1/2}$$

Clausing and Chao [equation (2-19)]:

$$h_c = \frac{2\,X\,k_h}{\pi b\,g(X)} \qquad X = 1.285\left[\frac{P_a}{E}\frac{b}{\delta_{cc}}\right]^{1/3} \qquad X < 0.65.$$

In order to reduce the foregoing equations to a more useful form, it is necessary to consider the physical contact situation. The area of the total solid-to-solid contact may be written as:

$$A_c = n\,\pi\,a^2$$

The loads which may be supported by the small contact spots in the elastic deformation range are very small. Thus, it may be assumed that the pressure at each contact spot would be equal to the yield pressure of the softest contact surface. The yield pressure, however, is nearly equal to the Meyer hardness, and the load on the contact in terms of known quantities may be written as:

$$F = H_M A_c = P_a A_a$$

The contact area ratio may then be written in terms of the apparent interface pressure. The contact area ratio would vary as P_a if the simplifying assumptions concerning the Meyer hardness are

considered valid [17, 58]. Should the contact surfaces be very

smooth or the contact subjected to very low loads, the deformation

could be elastic. This would permit use of the Hertz equation for

elastic deformation [77], and the contact area ratio would be

proportional to $P_a^{2/3}$ [17].

There are, however, a number of factors involved in actually

expressing the solid-solid contact area as a function of compres-

sive load. A substitution for the contact area ratio often made is:

$$\alpha = \frac{A_c}{A} = \frac{P_a}{\xi \, H_D} \qquad (2-23)$$

where ξ is an empirical deformation or accommodation coefficient.

This accommodation coefficient would be unity if full plastic flow

existed and no additional factors such as work-hardening or surface

films were present. The hardness number used should be either the

Vickers or Meyers value since these numbers are defined in terms

of the projected area of indentation, i.e., the area available for

heat transfer [58]. Generally, the value of the accommodation

coefficient is less than unity and is a rather complex function of

many factors. Providing the appropriate function is selected for

ξ , equation (2-23) will be valid for both elastic and non-elastic

surface deformation.

The relationship involving pressure and hardness given above

(or a similar function of pressure developed by the investigators)

was combined with the conductance expression at vacuum conditions

to yield the following equations for similar surfaces:

Cetinkale and Fishenden:

$$h_c = \frac{k_h \, P_a}{\xi \, H_M \, a \, \text{Tan}^{-1} \, [\frac{r_d - a}{a}]} \qquad (2\text{-}24)$$

Tachibana:

$$h_c = \frac{k_h \, P_a}{(\delta_T + \delta_\ell) \, \xi \, H_B} \qquad (2\text{-}25)$$

Fenech and Rohsenow:

$$h_c = \frac{k_h \, P_a}{(2\delta_{Fn} + 0.833a) \xi \, H_M} \qquad (2\text{-}26)$$

Laming:

$$h_c = \frac{2 \, k_h}{(1 - f)} \, (\frac{\text{Sin} \, \theta \, P_a}{\pi \, \lambda_1 \lambda_2 \, H_M})^{1/2} \qquad (2\text{-}27)$$

Clausing and Chao:

$$h_c = \frac{0.8175 \, k_h \, [\frac{P_a}{E} \, \frac{b}{\delta_{CC}}]^{1/3}}{b - 1.811 \, b \, [\frac{P_a}{E} \cdot \frac{b}{\delta_{CC}}]^{1/3} + 0.6275 \, b \, [\frac{P_a}{E} \, \frac{b}{\delta_{CC}}] \ldots} \qquad (2\text{-}28)$$

It has generally been assumed that the accommodation coefficients are not functions of pressure.

Each of the preceding expressions, equations (2-24) through (2-28), is a function of pressure to some degree. It would be instructive, then, to compare the behavior of these expressions at each of the limiting pressures, as well as the mid-range values shown in Figure 2-10. Analysis of equations (2-24), (2-25), and (2-26) appear to indicate a constant slope, dh_c/dP, however, the possible variation of δ or ξ with pressure could be included to provide better agreement

with experiment. Without this consideration the relationship of
Laming gives the conductance as dependent on the square rc t of
pressure whereas the expression of Clausing results in the conduc-
tance increasing much more rapidly as pressure increases. At the
limit of zero pressure, all of the above expressions yield a con-
ductance cf zero. As load pressure increases all equations result
in an increasing value of conductance; however, the Clausing equation
approaches a large value more rapidly than the others, and the slope
also increases with pressure. The Laming equation approaches a
large value less rapidly than the other equations considered in the
comparison.

The conductance is not only a function of apparent pressure but
also of the mean junction temperature -- though temperature does not
appear directly in the above expressions. The temperature effect
shows up as a variation of the thermophysical properties of the test
material. Thermal conductivity is one of the properties which is
highly temperature dependent and is included in all of the above
expressions. It may be seen that the conductance varies linearly
with thermal conductivity and thus indirectly with temperature.
As the temperature increases, the conductance increases, depending
upon the thermal conductivity-temperature relationship (Figure B-3).
Also, the contact area ratio varies inversely with the material
hardness or modulus of elasticity. As temperature increases the
modulus of elasticity for metals decreases (Figure B-4), yielding
a larger contact area ratio.

Another important variable affecting the contact conductance is the surface condition or effective gap thickness. The surface condition is generally a function of the roughness and flatness deviation and is represented in the above equations by several different parameters. The expressions of Cetinkale and Laming are difficult to analyze since no definite terms are directly related to the effective gap thickness. The surface wavelength and angle of orientation are included in Laming's expression but are not comparable to the surface finish parameters of roughness and waviness. The expressions of Tachibana, Fenech, and Clausing do represent the surface by an equivalent gap thickness between surfaces. Equations (2-25), (2-26) and (2-28) indicate that the conductance is inversely proportional to an equivalent gap thickness. Examining the equations of Tachibana, Fenech, and Clausing for very smooth surfaces, the expressions yield extremely large conductance values (or very low contact resistance). For perfectly flat surfaces, the expressions become infinite. These trends are also exhibited by the experimental data. For the case of very rough surfaces, these expressions yield quite low conductance values (or high contact resistance), again in accordance with the data.

Desirable Traits for Conductance Prediction Equations

Of the theoretical analyses presented, the expressions of Tachibana, Fenech, and Clausing seem to be the most useful at vacuum conditions. In particular, the relationships of Tachibana and Fenech show the most similarity, but do not show many of the expected trends.

If the accommodation coefficient in the Fenech and Tachibana equations were permitted to be a function of pressure, surface conditions, and temperature, perhaps closer agreement between data and theories could be expected.* The derivatives of conductance with respect to pressure and effective gap thickness would behave satisfactorily if the accommodation coefficient were not a constant. The Clausing equation more adequately represents the magnitudes and trends expected at the limiting cases; however, the limitation of $X = 0.65$ imposed on the equation prevents it from accurate magnitude prediction, as will be shown in Chapter IV.

In summary, an equation for thermal contact conductance should:

1) Reduce to an expression of the form

$$R_c = \frac{1}{Bka}$$

in the limiting case of a single contact;

2) Predict an increase in conductance with apparent pressure as a function of $P^n (n > 1)$. The derivative of conductance with respect to pressure should tend toward a small finite value as pressure approaches zero, and as pressure increases, the slope should become infinite;

3) Predict a relatively high conductance for smooth surfaces and a low conductance for rough surfaces. The derivative of conductance with respect to the surface parameter should indicate that the slope increases as the surface approaches a perfectly flat, polished condition, and as the surface becomes rougher, the slope should approach zero;

4) Predict an increase in conductance with increased mean junction temperature.

---

*A modified accommodation coefficient including these variables is developed in Chapter IV.

CHAPTER III

EXPERIMENTAL INVESTIGATION

An experimental investigation was conducted to obtain contact
resistance data in a vacuum environment. Data were obtained for
aluminum, stainless steel, brass, and magnesium contacts with four
different types of surface finishes. Apparent interface pressures
ranged from 25 to 800 psi, and mean junction temperatures from -80°F
to 320°F. The experimental apparatus is described in the first sec-
tion of this chapter. Experimental data from the present investiga-
tion are analyzed in the remaining section of this chapter.

I. EXPERIMENTAL APPARATUS

The experimental apparatus used to investigate thermal contact
conductance was made flexible enough to subject the test specimens
to various environmental and physical conditions. The instrumenta-
tion incorporated in the apparatus was made sophisticated enough to
insure accurate measurement of the test conditions. General speci-
fications for the experimental apparatus were based on the experience
and recommendations of Blum [14], Clausing and Chao [19,20], Fried
[34,35,36,37], Stubstad [72,73], and others [38,48,50]. A photo-
graph of the thermal contact resistance test facility is shown in
Figure 3-1. A more detailed explanation of the construction and
operation of this test facility is given by Abbott [1] and Smuda,
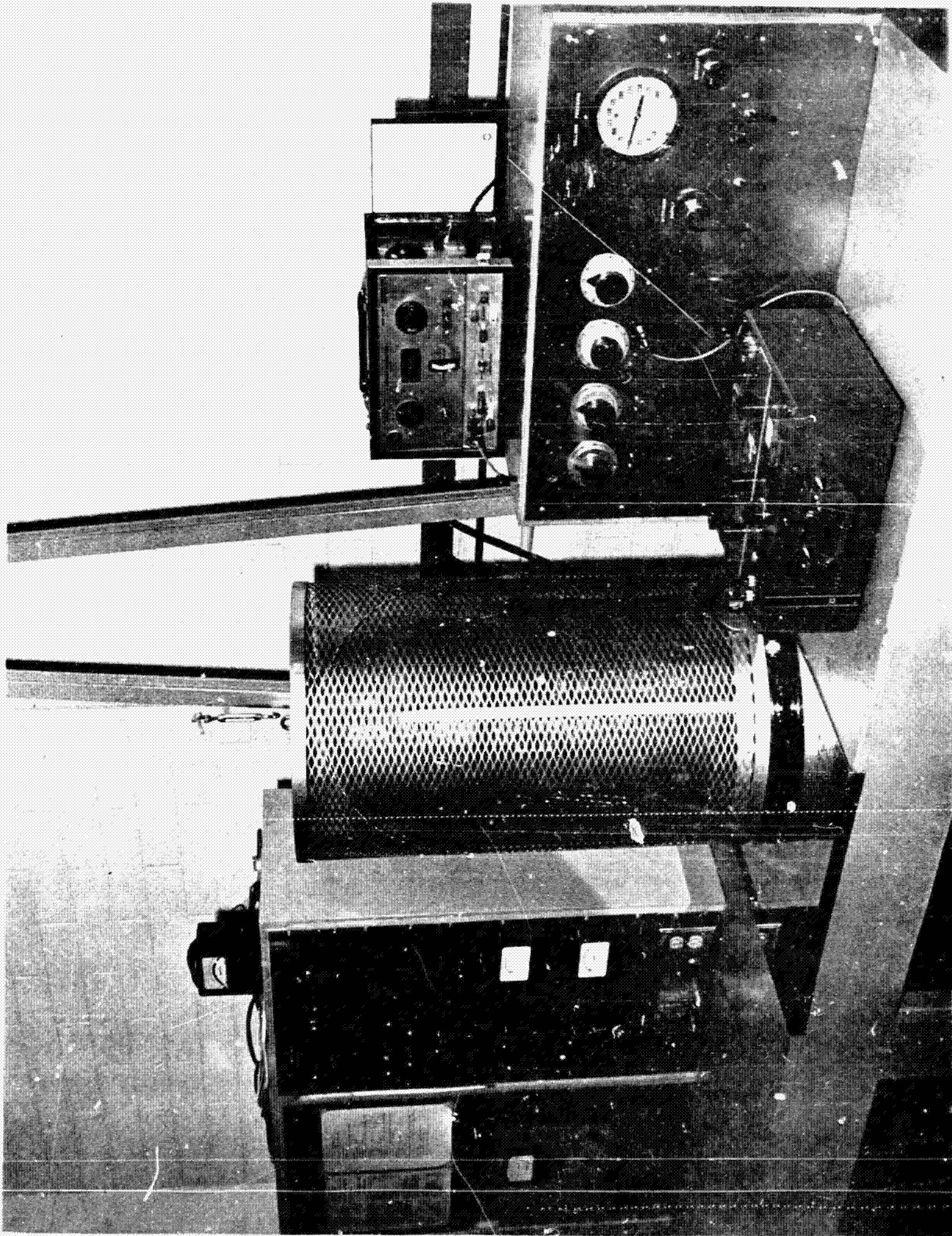
Figure 5-1. Photograph of the Thermal Contact Resistance Test Facility.

et al [69].

Vacuum System

A vacuum system was incorporated into the experimental apparatus for two primary reasons. First, the interstitial fluid present in an interface transfers heat across the junction by convection. It was desirable to eliminate all modes of energy transfer but conduction. Second, contact conductance is of vital concern to the space industry because it has a substantial effect on the heat transfer in, and the heat dissipation from space vehicles. Hence, it was necessary to simulate a space environment as nearly as possible by using a vacuum chamber for the investigation of interface conductance.

Ascoli and Germagnoli [8], Shlykov and Ganin [67], and Stubstad [72] have shown that the convection or conductivity effect of gas begins to decrease at approximately 70 Torr and measurably disappears at 10^{-1} Torr. Other investigators have stated that a vacuum in the range of 10^{-4} Torr is sufficient to negate the effect of interstitial fluids. Since a small pressure gradient exists in any vacuum facility [11, 24, 63], a system capable of operating in the range of 10^{-5} Torr or lower was constructed.

This vacuum system was composed of a bell jar and base plate, an oil diffusion pump, a mechanical forepump, a chevron cooling baffle, high vacuum valves, and appropriate vacuum measuring devices, as recommended by Dushman [27], Lafferty [54], and others. Details of the vacuum system have been given by Smuda, et al [69]. Operation of the system generally yielded a chamber pressure on the order of

1×10^{-5} Torr after two hours of operation, and as low as 1×10^{-6} Torr after twelve hours of operation.

Test Specimens

Design of the test specimens was a major consideration for several reasons. First, their size and shape dictated the design criteria for most of the other test section components. Second, the technique used to evaluate the thermal contact conductance required uniform heat flux above and below the interfaces. Finally, it was desirable to obtain as much data as possible for each specimen test, since the time required to reach steady state conditions varied from three to twelve hours or more.

A basic cylindrical configuration was specified and fabricated in three pieces.* These components were installed as a vertical column under axial load with the contacting surfaces located at two stations along the column. The completed specimen system was located in the vacuum chamber as shown in Figure 3-2.

Apparatus Instrumentation

The validity of the results obtained by experimentation depends greatly upon the accuracy of the instrumentation used. Instrumentation is required for the measurement of the heat flux (i.e., the electrical power input), the force applied to the interface, temperatures, and other variables.

---

* Detailed drawings are given in Appendix B.
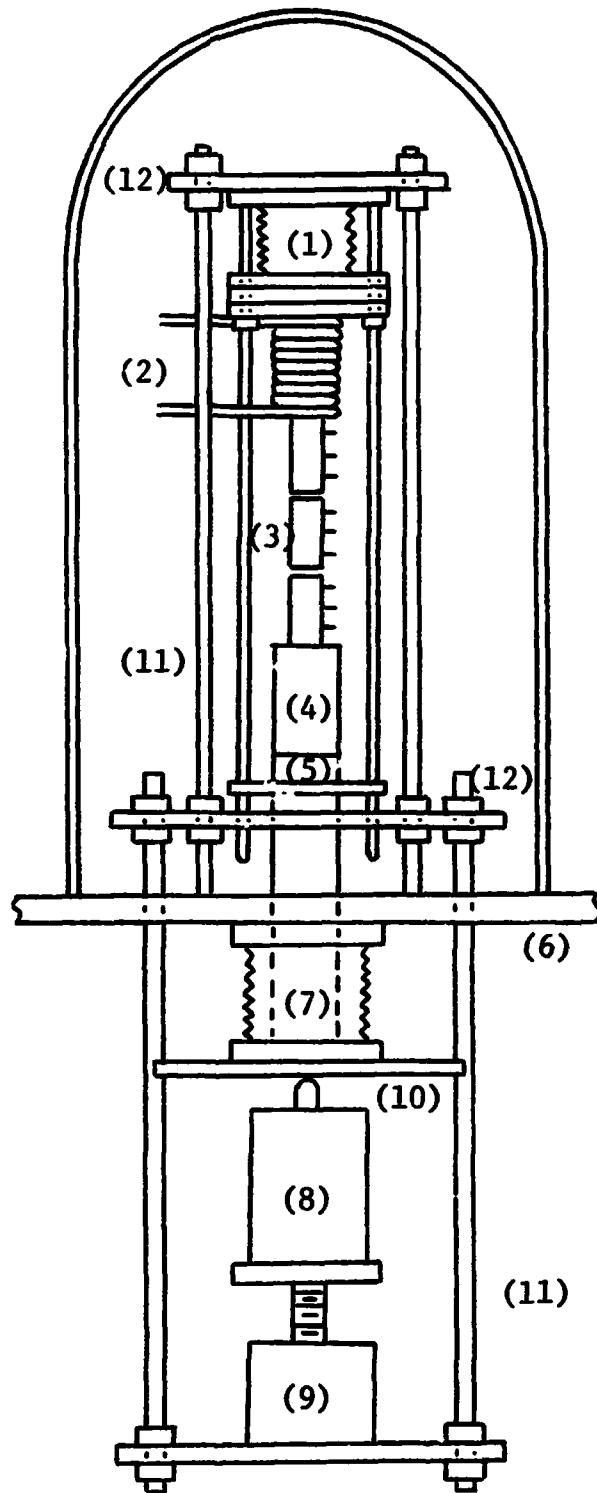
(1)	Nitrogen Load Bellows	(7)	Passthrough Bellows
(2)	Heat Sink	(8)	Load Cell
(3)	Test Specimens	(9)	Mechanical Screw-Jack
(4)	Heat Source	(10)	Guide Plate
(5)	Guard Heater	(11)	Support Rods
(6)	Base Plate	(12)	Support Plate

Figure 3-2. Schematic Diagram of the Experimental Apparatus.

In light of the requirements established by the heat source location, the temperature criteria, and the dimensions of the specimens, a 300 watt Acrawatt strap type circumferential heater was used as the source. The heat source was insulated and surrounded by aluminum foil to reduce radial heat losses. The heat sink was constructed from a cylindrical copper block, drilled and tapped to accept the threaded end of the metal test specimen. A copper cooling coil was silver soldered to the outside surface of the copper cylinder. Water and liquid nitrogen were used to provide a wide variation in the test temperatures.

The source end of the specimen with band heater was insulated axially and radially to minimize the heat losses. To shield other components and further reduce the losses, an aluminum radiation shield was located about one inch away from the insulated heater. An aluminum cap was placed on top of the cylinder formed by this outer shield to prevent radiation to the instrumented section of the specimen. The axial insulator was composed of alternating layers of one-sixteenth-inch aluminum sheeting and asbestos board insulating material. Thermocouples were located in the aluminum disks for monitoring the axial temperature gradient.

For better control of the heat losses from the source, an axial guard heater was installed below the insulator. The guard heater provided a positive means of controlling the conduction heat losses along the specimen by accurate control of the temperatures on each side of the axial insulator. This temperature control reduced the time necessary for establishing steady state conditions.

A regulated d.c. voltage power supply was used to provide power for the main heater [70]. Shunts were used to permit current and voltage measurement on a millivolt potentiometer, thus increasing the resolution of the measurements.

The apparent mechanical pressure applied to an interface has a major influence on the resulting thermal contact conductance. For load application to the test specimens, a high pressure nitrogen gas bellows chamber was constructed as an integral part of the test apparatus. The effect of load pressure was determined by varying the nitrogen gas pressure in the bellows chamber. In the present sense, apparent interface pressure is defined as the load force divided by the cross-sectional area of the cylindrical test specimens. The load force was determined from a compression load cell located in the specimen column, and a strain indicator.

Specimen Preparation

The finish of bare junction surfaces has a strong effect on the interface conductance [13, 57, 84, 85]. Since one of the objectives of this investigation was to obtain experimental data for the development of a semi-empirical equation for the prediction of contact conductance, it was desirable that a wide range of surface finishes be used. Three different surface finishes were therefore selected for each test material; one as smooth as could reasonably be obtained, a second moderately rough, and a third extremely rough.

All surfaces were finished on a lathe, lapped with a fine lapping compound, as described by Smuda, et al [69], and polished

on emory paper. The moderately rough surfaces were finished by sanding the previously polished surfaces with "3M" Garnett paper (grade 7WCE2), yielding a surface with scratches of random orientation. An extremely rough set of surfaces was made by peening the polished surfaces with a small ball-peen hammer. These three types of surfaces represented a wide range of surface finish.

The surface finish is usually described by the rms, roughness and the waviness or flatness deviation [4]. These are two separate and distinct characteristics. Surface roughness is considered to be a measure of the finishing process. On the other hand, surface waviness is considered to be the variations in the overall surface configuration that result from such things as warping or periodic oscillations in the finishing process.

The specimen surface measurements for this investigation were made using both a Bendix Micrometrical Proficorder and Profilometer. Since the results given by Proficorders and Profilometers represent only one trace across the surface, several traces were made on each type of surface to assure that the measured flatness deviation and roughness would be representative of the surface. At least one trace was then made for each specimen surface used in the investigation. The resulting flatness deviation and roughness for the test surfaces are listed in Appendix B.

Temperature Measurement

The accuracy of the determination of interface contact resistance

is greatly dependent on the accuracy of the temperature measurements. Hence, the precision of the thermocouples and thermocouple readout system were of major importance in the experimental program. Number 30 gage copper-constantan thermocouples were selected since they were easy to fabricate and dependable over the range of temperatures from -300 to 750°F. These thermocouples exhibited an accuracy of ±0.5°F when calibrated [69]. The thermocouple outputs were measured with a Leeds and Northrup Model 8686 millivolt potentiometer. The uncertainty of the potentiometer was five microvolts, which represents 0.2°F for the copper-constantan thermocouples through the range of temperatures considered [66].

Abbott [1] tried several techniques for the fabrication of thermocouples and found that the best results were obtained when the bare parts of the wires were twisted together tightly for about one-fourth of an inch, the joint silver-soldered, and the excess wire cut off to the point where the wires first made contact. This procedure was used for the construction of all thermocouples used in this investigation. After the thermocouples were fabricated, they were checked for continuity.

To measure the center-line temperatures of the specimen, thermocouples were mounted in holes 0.046 inches in diameter and 0.531 inches deep. The leads were wrapped once around the specimen to minimize heat losses through the wire [10, 23, 49]. The thermocouples were held in position by packing them in the holes with aluminum powder. A considerable amount of care was taken to insure that the thermocouple and insulation were not damaged during this

operation. The resistance of each thermocouple was checked before
and after installation. If the resistance varied between the read-
ings, it was assumed that damage had occurred and the thermocouple
was then replaced.

The surface temperatures were measured by placing thermocouples
in holes 0.046 inches in diameter and 0.062 inches deep, diametric-
ally opposed to the middle center-line hole in each specimen. The
leads were wrapped twice around the specimen for the purpose of
minimizing heat losses and for support of the thermocouple lead wire.

Thermal Conductivity

Since the thermal conductivity of aluminum 2024 varies consider-
ably with heat treatment, experimental conductivity data were obtained
for the aluminum used in this investigation to affirm the use of
published values [69]. The thermal conductivities for the other
test materials do not change appreciably with heat treatment; there-
fore handbook values were used. The conductivities for aluminum 2024,
brass alloy 271, magnesium AZ31B, and stainless steel 304 used in
this investigation are given in Appendix B.

Development Tests

The effects produced by the installation of radiation shields,
guard heaters, and insulation, by polishing the surface of the
specimen. and by various heater installation techniques were
evaluated experimentally in a series of tests conducted by Abbott
[1]. The tests were selected so that the results could be directly

compared to indicate the relative effectiveness of each test section configuration. Clausing and Chao [20] indicated that heat losses from the test specimens were a major source of concern because such losses created a non-uniform heat flow. Hence, the reduction of surface heat losses was the principal factor considered in deciding which of the test section configurations was the most desirable.

A series of tests was performed using the experimental apparatus to determine a suitable test section configuration for the three component specimens. Several different radiation shield combinations were tested to determine which type of shield would minimize the surface heat losses and permit a more uniform temperature gradient in the test specimens. The resulting shields, composed of aluminum foil and WRP Felt, were secured around the heated specimen, and a split aluminum and mica disk was placed across the top of the lower shield to completely enclose the heated specimen without touching it. A photograph of the assembled test section is shown in Figure 3-3. Use of this test section yielded relatively uniform temperature gradients with minimum heat losses.

Test Program

To determine contact conductance values experimentally for comparison with other data, several variables had to be measured. The apparent pressure at the interface, the temperature gradients in the specimens, and the power input were measured for each steady state position. The length of time required to obtain steady state conditions ranged from two to twelve hours for each data point. A
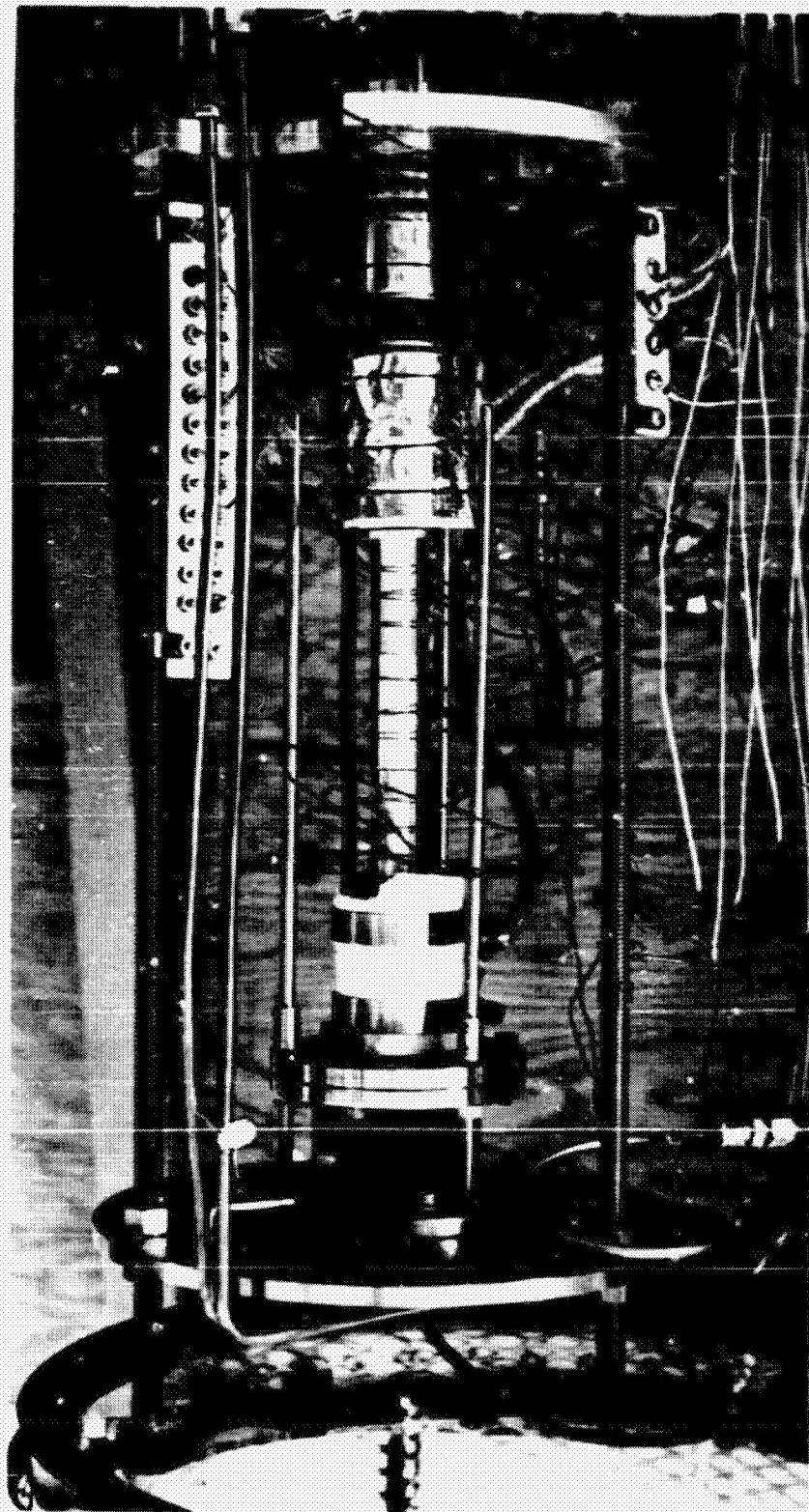
Figure 3-3. Photograph of the Assembled Test Section.

detailed explanation of the operating procedure is given by Smuda, et al [69].

The apparent interface pressure was varied from approximately 30 to 800 psi. The temperature in the center specimen was maintained at approximately 250°F when using the water coolant and 80°F when using the liquid nitrogen coolant. The power was varied as necessary to maintain the appropriate temperatures in the center specimen. The results of these tests are tabulated in Appendix B.

A heat loss calibration was made for each specimen material in order to determine the heat flux in the specimens. This value was found to compare favorably with the heat flux calculated using the thermal conductivity and temperature gradient.

II. ANALYSIS OF THE EXPERIMENTAL DATA

The experimental data of the present investigation were analyzed in the manner described in Chapter II. Both the magnitudes and trends of these data were compared with the criteria established. The results for aluminum, stainless steel, brass, and magnesium are presented here with discussion of their individual characteristics.

Aluminum

The contact conductance for annealed aluminum 2024 is shown as a function of pressure in Figure 3-4. Data for all four surfaces as well as different mean junction temperatures are given for purposes of comparison. The spread between the conductance curves is attributable to the wide range of both surface parameter (defined in
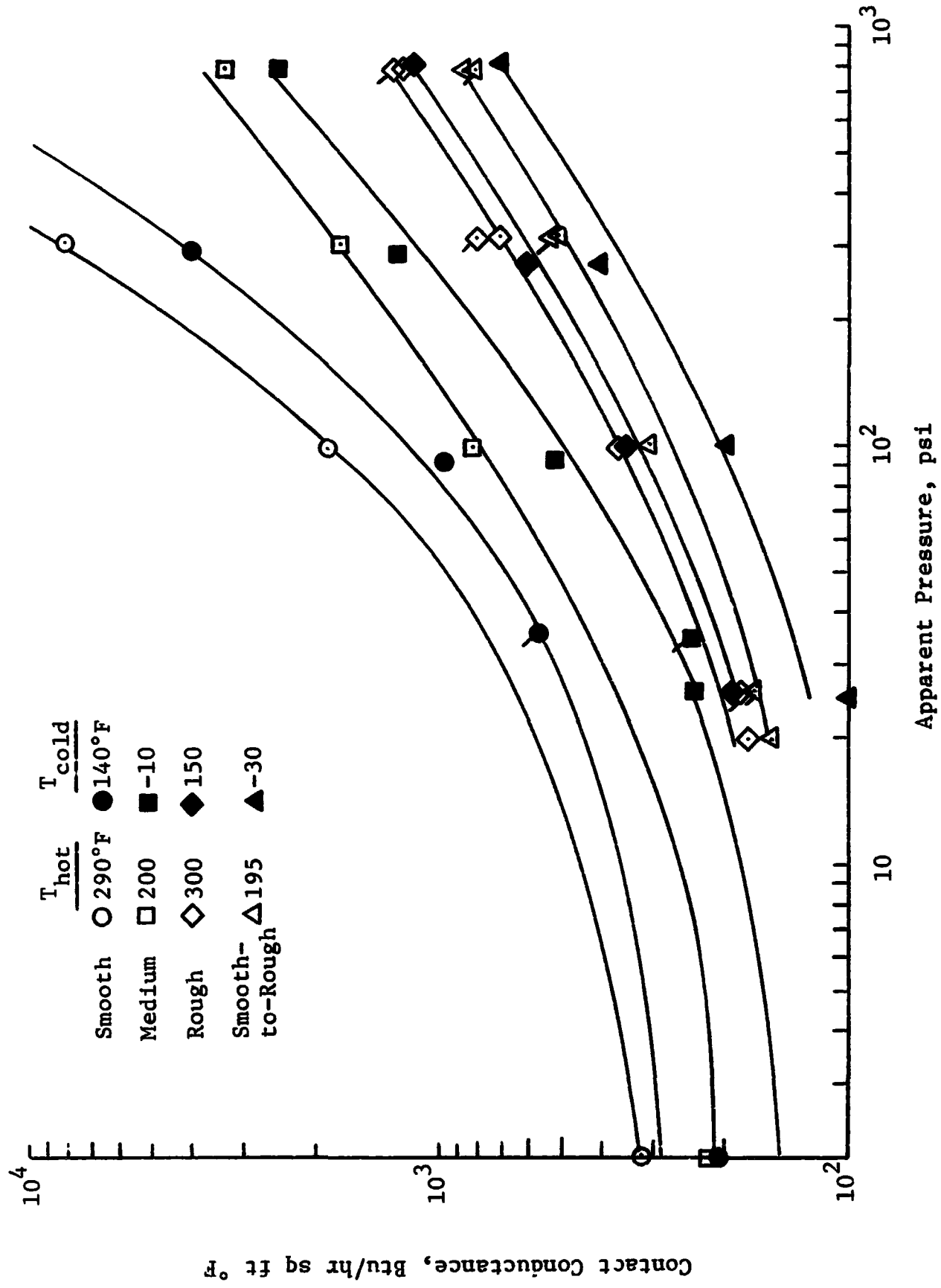
Figure 3-4. Variation of Contact Conductance with Apparent Interface Pressure for Aluminum 2024.

Chapter II) and mean junction temperature.

Several check runs were made for the aluminum data. These are noted by the flagged symbols in Figure 3-4. The manner in which these check data points were obtained is given in Appendix B. It should be noted that the check runs for the rough and smooth-to-rough surfaces were repeatable within 5 percent. The check runs for the low temperature smooth and medium surfaces were obtained at pressures different from those of the original data, in order to fill out the curve. These check data points fell within 7 percent of the curve through the original data points.

The aluminum data exhibit the trends required by the criteria of Chapter II. The conductance approaches infinity as pressure increases, and as pressure tends toward zero, the data seems to approach a finite value. Further, the effect of mean junction temperature is apparent in that for similar surface conditions, the low temperature curve is slightly lower than the high temperature curve. The variations in the distance between the curves may be explained by the variations in the range of the mean junction temperature.

The derivative of conductance with respect to apparent interface pressure (i.e., the slope of the curves in Figure 3-4) appears to increase as pressure becomes large. This increase is more rapid for the smoother than for the rougher surfaces. It may also be noted that the slope increases for increased mean junction temperature.

A majority of these aluminum data appear to be acceptable, although some scatter exists in the data for smoother surfaces. This

u..explainable scatter for smooth surfaces has also been experienced
by other investigators [19, 26].

Stainless Steel

Conductance data for stainless steel is shown as a function of
apparent interface pressure in Figure 3-5. The smooth and rough
contacts show little difference between the high and low mean junc-
tion temperature runs. The medium and smooth-to-rough contact
curves exhibit a much greater change in conductance with mean
junction temperature. These differences may be attributed to the
variation of thermal conductivity with temperature, and the magni-
tude of the mean junction temperature.

The data are relatively consistent and exhibit the trends
which would be expected. The trends of the conductance and deriva-
tives of the conductance with respect to pressure, temperature, and
surface parameter behave in the same manner as those for the aluminum
data.

The stainless steel data appear to be among the most accurate
and consistent of all the data, and satisfy the criteria established
in Chapter II.

Brass

The brass data are presented as a function of apparent interface
pressure in Figure 3-6. Like aluminum and stainless steel, the
conductance and derivatives of the conductance are consistent wit..
the criteria established in Chapter II. Note that the effect of mean
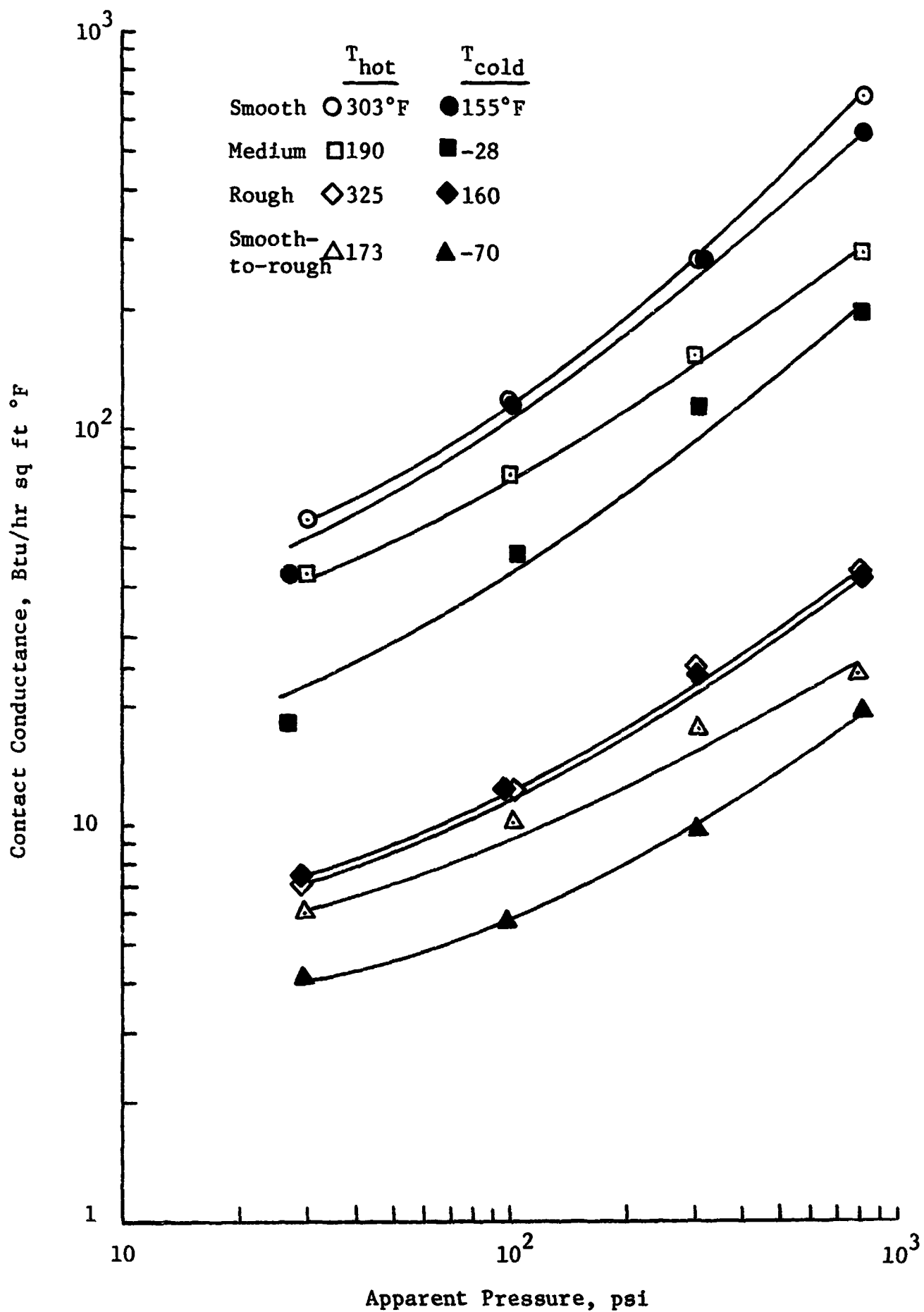
Figure 3-5. Variation of Contact Conductance with Apparent
Interface Pressure for Stainless Steel 304.
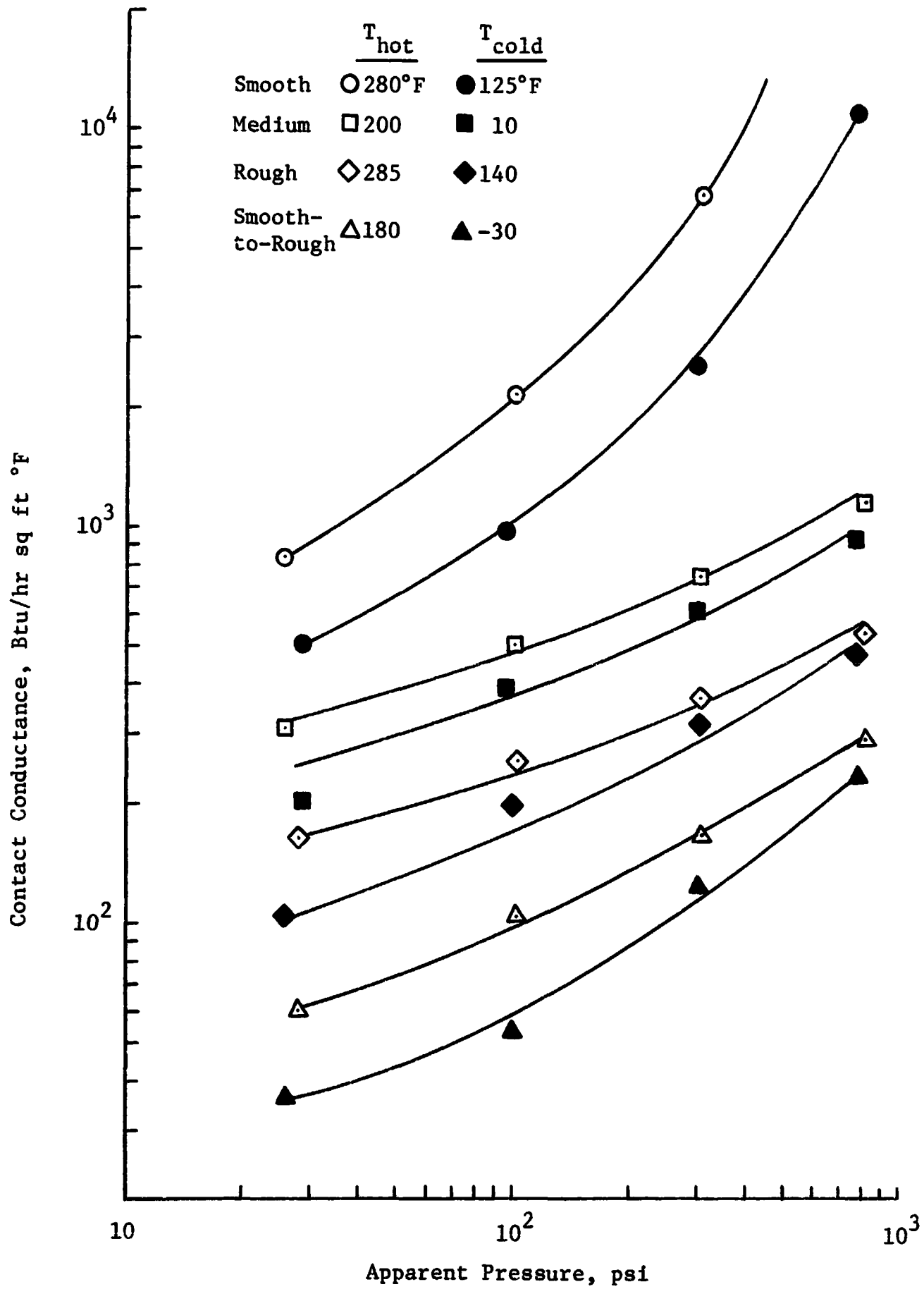
Figure 3-6. Variation of Contact Conductance with Apparent
Interface Pressure for Brass Alloy 271.

junction temperature is quite prominent. The average difference between mean junction temperature for hot and cold data of the same surface is approximately 175°F. This difference in temperature causes the spread in the curves. As expected, the smooth surface curves approach infinity more rapidly than those for the rougher surfaces; however, all curves show an increasing slope with increasing pressure.

The brass data, then, are consistent both in trend and magnitude. These data also appear to compare well with the trends of the aluminum and stainless steel data of this investigation.

Magnesium

The conductance data for magnesium AZ31B presented as a function of apparent interface pressure in Figure 3-7, are not as consistent as those for the other test materials. Prior to the experimental testing, it was noted that a slight oxide film was present on the smooth and medium surfaces. The surfaces were then polished and thoroughly cleaned, but the effect of the surface film apparently was not completely removed. The presence of a visible oxide film on magnesium surfaces was also noted by Clausing and Chao [20]. The effect of this film on their experimental data was treated in Chapter II.

The low temperature data for the smooth surface do not agree in magnitude with the high temperature data. However, the slopes of the two smooth surface curves do show good agreement. The disagreement of the smoother surface data results from a discrepancy in the temperature drop across
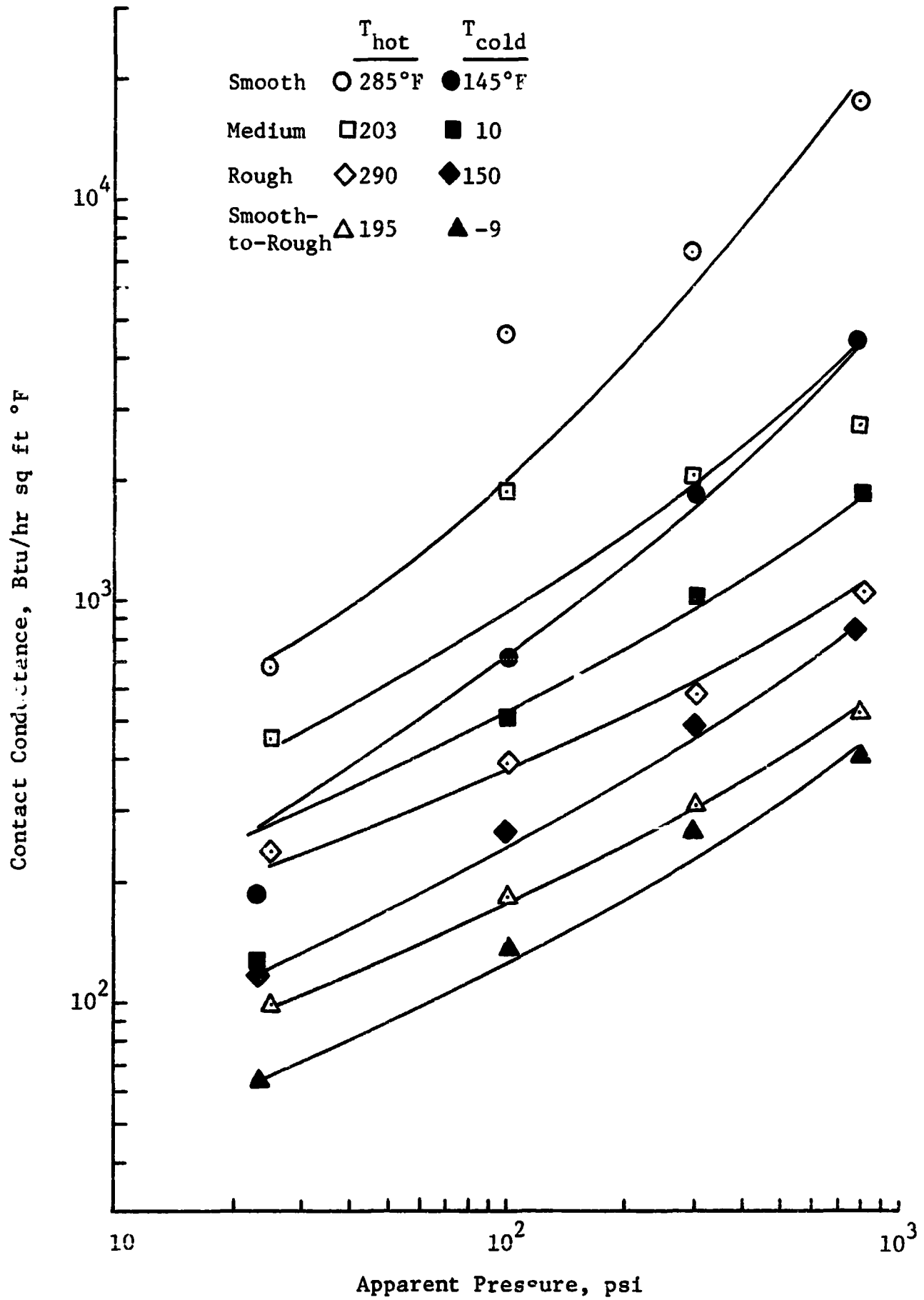
Figure 3-7. Variation of Contact Conductance with Apparent
Interface Pressure for Magnesium AZ31B.

the interface. Specific reasons for this discrepancy have not been found, although several possibiliti(es) exist. The smooth surfaces could have been contaminated, or the surfaces misaligned. The data may have been taken at other than steady-state conditions; however, results for the medium surfaces appear to be satisfactory.

The slopes of the curves for magnesium in Figure 3-7 appear to increase as pressure becomes large. The effects of mean junction temperature and surface parameter are also apparent. The trends exhibited by these magnesium data compare favorably with the criteria for experimental data established in Chapter II.

Dissimilar Metals

Although the objective of this work was not to study the effects of dissimilar metals, a series of data were obtained for two aluminum-stainless steel junctions. These junctions were composed of a smooth stainless steel surface against a rough aluminum surface (SS1 → AL5), and a rough aluminum surface against a rough stainless steel surface (AL6 → SS7). The heat flux passed from stainless to aluminum and from aluminum to stainless, respectively. The resultant data are tabulated in Appendix B and shown graphically in Figure 3-8.

The results appear to be consistent in that the data fall in a smooth curve. The slope of these curves, like those for similar metals, increases as pressure becomes large. The magnitude of the smooth-to-rough data is larger than that of the rough surface data, in contrast to the data shown in Figure 3-4 through 3-7, as if the
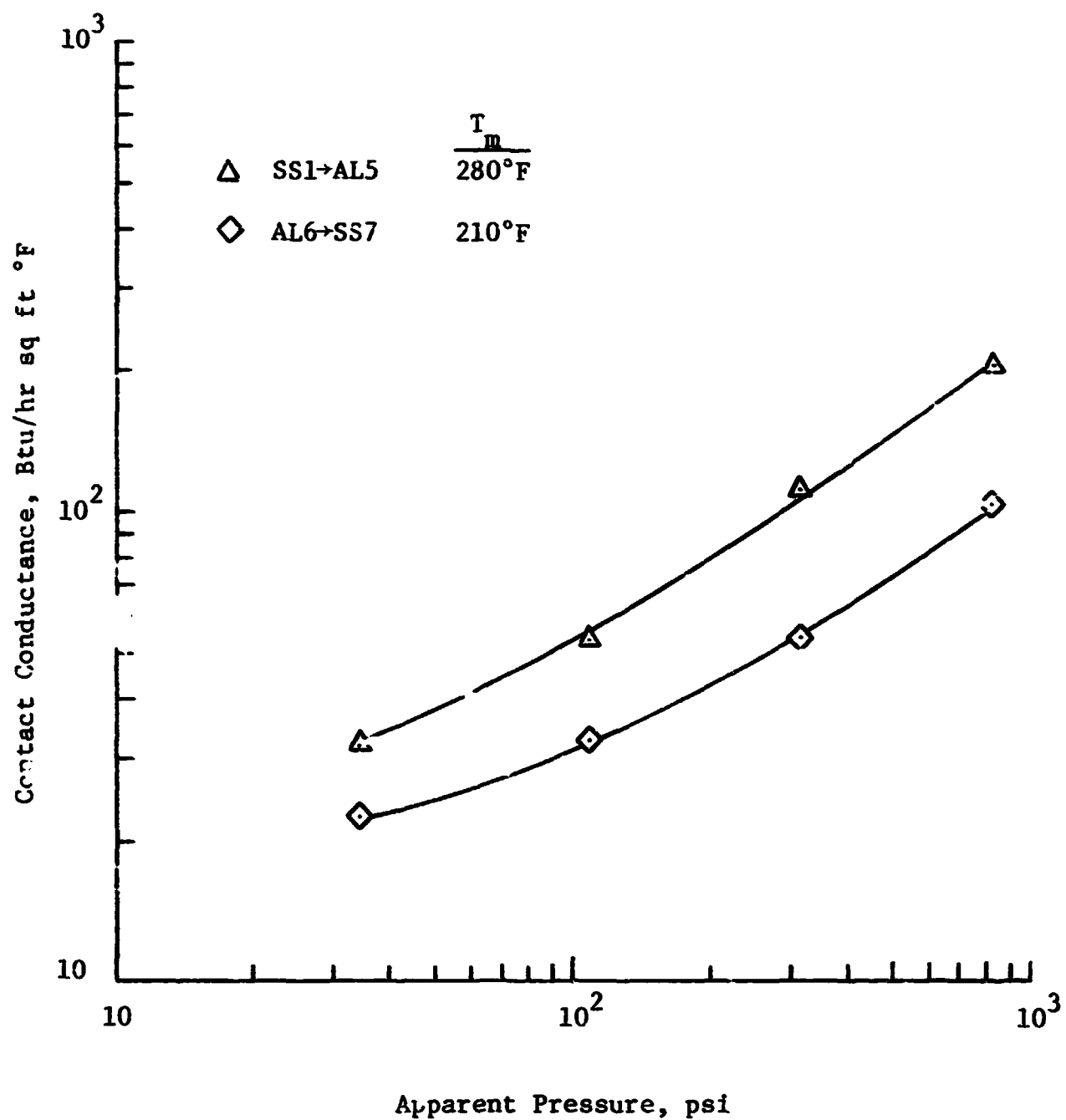
Figure 3-8. Variation of Contact Conductance with Apparent Interface Pressure for Aluminum-Stainless Steel Junctions.

surface parameter for the harder material is predominant.

Summary

The experimental contact conductance data for aluminum, stainless steel, brass, and magnesium are consistent and behave as expected, with few exceptions. These data compare well both in magnitude and trend with the criteria established in Chapter II. These results were used to establish the constants of a semi-empirical relationship for the prediction of contact conductance.

CHAPTER IV

ANALYSIS AND DISCUSSION

Numerous approaches to the problem of predicting thermal contact
resistance of bare metallic surfaces have resulted in several semi-
empirical equations, as discussed in Chapter II. Although some
authors stated that good correlation existed between their theory
and experiment, the correlation was generally limited to those data
obtained by the particular author. In this chapter an attempt is
made to analyze carefully those theories exhibiting some success,
and where possible, to extend the theories for purposes of more
general application. In addition, a dimensionless correlation for
the prediction of contact conductance is developed. The results
of this correlation are then compared with previous theories and
experimental data.

I. PUBLISHED THEORIES

The expressions for contact conductance developed by Cetinkale
and Fishenden [17] and Laming [55] do not lend themselves to compari-
son with experimental data due to lack of information regarding their
constants. Since the expression developed by Tachibana [74] behaves
much like that of Fenech, only the expressions developed by Fenech
and Rohsenow [32] and Clausing and Chao [20] will be discussed.

Comparisons with experimental data will be made to establish the
degree to which thermal contact conductance can be predicted using
these equations.

Fenech and Rohsenow

The approach and assumptions used by Fenech in his analytical
treatment of contact conductance were reviewed in Chapter II. To
further substantiate his analysis, Fenech obtained experimental data
from non-idealized metallic surfaces in contact and compared these
data with his theory. Results of these tests showed excellent agree-
ment considering the degree of uncertainty in the high conductance
measurements and the limited amount of data obtained in Fenech's
investigation.

The basic equation for contact conductance derived by Fenech
was given in equation (2-13). This equation, reduced to vacuum
conditions by Henry and Fenech [45], is given as:

$$h_c = \frac{\frac{\alpha}{1 - \alpha}}{\frac{\delta_1}{k_1} + \frac{\delta_2}{k_2} + (\frac{1}{k_1} + \frac{1}{k_2}) \frac{1}{4.26} (\frac{\alpha}{n})^{1/2}} \tag{4-1}$$

For the case of similar surfaces, $\delta_1 = \delta_2 = \delta_{FR}$, and introducing
the mean harmonic thermal conductivity, equation (4-1) reduces to:

$$h_c = \frac{k_h \frac{\alpha}{1 - \alpha}}{2\delta_{FR} + 0.47 (\frac{\alpha}{n})^{1/2}}$$

This form of the equation is not useful for calculation of
contact conductance since the values for the area ratio and the

number of contact spots are not known. Fenech states that for the
results of his armco iron-aluminum data, the radius of the contact
spot and the number of spots could each be repre;ented as a function
of the apparent interface pressure. The relationships he developed
for these variables would only apply to his particular data, as
indicated by Bloom [13]. Determination of the number of contact
spots and the contact area ratio by use of Fenech's graphical
technique is tedious and would be impractical for actual engineering
application.

The denominator of the above expression may be further simplified
by substituting for α and n. The conductance expression then becomes:

$$h_c = \frac{k_h \cdot \frac{\alpha}{1 - \alpha}}{2\delta_{FR} + 0.833\ a} \qquad (4\text{-}2)$$

Fenech suggested that the contact area ratio could be represented by
the ratio of apparent interface pressure to material hardness. The
validity of this assumption, however, is limited to the higher pressure
ranges. Substitution of such a ratio for the contact area generally
requires the use of an accommodation coefficient, as discussed in
Chapter II. Fenech has assumed that the fraction $\frac{\alpha}{1 - \alpha}$ is approx-
imately equal to α since α is very small. Applying this simplification
to equation (2-23), the contact conductance expression may be written
as:

$$h_c = \frac{k_m\ P_a}{(2\delta + 0.833a)\xi\ H_M} \qquad (4\text{-}3)$$

The resulting expression appears easy to use; however, several unknown
values remain. For purposes of the present investigation, the

effective gap thickness and contact spot radius were selected as
the flatness deviation and roughness deviation, respectively, as
suggested by Clausing and Chao [19,20]. The remaining unknown
quantity, the accommodation coefficient, was then determined by
an empirical fit of the published experimental data given in
Appendix A.

By fitting the data with the above expression, it was necessary
that the accommodation coefficient be a function of apparent inter-
face pressure, the flatness deviation, and the modulus of elasticity.
The coefficient appears to be a strong function of flatness deviation
and a relatively weak function of pressure and modulus of elasticity.
The empirically determined coefficient was

$$\xi = e^{-\dfrac{5.2 - 5.66 \times 10^3 \, \dfrac{P_a}{E}}{\log(FD) \cdot FD^{0.257}}} \tag{4.4}$$

The refinement of this accommodation coefficient was discon-
tinued since the basic form of the equation did not have the correct
pressure dependence for low pressures. Further, published data
did not represent a sufficient range of mean junction temperatures
to enable determination of a temperature effect. The expression
for calculating contact conductance in terms of generally reported
quantities may be found by combining equations (4-3) and (4-4).

In order to determine the effectiveness of this expression,
it must be analyzed in terms of the criteria established in Chapter
As pressure increases, the conductance increases to infinity and
as   goes to zero the conductance goes to zero.

It will be noted, too, that the expression does not satisfy the criteria for temperature and surface finish established in Chapter II.

Figures 4-1 and 4-2 show comparisons made with experimental data. Those data presented in Figure 4-1 represent selected mid-range conductance data of other investigators (Appendix A). The modified Fenech equation does show the same trend as the data; however, as pressure becomes small the curve of the modified theory deviates from the data by a considerable amount. The order of magnitude predicted by the equation is satisfactory for mid-range data. It deviates appreciably, however, for extremely smooth and extremely rough surfaces. It should be noted that the agreement is better for aluminum than for other materials.

The comparisons with data of the present investigation, shown in Figure 4-2, follow the same trends as those in Figure 4-1. Again the magnitude and slopes show better agreement with aluminum than with other data. The order of magnitude prediction for most data, however, is not very close.

The modified Fenech equation was developed in order to see how closely conductance values could be predicted from an expression obtained by a direct fit of experimental data. Since many simplifying assumptions have been made in determination of the accommodation coefficient, it would appear that equation (4-5) would only predict order of magnitude conductance data at best. Even then, its prediction would be valid only for a limited range of pressures and temperatures, due to the limitations of the original equation.
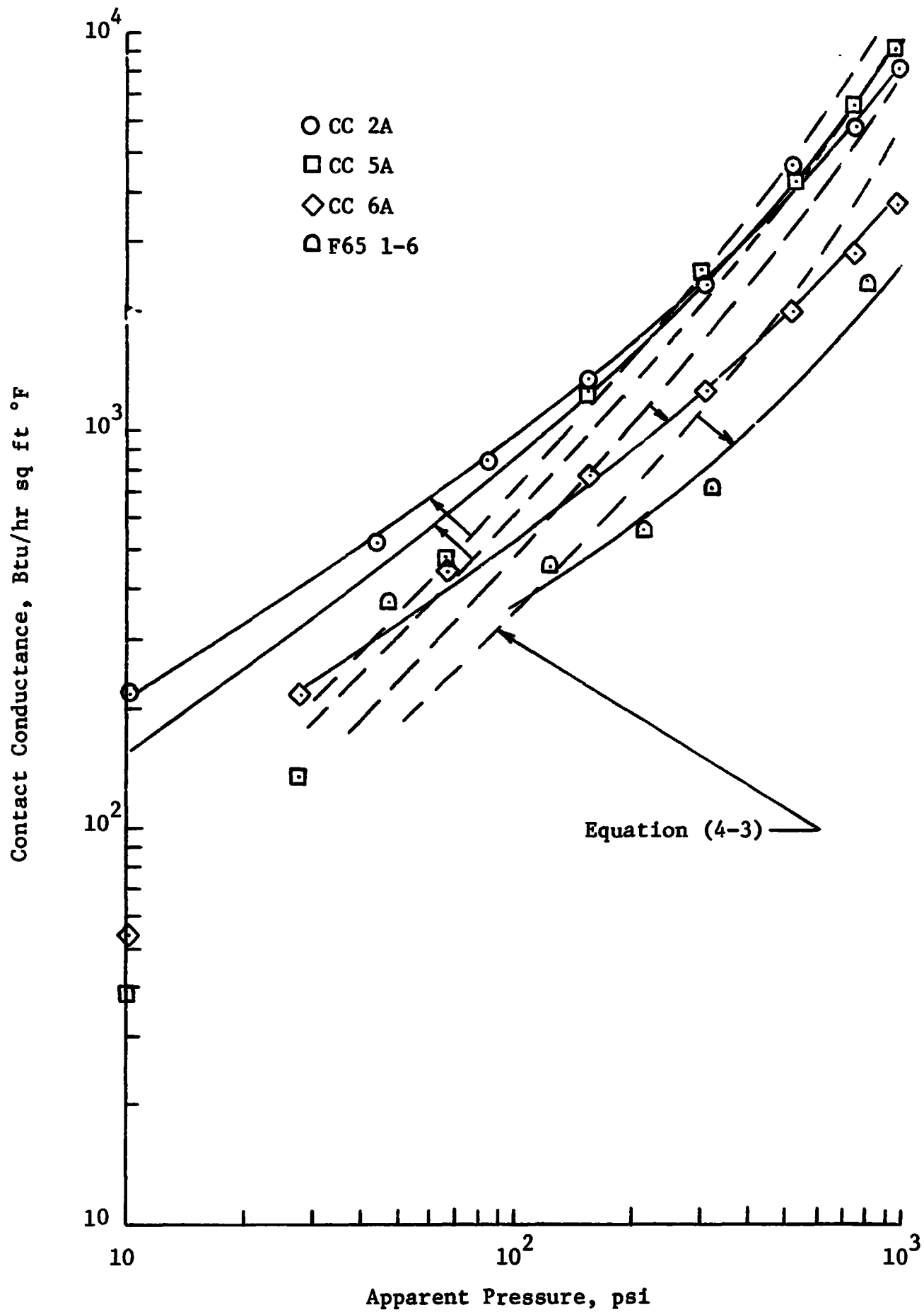
Figure 4-1. Variation of Selected High Temperature Contact
Conductance Data with Apparent Interface Pressure
-- Comparison with Modified Fenech Equation.
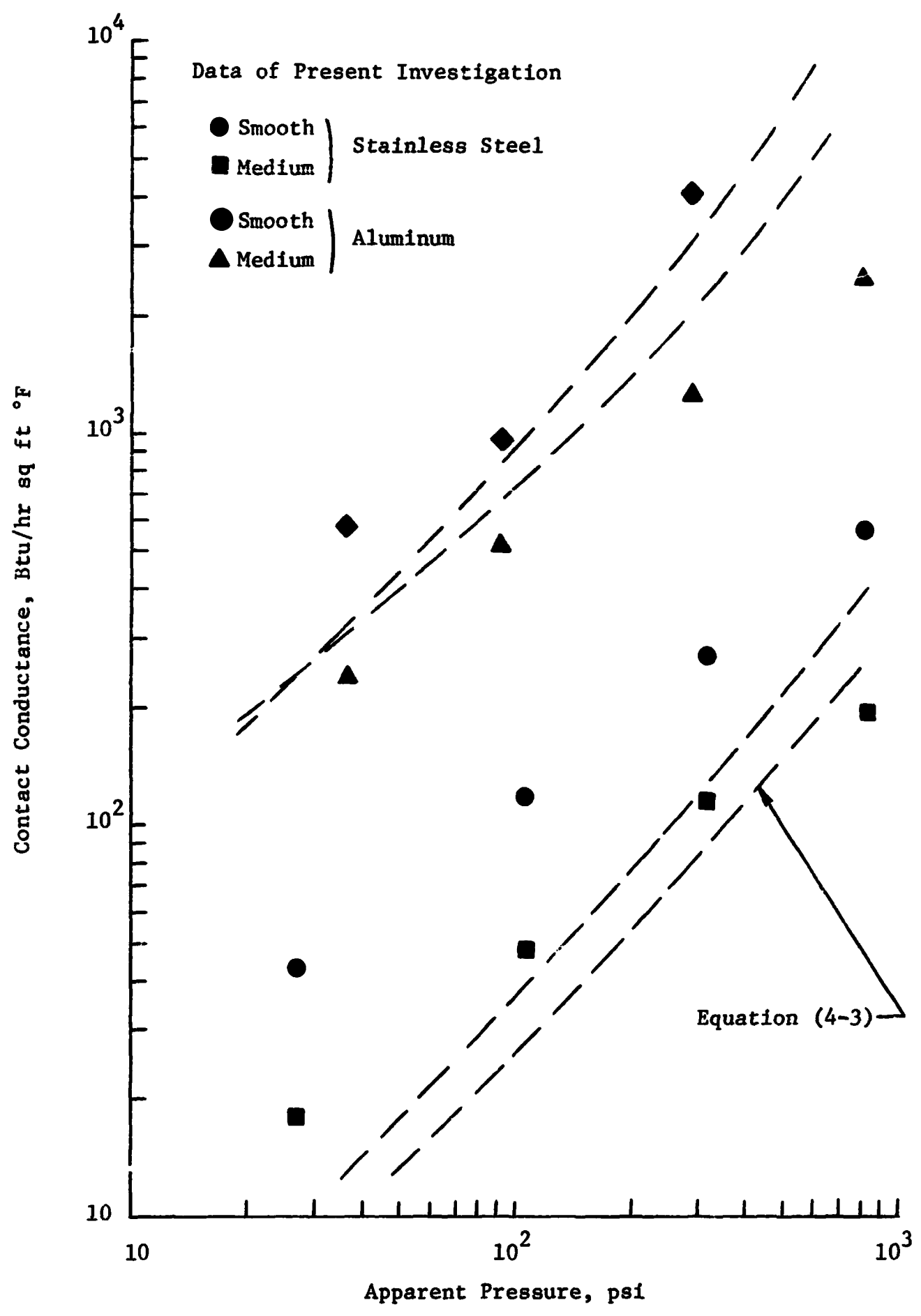
Figure 4-2. Variation of Selected Low Temperature Contact
Conduct ince Data with Apparent Interface Pressure
-- Comparison with Modified Fenech Equation

Clausing and Chao

The theoretical analysis presented by Clausing was justified
by comparison with experimental data for several different metals.
The data obtained in his experimental investigation were limited
to contacting surfaces in which the macroscopic resistance was
dominant. Although fairly good agreement was found between theory
and experimental data of all test materials when comparing Clausing's
dimensionless conductance with the elastic conformity modulus, good
magnitude prediction of contact conductance was possible only for
a few isolated sets of data.

The macroscopic contact conductance was given as:

$$h_c = \frac{2 \, X \, k_h}{\pi b \; g(X)}; \quad X = 1.285 \, \{(\frac{P_a}{E}) \; (\frac{b}{\delta_{cc}})\}^{1/3} \qquad (4\text{-}5)$$

where the series $g(X)$ is given in equation (2-46). Clausing assumed
that the total flatness deviation would be the sum of the surface
flatness deviations, and that the radius of the contact spots could
be represented by the rms surface roughness. The test parameters
for Clausing's experimental data are listed in Appendix A. Included
in the appendix are the surface parameters, thermal conductivity,
and modulus of elasticity. The above equations were programmed on
a digital computer to permit analysis of Clausing's experimental
data and theory, and data from other investigators.

Figure 4-3 shows the reciprocal of the dimensionless conductance
(the equivalent length per unit radius) compared with the elastic
conformity modulus for brass, stainless steel, magnesium, and aluminum,

Experimental Data of Clausing and Chao

○ Brass
□ Magnesium
◇ Stainless Steel
△ Aluminum

(Rough Surfaces)

—— Theory

$$\frac{P_a}{E}\frac{b}{\delta_{CC}} \times 10^2$$

$\dfrac{k}{h_c b}$
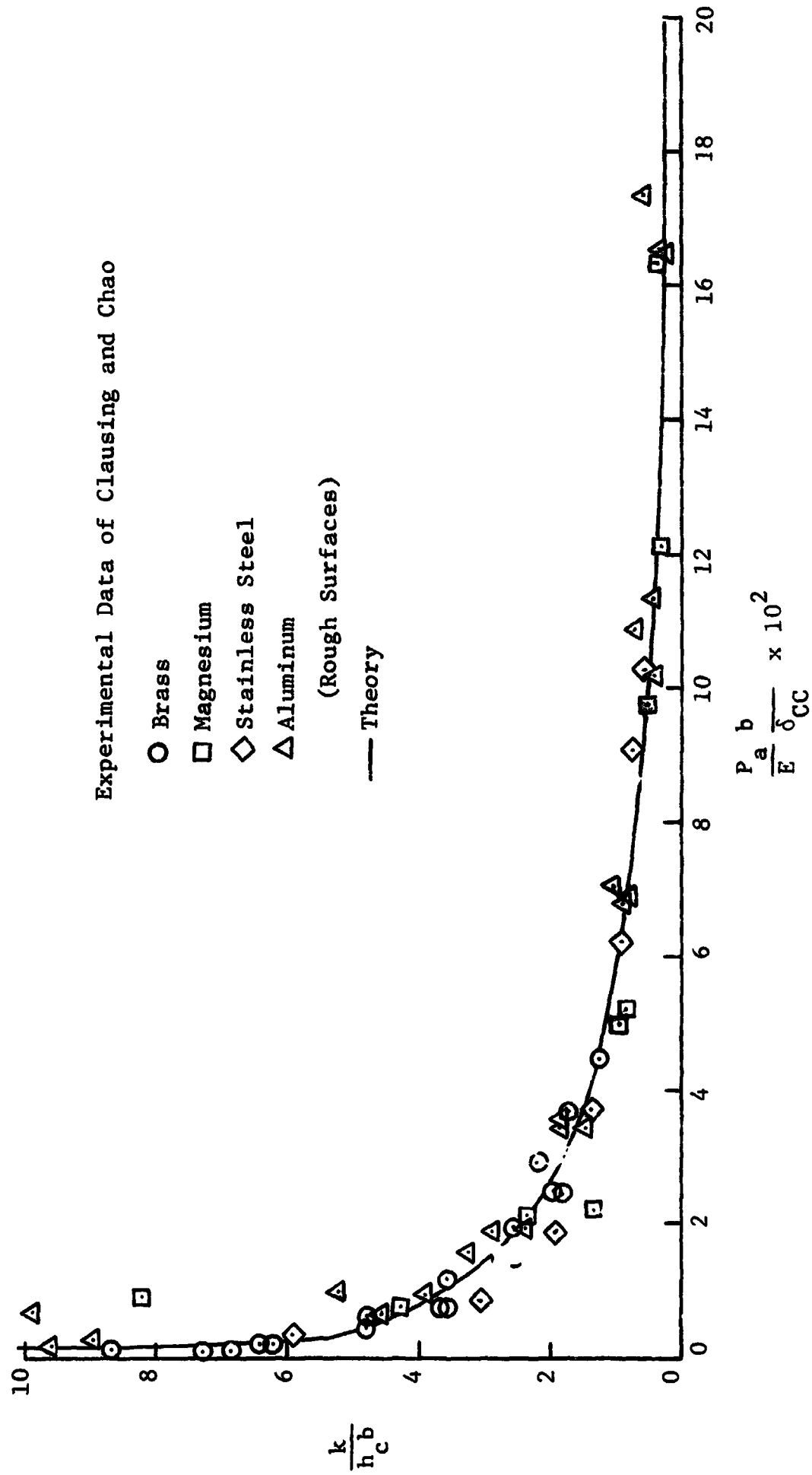
Figure 4-3. Variation of Dimensionless Conductance with Dimensionless Pressure, as Presented by Clausing and Chao [20].

as presented by Clausing. It should be pointed out that although the theory and experimental data appear to agree well, the data shown are only for rougher surfaces.

Contact conductance values for brass, stainless steel, and magnesium data are plotted as a function of apparent pressure in Figure 4-4. These experimental data are compared with contact conductance values predicted by equation (4-6). The theoretical curves for brass show the same trend and approximate magnitude as the experimental data for the range of pressures 50 to 1,000 psi. The theoretical values for magnesium also show the same trend as the experimental data; however, the theory does not adequately predict magnitude values, especially for smoother surfaces. At pressures below fifty psi, the experimental data deviate appreciably from the predicted values. For stainless steel, extreme deviations occur below 100 psi. The predicted values for smoother stainless steel surfaces terminate at approximately 250 psi. The theory, then, is applicable only for this small range of pressure.

Comparison of experimental data with theory for aluminum is shown in Figure 4-5. It may be noted that the data for surface flatness deviations of 220 to 230 microinches and surface roughness deviations greater than twelve microinches show fair agreement with theory. This agreement holds only for pressures between 100 and 500 psi. When the theory is extended beyond Clausing's limit (X = 0.65, approximately 600 psi), the curve deviates from the experimental data in an exponentially increasing manner. Comparison of Clausing's theory with his data indicates that the range of applicability is greatly
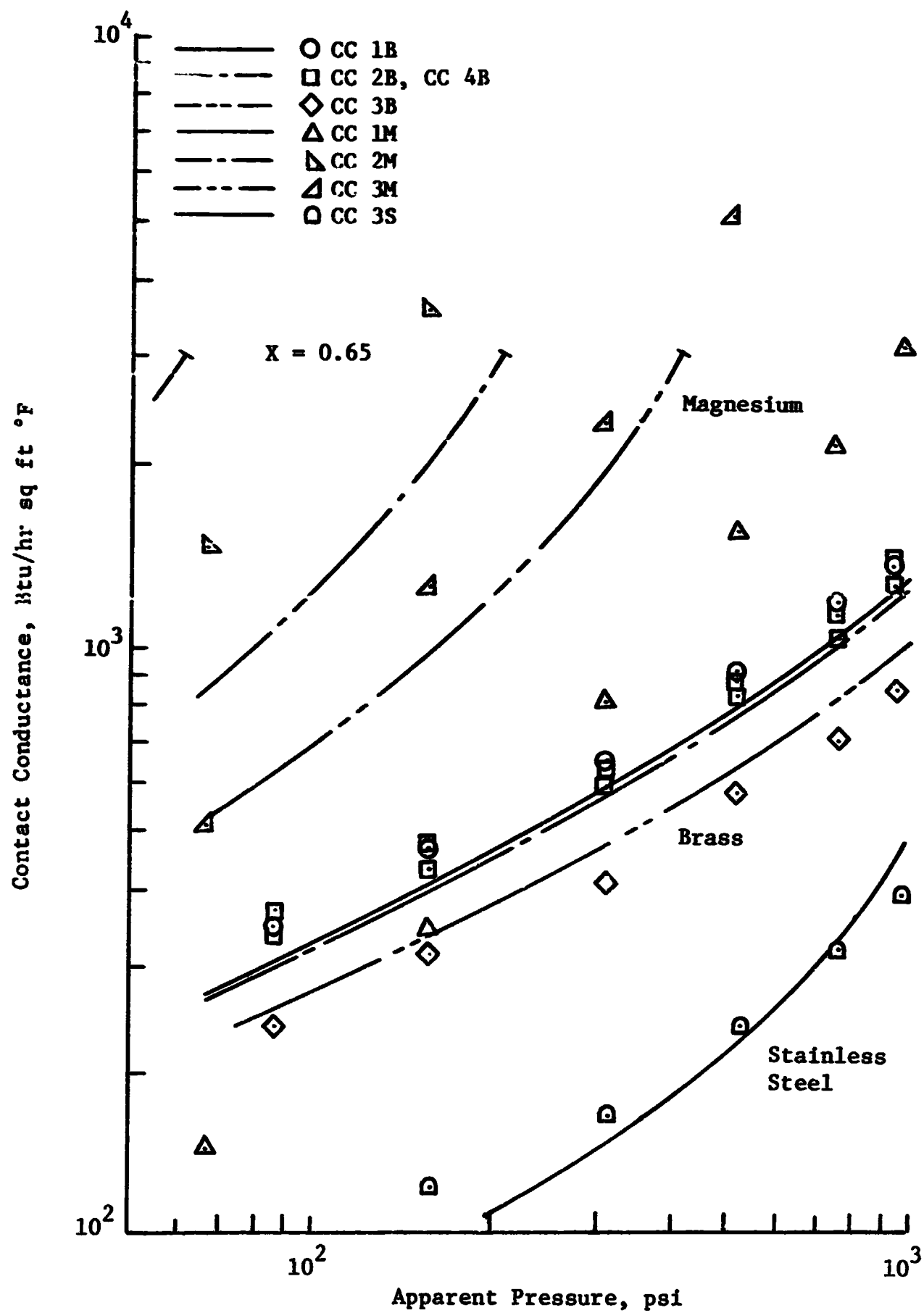
Figure 4-4. Variation of Brass, Magnesium, and Stainless
Steel Contact Conductance with Apparent Interface
Pressure -- Comparison with the Clausing Equation.
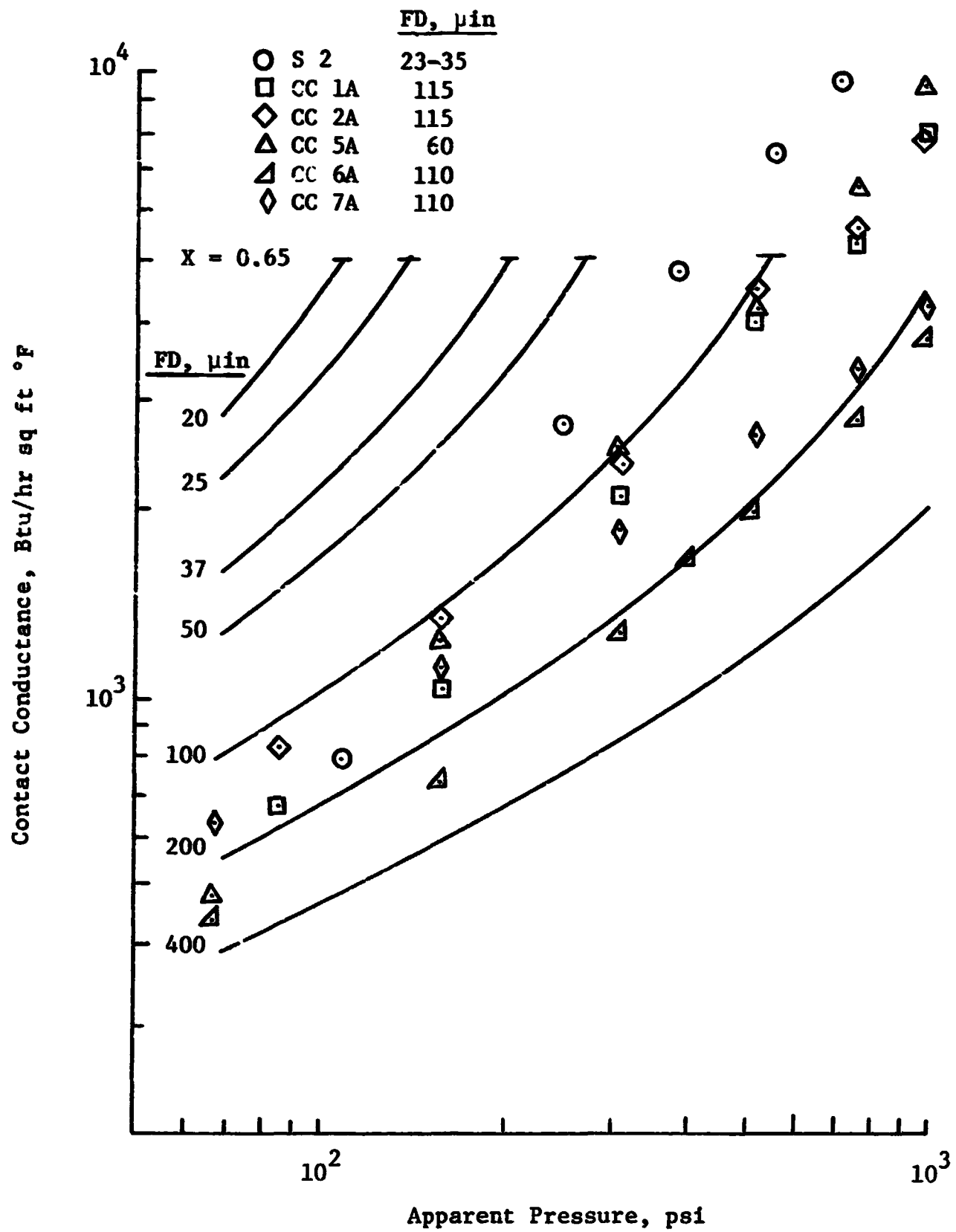
Figure 4-5. Variation of Aluminum Contact Conductance
with Apparent Interface Pressure — Comparison
with the Clausing Equation.

influenced by the factor X. Further analysis of the macroscopic conductance shows that some of the experimental data obtained by Clausing do not vary consistently with the flatness deviaticr as might be expected. This peculiarity in the data is discussed by Smuda, et al [69].

Aluminum data obtained at Arizona State University are also compared with Clausing's theory in Figure 4-5. Note that his equation shows better agreement with these smooth surface data than with his own data for similar surface conditions. For both Clausing's data and that obtained at Arizona State University, the predicted values for the conductance of smooth surfaces diverges substantially and over-predicts the magnitude by factors of ten or more.

There may be several reasons why the Clausing equation does not better predict the experimental data. Perhaps the experimental technique used in obtaining the data did not permit accurate alignment of the specimens, thus causing some error in the assumed region of contact. More likely, the elastic conformity modulus may not properly represent the pressure-surface dependence.

Other factors may influence the usefulness of the Clausing theory. The spherical contact model with which the data were obtained does not represent the surfaces generally used in engineering applications. In addition, the assumption of elastic deformation at the contact would apply only to specific conditions. A full treatment of the problem should include the effects of plastic deformation. Further, due to the nature of the macroscopic constriction

resistance solution [i.e., as X → 1.0, g(X) → 0] and the parameters

selected for the elastic conformity modulus, the predicted values of

thermal contact conductance tend to infinity at finite loads.

Analysis of the theory suggests that a modification to include

the conductance due to the microscopic asperities would decrease

the predicted conductance at higher pressures. This modification

would permit more favorable correlation of the theory with experi-

mental data.

The development by Clausing and Chao of a theoretical equation

for the prediction of contact conductance makes possible limited

prediction of conductance values. Its application is restricted to

rough contact surfaces and cases in which the macroscopic constric-

tion resistance dominates. Since a majority of surfaces and

geometry used in engineering applications where contact resistance

occurs are flat, machine surfaces, the roughness and flatness

deviations would be small. Clausing's theory would be of little

use for predicting contact conductance for such conditions. A good

theory for contact conductance should be able to predict conductance

values for smooth as well as rough surfaces.

II. DIMENSIONLESS CORRELATION

Although it is difficult to specify the exact variables affect-

ing thermal contact conductance, analysis of the assumed parameters,

performed by Clausing and Chao [20], resulted in the grouping:

$$\frac{hb}{k} = f \left(\frac{P_a}{E} \quad \frac{b}{\delta_{cc}} \right)$$

Clausing used this result for the correlation of some of his data

(Figure 4-3), deeming the relationship applicable only to rough

surfaces. Clausing's data and parameters, as well as other experi-

mental data, are plotted in a different manner in Figure 4-6, to give

a better perspective of the agreement. The scatter present may be

attributed primarily to variations in the mean junction temperature,

and the manner in which the surface parameter is defined. In Claus-

ing's work, the mean junction temperature ranged from $160°F$ to $340°F$;

thus temperature effect was minimized. The mean junction temperature

of published experimental data, however, ranges from $-250°F$ to $500°F$.

Its effect on conductance is obvious indeed.

It was shown that the equation derived by Fenech and Rohsenow

could be simplified in form by neglecting an interstitial fluid and

by assuming similar surface characteristics for both sides of the

contact (pp. 95-96). With these simplifications the denominator

of equation (4-2) can be denoted as δ, a parameter which can be

described as the effective thickness or depth of influence of the

contact. The ratio of the actual contact area to the total cross-

sectional area of the junction is represented by α. In dimensionless

form

$$\frac{h_c \delta}{k_h} = \frac{\alpha}{1 - \alpha} \qquad (4-6)$$

The results of several other investigators can also be reduced to

this general form; however, the difficulty still remains that δ and

α must be defined in terms of the controlled test variables.
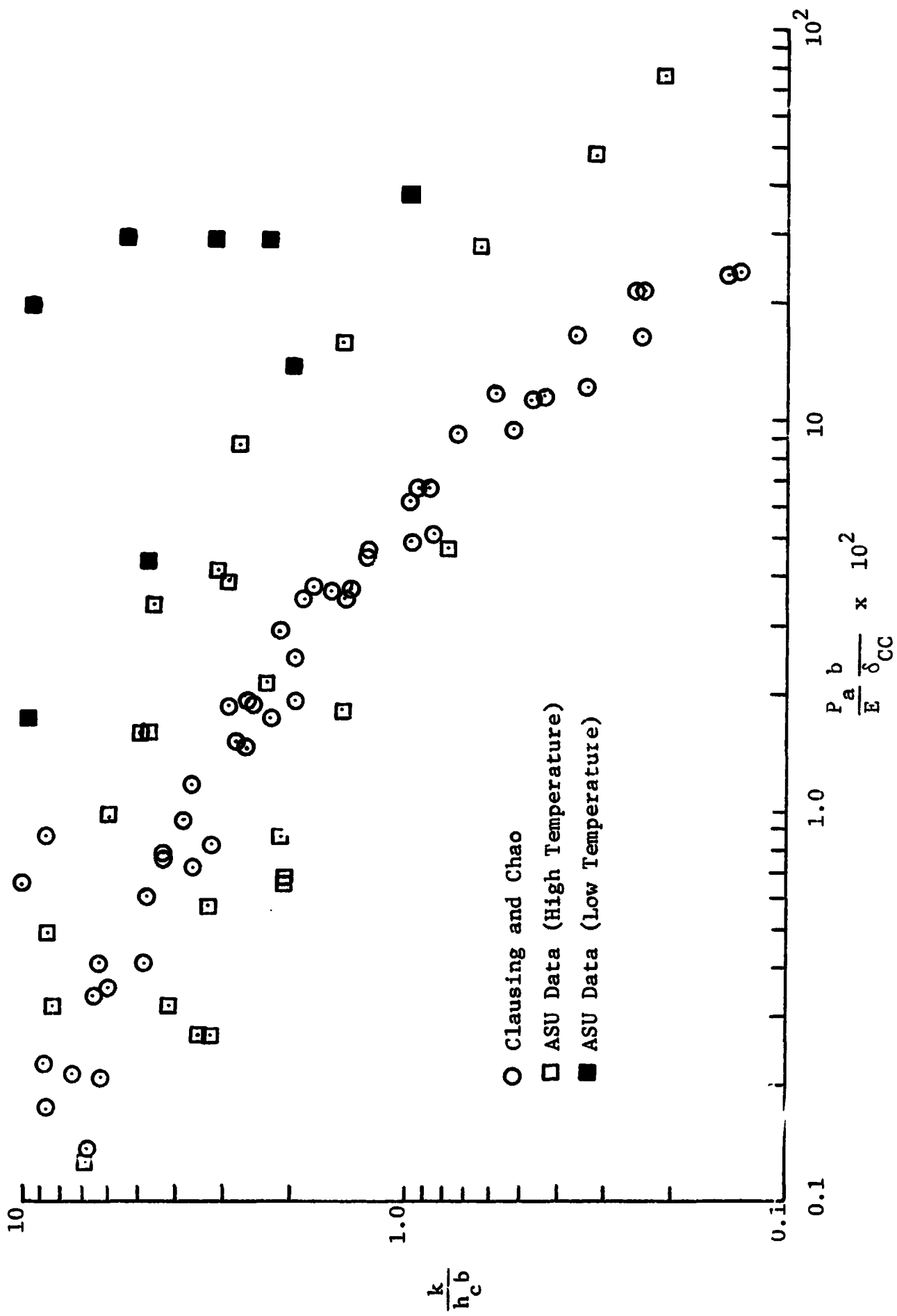
Figure 4-6 Variation of Dimensionless Conductance with Dimensionless Pressure for Published Data.

Earlier attempts at dimensionless correlation and dimensional analysis of the variables effecting contact conductance have yielded very few useful results [17, 19, 42, 47, 76, 81]. A number of different parameter groupings have been found; however, these groups only correlated a small amount of published experimental data.

Since it was desirable that the required material properties and surface parameters for predicting h be easily obtained, the functional relationship for h was derived in terms of the assumed variables of load pressure, mean junction temperature, surface roughness and flatness, and the material properties. Hudack [47] had shown that the parameter $\frac{P_a}{E} \beta T_m$ could be used to correlate thermal conductance data for aluminum 7075. Other investigators have also used various combinations of $\frac{P_a}{E}$ and $\frac{b}{\delta}$ for their correlations. Clausing had demonstrated some success with a correlation of the dimensionless parameter $\frac{hb}{k_m}$ (Figure 4-6). Thus the dimensionless parameters were:

$$P^* = \text{dimensionless pressure} = \frac{P_a}{E}$$

$$T^* = \text{dimensionless temperature} = \beta T_m$$

$$\delta^* = \text{dimensionless surface parameter} = \frac{\delta}{b}$$

$$\psi = \text{thermal conductance number} = \frac{h_c \delta}{k_m}$$

The experimental results of this investigation were plotted in the form of $\frac{hb}{k_m}$ as a function of P*T*, since the surface parameter δ was as yet undefined. This variation of dimensionless conductance with P*T* for stainless steel 304 is shown in Figure 4-7.

It was necessary to specify values for the initial surface para-
meters which would cause the curves such as those in Figure 4-7 to
agree. This was done by taking ratios of $\frac{hb}{k_m}$ between surfaces at con-
stant values of P*T*. An initial value of δ_o = d was chosen for the
smooth-to-smooth surfaces, and the remaining values of δ_o for other
contacting surfaces were calculated at 20 psi. In Figure 4-8 initial
refers to correspondence of the $\frac{hb}{k_m}$ curves . 20 psi. To check the
values the curves were also made to coincide at a load pressure of
800 psi (final in Fig. 4-8).

Study of this surface parameter indicated that it was a function
of d, defined by equation (2-22) such that:

$$\delta_o = f(d) = f \ \{(FD+2RD)_{\substack{rough \\ surface}} - \frac{1}{2} (FD+2RD)_{\substack{smooth \\ surface}} \} \qquad (4-7)$$

Plots were then made of $\frac{h_c b}{k_m}$ as a function of δ_o^*, for constant
values of P*T*. It was found that $\frac{h_c b}{k_m}$ varied with δ_o^* in an
exponential manner, i.e., the curves yielded straight lines on
semi-log graph paper as shown in Figure 4-9. The straight lines,
however, were offset by a variation in slope as a function of P*T*.
After further consideration it was found that the product P*T*/δ*
was a dimensionless parameter which would correlate the family of
exponential curves, at constant values of P*T*. Since the surface
parameter has the dimensions of length, the functional form for δ
was selected as:

$$\delta = \delta_o \ e^{-m \ P*T*/\delta_o^*} \qquad (4-8)$$

where the value for m must be selected for the best fit of the data.
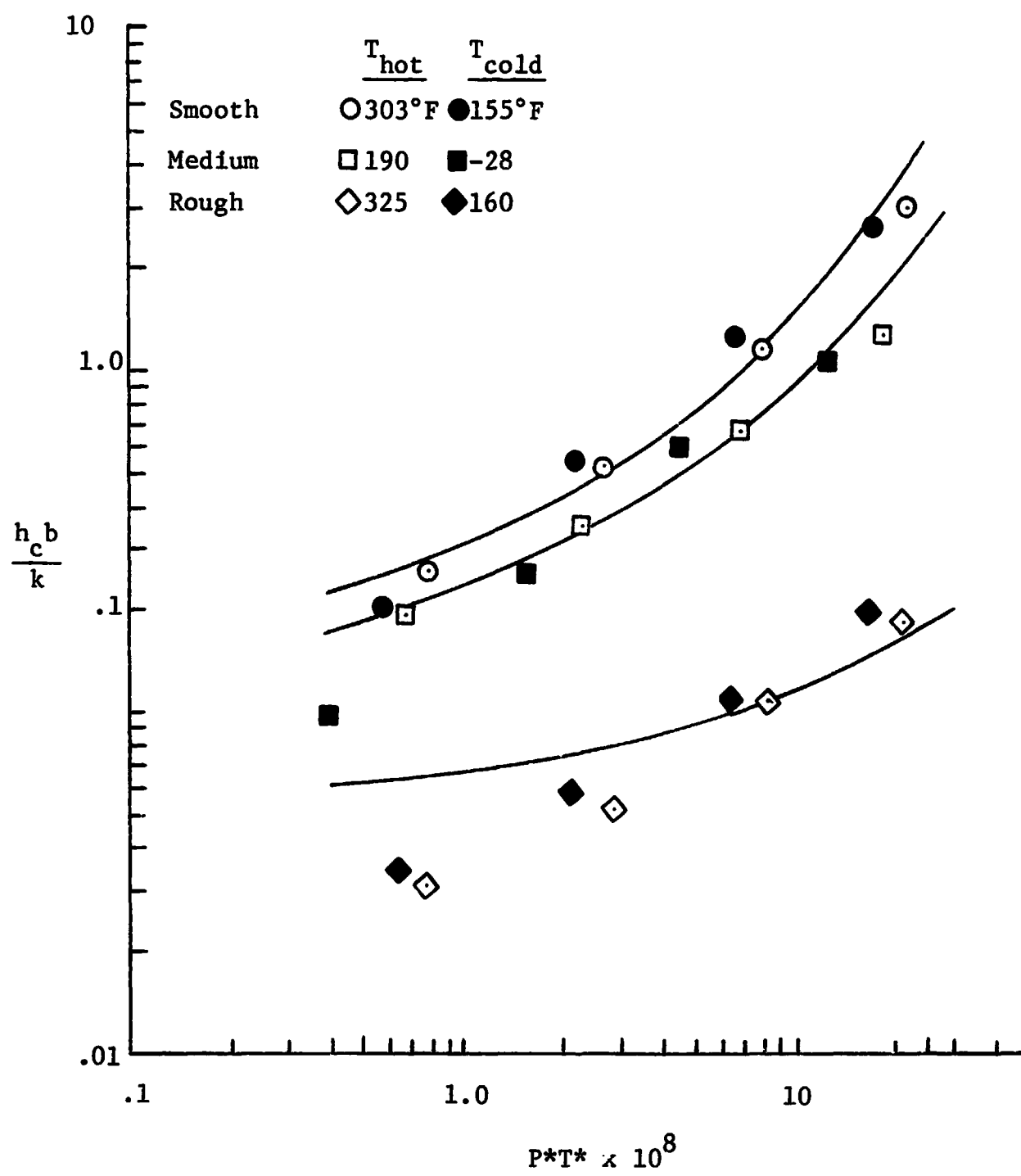
Figure 4-7.   Variation of Dimensionless Conductance
with Dimensionless Pressure and Tempera-
ture for Stainless Steel 304.
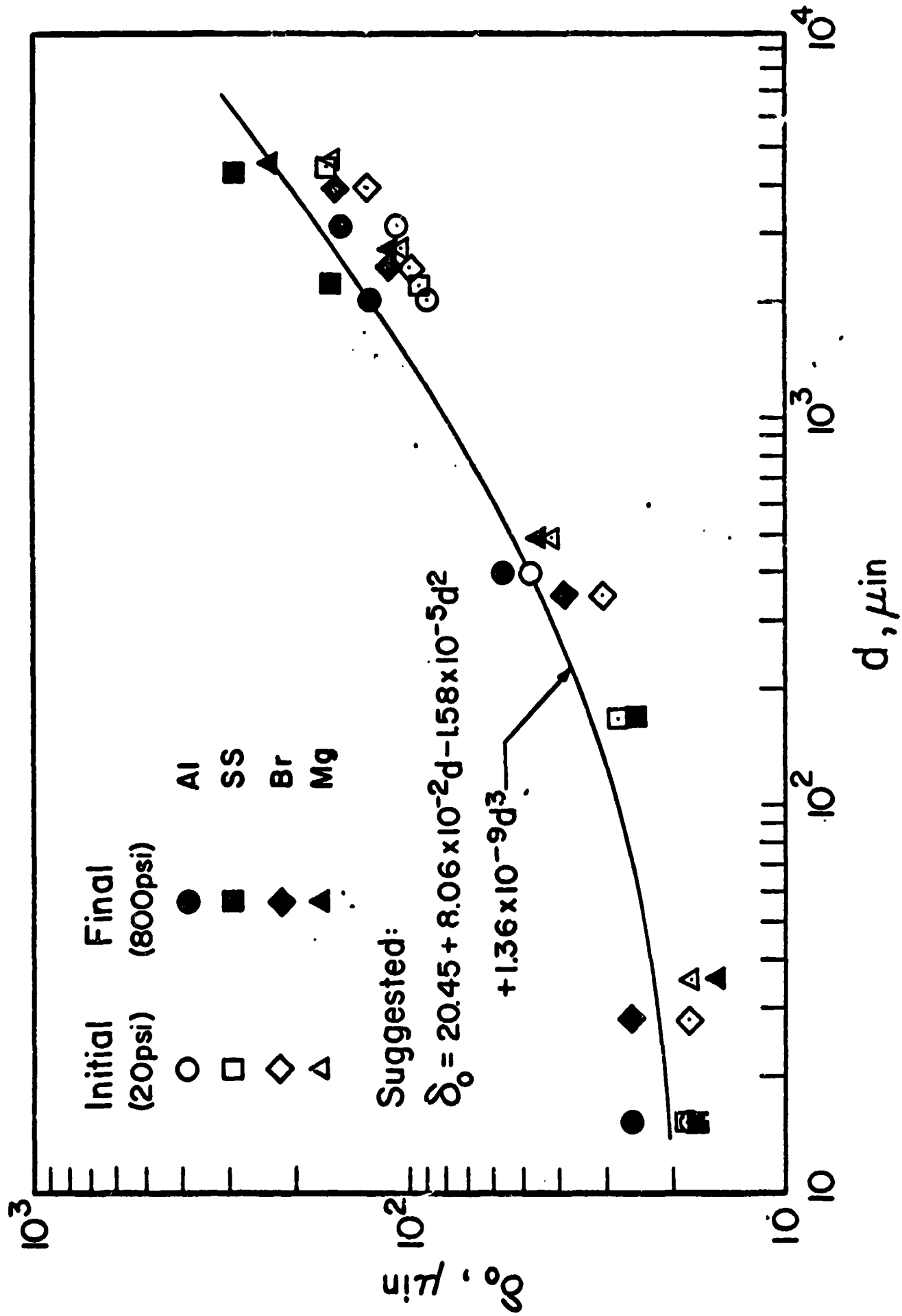
Figure 4-8. The Relationship between the Surface Parameter δ_o and the Flatness and Roughness Deviations
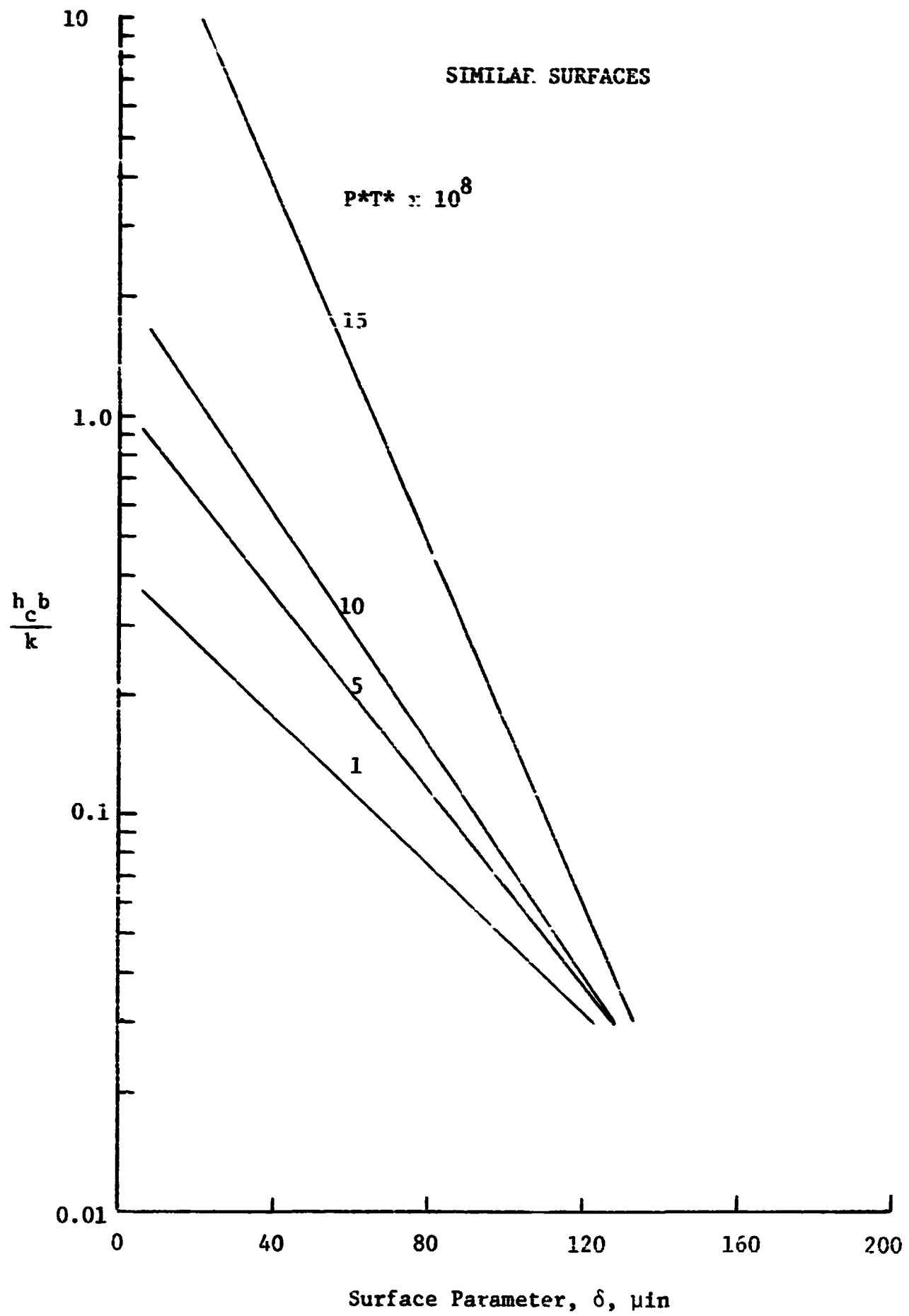
Figure 4.9   Variation of $\frac{h_c b}{k}$ with Surface Parameter for Constant P*T*.

This function behaves as required for the limiting cases of pressure
and temperature. As pressure increases, the surface parameter or
effective gap thickness becomes smaller. At zero pressure, the
effective gap thickness is just the initial value.

The thermal conductance number, $\psi = \dfrac{h_c \delta}{k_m}$, was then plotted as
a function of P*T*, with the constant m selected for approximate best
fit to be 180.0. The resulting plot is shown in Figure 4-10. In-
cluded in the figure are all of the published data listed in Appendix
A, as well as the data of the present experimental investigation. The
data are representative of seven different investigators, with
approximately 400 data points. The data shown include mean junction
temperatures of -250°F to 500°F, apparent interface pressures of 10
to 7,000 psi, surface flatness deviations of 15 to 4,500 microinches,
and surface roughnesses of 3 to 120 microinches. Data for aluminum,
stainless steel, brass, and magnesium are included. It may be
seen that for a majority of the data, extremely good correlation
exists. The spread of data points is to be expected due to the
variation in surface parameters. Also no two investigators measure
or present their data in the same manner. Further, some of the data
are correlated on assumed information, since all of the experimental
characteristics were not listed by the investigator. The correlation
of such a large amount of published experimental data suggests that
the correlating parameters are a decided improvement over existing
relationships.
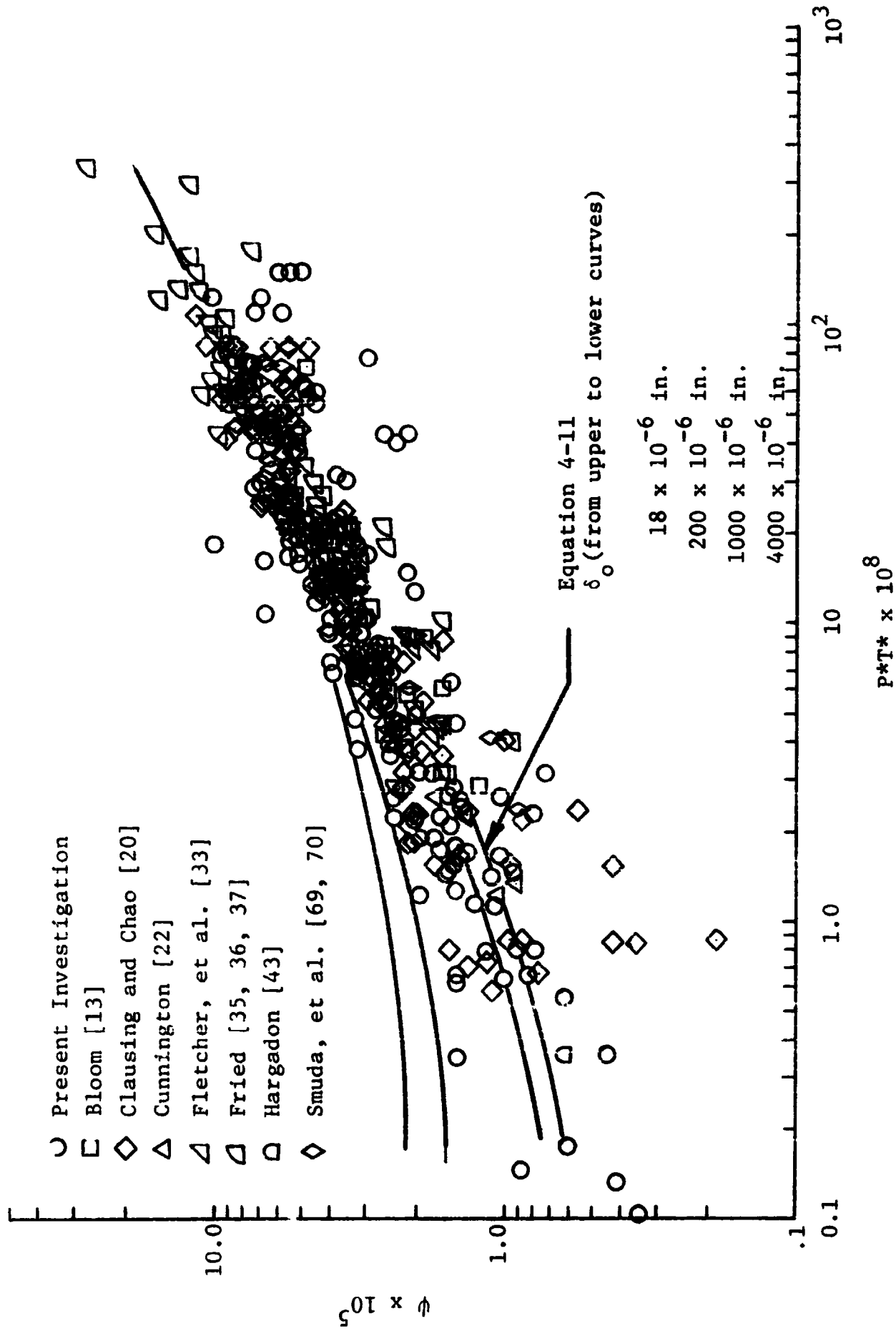
Figure 4-10. Variation of Thermal Conductance Number with Dimensionless Pressure and Temperature for All Data.

More scatter was noticed below the correlation curve, especially at the higher and lower load pressures. This scatter may be explained in several ways. At higher load pressures, those surfaces with oxide films or other contaminants would result in lower measured conductance values. Also, at high load pressures the interface temperature difference is small and in some instances is the same as the uncertainty, thus permitting errors of 100 percent or more. At low load pressures, measured conductance values exhibit a wide range of scatter. This may partially be explained by the variations in load application mechanisms used by different investigators. Other reasons might be the alignment of the test surfaces, uncertainty in the material properties, and incorrectly reported surface characteristics.

As a result of the excellent correlation shown in Figure 4-10 the expression for thermal contact conductance may be written as:

$$\psi = f(P*T*, \delta_o*) \ \frac{\alpha}{(1 - \alpha)}$$

In order to establish the functional form of the contact area ratio, several criteria must be met. For example, the contact area ratio must be a function of temperature and pressure, and at low or zero load pressures, the contact area ratio must be a function of the surface

parameter. In addition, the shape of the correlation curve will dictate
the functional form. One expression which satisfies these requirements
is:

$$\psi = \frac{\alpha}{1 - \alpha} = \{C_1(\delta_o{}^*) + C_2 \ P* \ T*\}^{\ n} \qquad (4-9)$$

from which the area ratio would be

$$\alpha = \frac{\{C_1(\delta_o{}^*) + C_2 \ P*T*\}^{\ n}}{1 + \{C_1(\delta_o{}^*) + C_2 \ P*T*\}^n}$$

Hence, for the limiting cases of pressure

$$\underset{P \to o}{Lim \ \alpha} = \frac{C_1(\delta_o{}^*)}{1 + C_1(\delta_o{}^*)} \quad ; \quad \underset{P \to \infty}{Lim \ \alpha} = 1$$

Further, the coefficient $C_1(\delta_o*)$ must be very small, thus satisfying
the low load contact area ratio and conductance requirements. This
particular selection would include any possible radiation effects as
the load pressure is reduced to zero.

In order to substantiate the validity of equation (4-9), it is
necessary to consider its behavior at all limiting conditions. Checking
the limiting cases for pressure, the value of $\frac{h_c \delta_o}{k_m}$ approaches infinity
and $C_1(\delta_o*)^n$ in the limiting cases of P* approaching infinity and zero,
respectively. The slope of the conductance curve as a function of P*
approaches infinity and a small value for limit as P* becomes large and

as P* goes to zero, respectively.

These results are as expected from the criteria established in Chapter II. The relationship with mean junction temperature behaves very much like that with pressure. As temperature increases, the conductance increases, and as temperature decreases, the conductance becomes smaller. The rate of change of conductance with mean junction temperature behaves in the same manner. These trends are also in agreement with those resulting from the data analysis of Chapter II. The relationship with the surface parameter indicates that as the surface becomes smoother, the conductance becomes large, and as the surface becomes very rough, the conductance becomes small. The rate of change of conductance with surface parameter approaches infinity as the surface parameter tends to zero and approaches zero as the surface parameter becomes large.

The coefficients for the prediction equation were found in the following manner. For large load pressures, the term $C_1(\delta_o)$ was first considered negligible and the logarithm of equation (4-9) was plotted in the form:

$$\log \psi = n \log C_2 + n \log P^*T^*$$

Approximate values for n and C_2 were selected from the slope and intercept of the plot, respectively. The resulting values were n = 0.58 and $C_2 = 0.020$. With all coefficients known except $C_1(\delta_o)$, the low load pressure data were used to obtain an average value of $C_1(\delta_o)$

for all data. The resulting value was $C_1(\delta_o) = 5.10 \times 10^{-6} \delta_o$.

These constants were then used to predict the conductance values for the measured data and the resultant error was calculated. Since these initial values for the constants were approximate, the constants were then refined by incrementing them and calculating the rms error for all data of this investigation. For the minimum rms error, the coefficients for equation (4-9) were

$$C_1(\delta_o{}^*) = 5.22 \times 10^{-6} \delta_o{}^*$$

$$C_2 = 0.036$$

$$m = 170$$

$$n = 0.56$$

The resulting conductance equation may be written as

$$h_c = \frac{k_m}{\delta_o} \, e^{170 \, P*T*/\delta_o{}^*} \{5.22 \times 10^{-6} \delta_o{}^* + 0.036 \, P*T*\}^{.56} \qquad (4-10)$$

and the dimensionless conductance parameter is

$$\psi = \{5.22 \times 10^{-6} \delta_o{}^* + 0.036 \, P*T*\}^{0.56} \qquad (4-11)$$

A comparison of Equation 4-11 with the present experimental data as well as those of previous investigators is illustrated in Figure 4-10 for δ_o

values of 18 (top curve), 200, 1000, and 4000 μ-in. At higher values
of P*T* the surface finish is noted to have a much smaller effect.

III. COMPARISON OF THE DIMENSIONLESS CORRELATION
WITH EXPERIMENTAL DATA

In order to justify the accuracy of the expression for contact
conductance developed in the previous section, comparisons must be
made with experimental data. Therefore, the predicted values of
conductance will be compared with experimental data of the present
investigation and with other published data. In additior, compari-
sons are made with existing relationships for the prediction of
contact conductance.

Present Experimental Data

Comparisons were made between predicted and measured conduc-
tance values for data of the present investigation. Equation (4-11)
appears to predict these conductance values within an average overall
error of 29 percent, with a maximum overall error of 47 percent for
the magnesium experimental data. Deleting several of the oxidized magnesium
data points results in an average overall error of 24 percent for the
remaining data. Pressures ranged from 20 to 815 psi, mean junction
temperatures from -85°F to 335°F, and surface flatness deviations
from 18 to 4,500 microinches.

The experimental data for aluminum 2024 are shown in Figure
4-11. Study of the curves suggests that the theory predicts the data

with an average overall error of 21 percent. The predicted trends compare well with those of the experimental data. It should be noted, however, that as pressure increases, the predicted values of conductance increase more rapidly than the experimental data. This slight deviation may be attributed to oxidation, as discussed in Chapter II.

The variation of contact conductance for stainless steel 304 is shown as a function of pressure in Figure 4-12. The predicted values of conductance are also shown for comparison. Note the excellent agreement for all data, with the exception of a few data points. The agreement is within an overall average error of 25 percent, with a maximum deviation of 57 percent for one or two data points.

The stainless steel are among the most consistent of the data, as shown in Chapter III. One reason for this good agreement is the range of interface temperature difference. At high load pressures, the ΔT_j for stainless steel is on the order of $10°F$, whereas the ΔT_j for aluminum, magnesium, and brass is on the order of 1 to $3°F$, similar to the uncertainty in ΔT_j. Therefore, errors of 100 percent might be expected for the softer materials; however, the error for stainless steel would be much smaller.

Equation (4-11) is compared with brass conductance data in Figure 4-13. The trends and magnitudes are well predicted. These
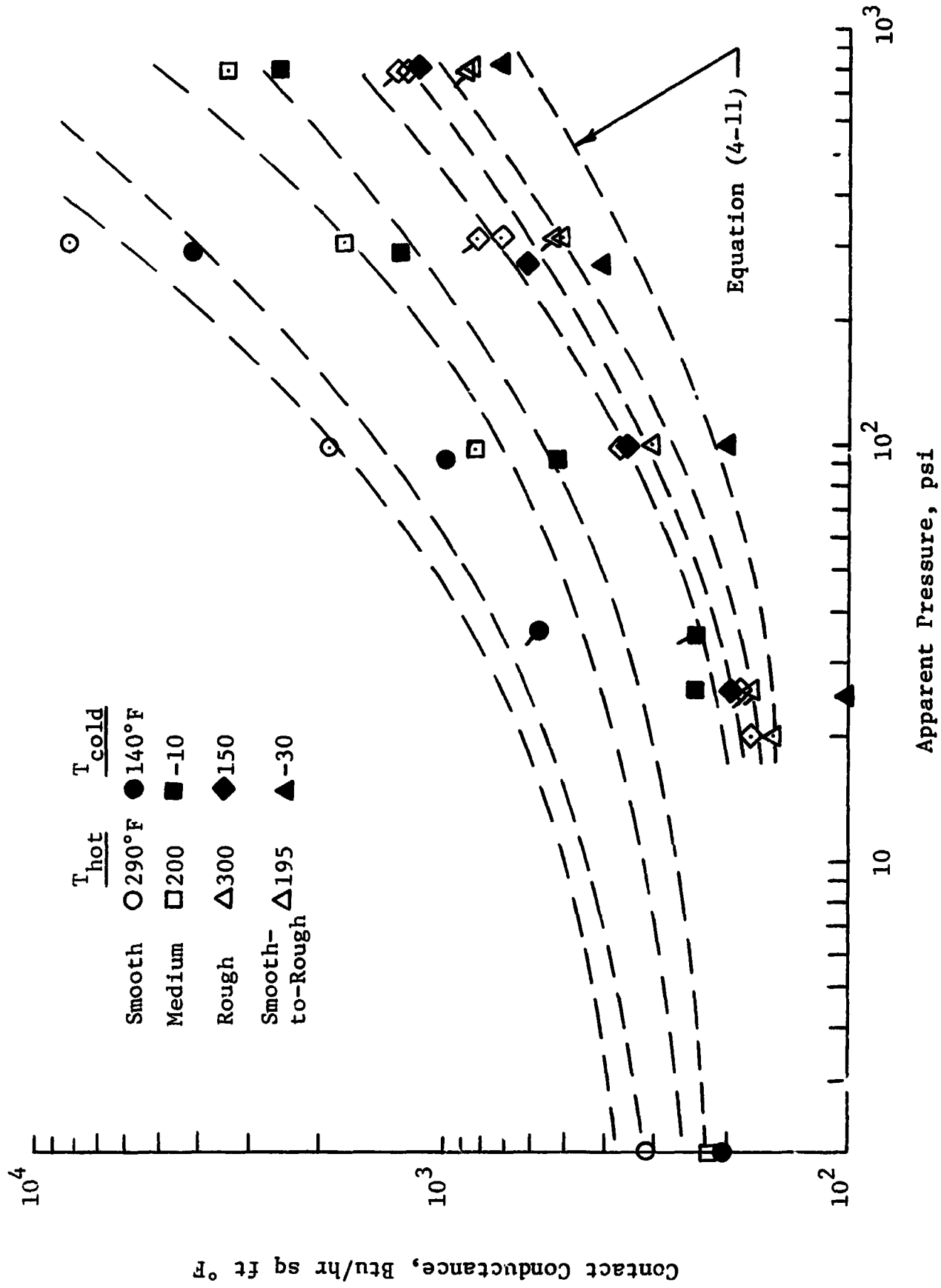
Figure 4-11. Variation of Contact Conductance with Apparent
Interface Pressure for Aluminum 2024 --
Comparison with Dimensionless Correlation
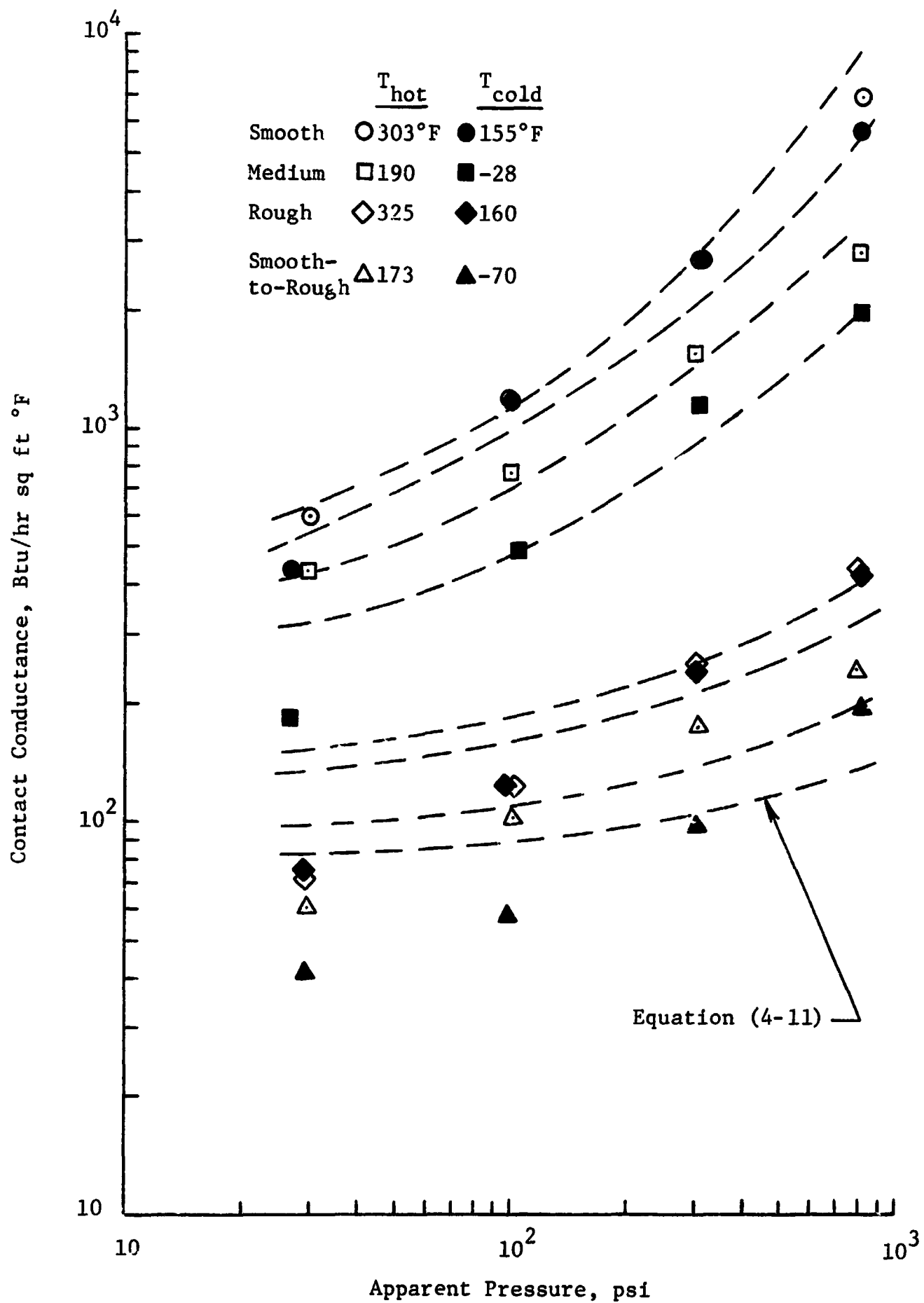
Figure 4-12. Variation of Contact Conductance with Apparent
Interface Pressure for Stainless Steel 304 --
Comparison with Dimensionless Correlation

data are predicted with an average overall error of 24 percent. The high temperature smooth data exhibit the proper trend but are somewhat under-predicted. As with aluminum, the predicted curves increase more rapidly than the data curves as pressure increases. This may be attributed to the small ΔT_j for brass, which causes conductance errors in the high load pressure data for this as for most other soft materials.

The contact conductance data for magnesium AZ31B are given in Figure 4-14 for comparison with predicted values. There appears to be quite poor agreement for the smoother surfaces; however, the agreement for the rougher surfaces is good. The proper trends are shown, but the magnitudes at the higher pressures are substantially over-predicted. As with brass, this over-prediction at the higher pressures may be caused by the error in the ΔT_j. The magnesium smooth and medium surfaces used in this investigation were visibly oxidized even after thorough cleaning, as discussed in Chapter III.

The fact that Equation 4-11 does not always accurately predict the magnitude of the conductance for the smoother surfaces might be explained in terms of a surface film. When two polished, flat surfaces are placed in contact, the oxide film which may be present, forms a relatively unbroken layer between the surfaces. As pressure is increased, the metal-to-metal contact becomes minimal and the oxide film becomes a dominant factor which causes the conductance to be lower than for oxide free surfaces.
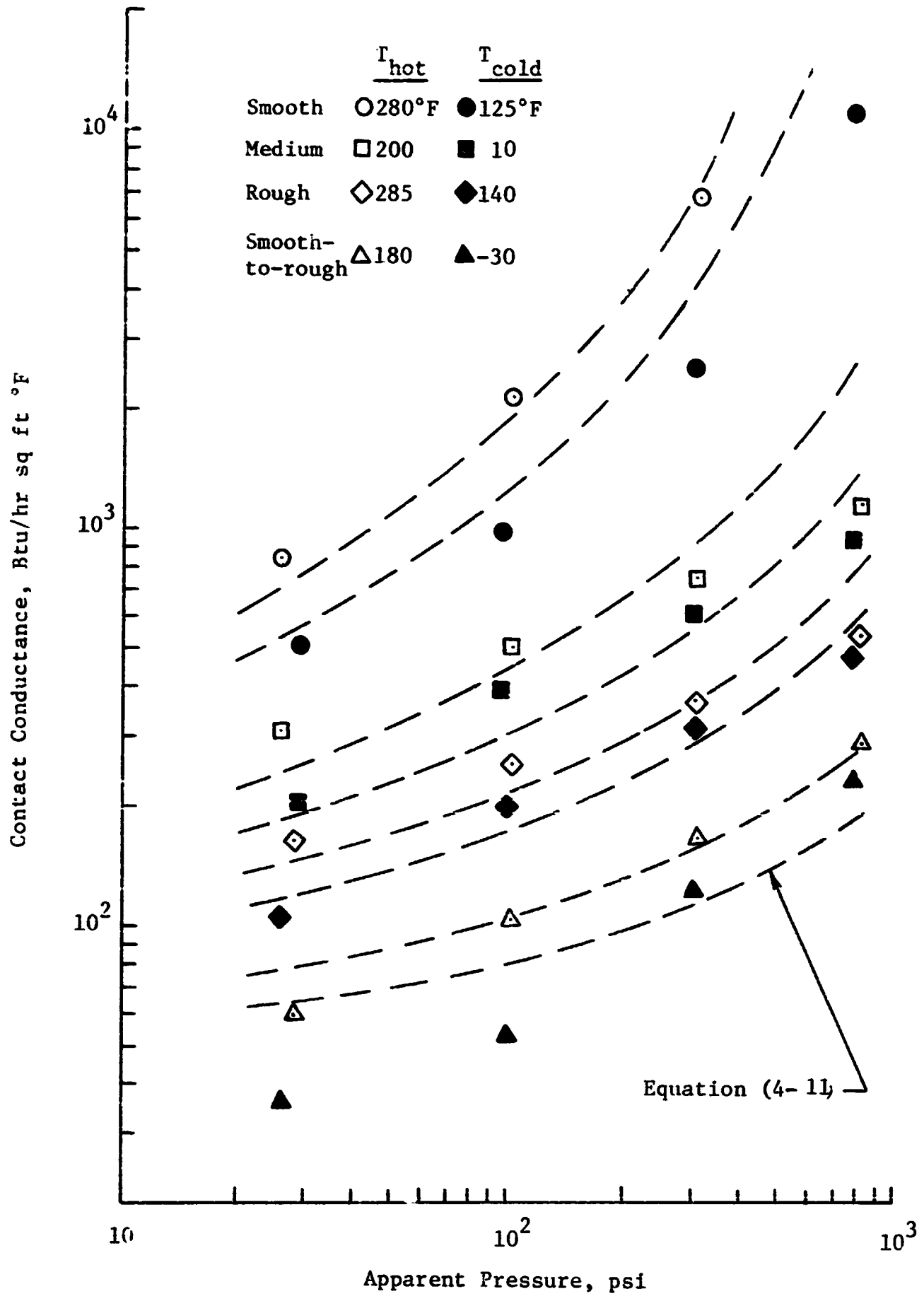
Figure 4-13. Variation of Contact Conductance with Apparent
Interface Pressure for Brass Alloy 271 --
Comparison with Dimensionless Correlation
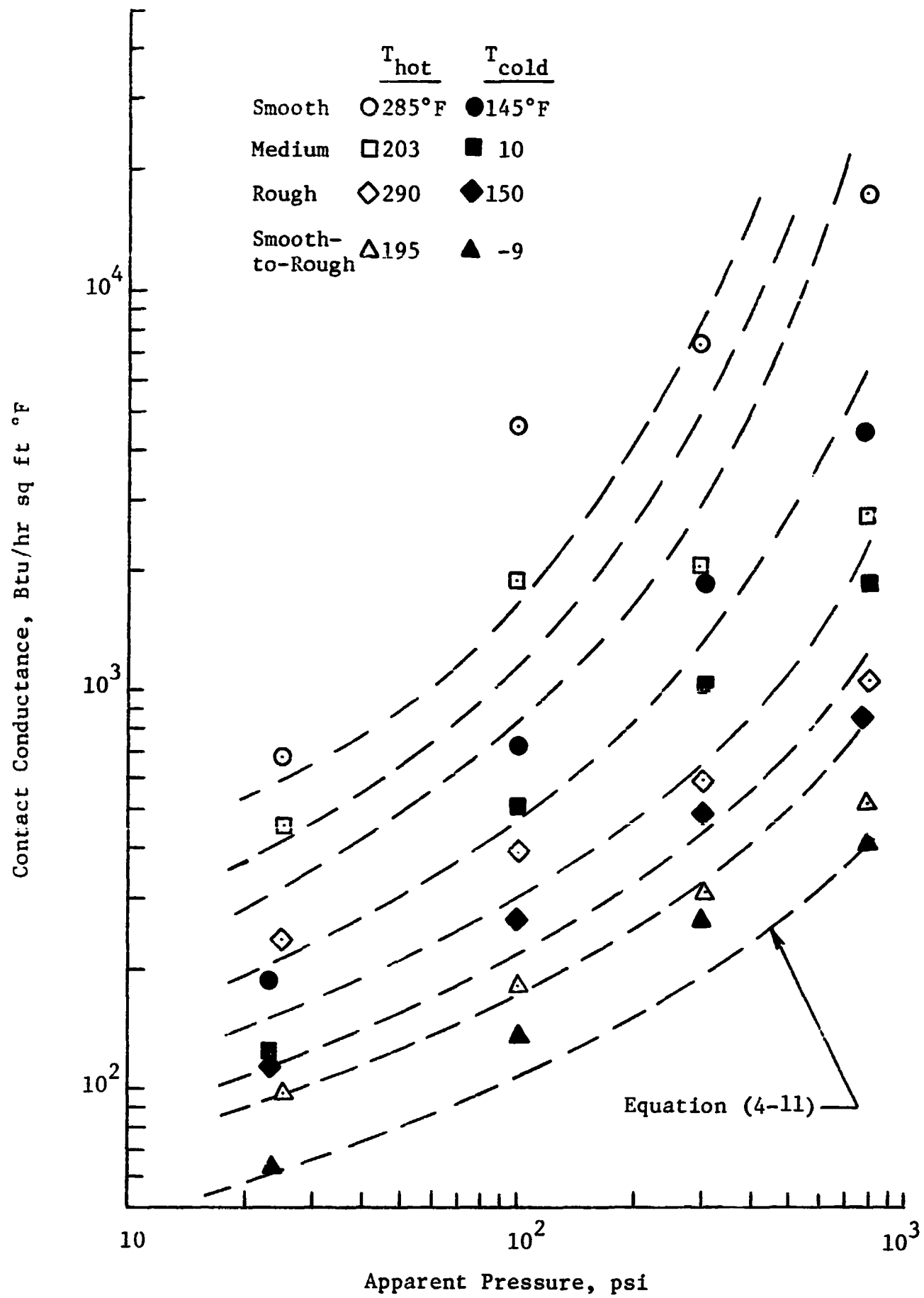
Figure 4-14. Variation of Contact Conductance with Apparent
Interface Pressure for Magnesium AZ31B --
Comparison with Dimensionless Correlation

Published Experimental Data

Experimental data of Bloom [13], Clausing and Chao [20], Fried
[37], and Smuda, et al. [69], are presented in Figure 4-15 for comparison
with the expression developed in the present analysis, equation (4-11).
A wide variation in test materials and mean junction temperatures is
represented. Note the excellent agreement for all of these data.

Experimental data of Cunnington [22], Fried [37], and Hargadon [43]
are presented in Figure 4-16 for comparison with equation (4-11), and
the modified Fenech and Clausing expressions [equations (4-3), (4-4),
and (4-5)].

As pressure increases, all of the equations predict the same
trend. At low pressures, the modified Fenech equation severely under-
predicts the experimental data because of the pressure dependence assumed
in the equation. The magnitude predictions by the expression developed
in this analysis compare well with the data, with an average overall
error of less than 24 percent. The expression of Clausing under-predicts
the experimental data by more than 100 percent in some cases. This
may be attributed to the manner in which the surface parameter is used in
his equation.

The predicted conductance data for most of the other published
experimental investigations agree equally well. Some data deviate
appreciably, however. In many cases, these deviations may be
attributed to assumed test information which was not presented in
the published work.
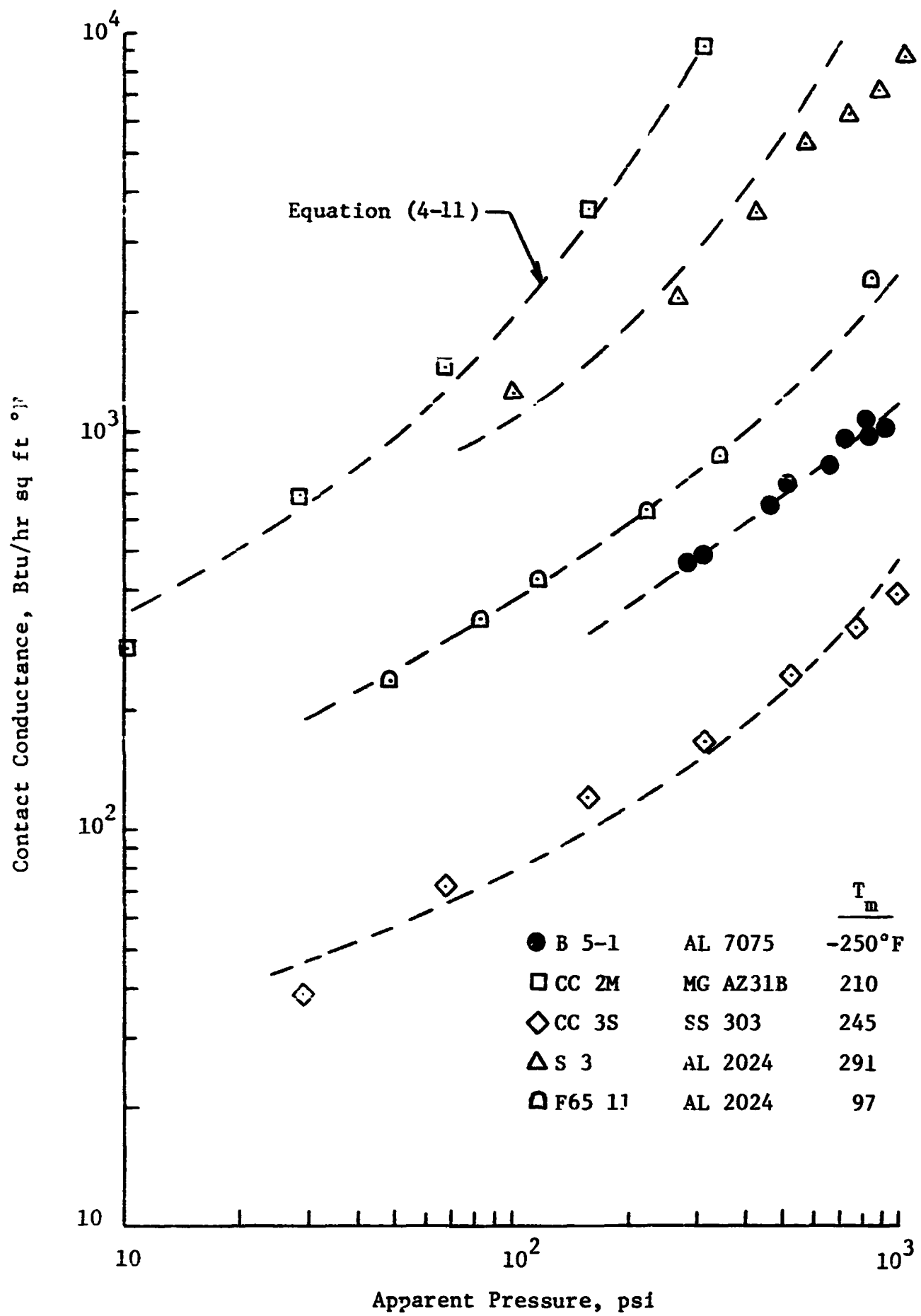
Figure 4-15. Variation of Contact Conductance wi·h Apparent
Interface Pressure for Selected Published Data
-- Comparison with Dimensionless Correlation
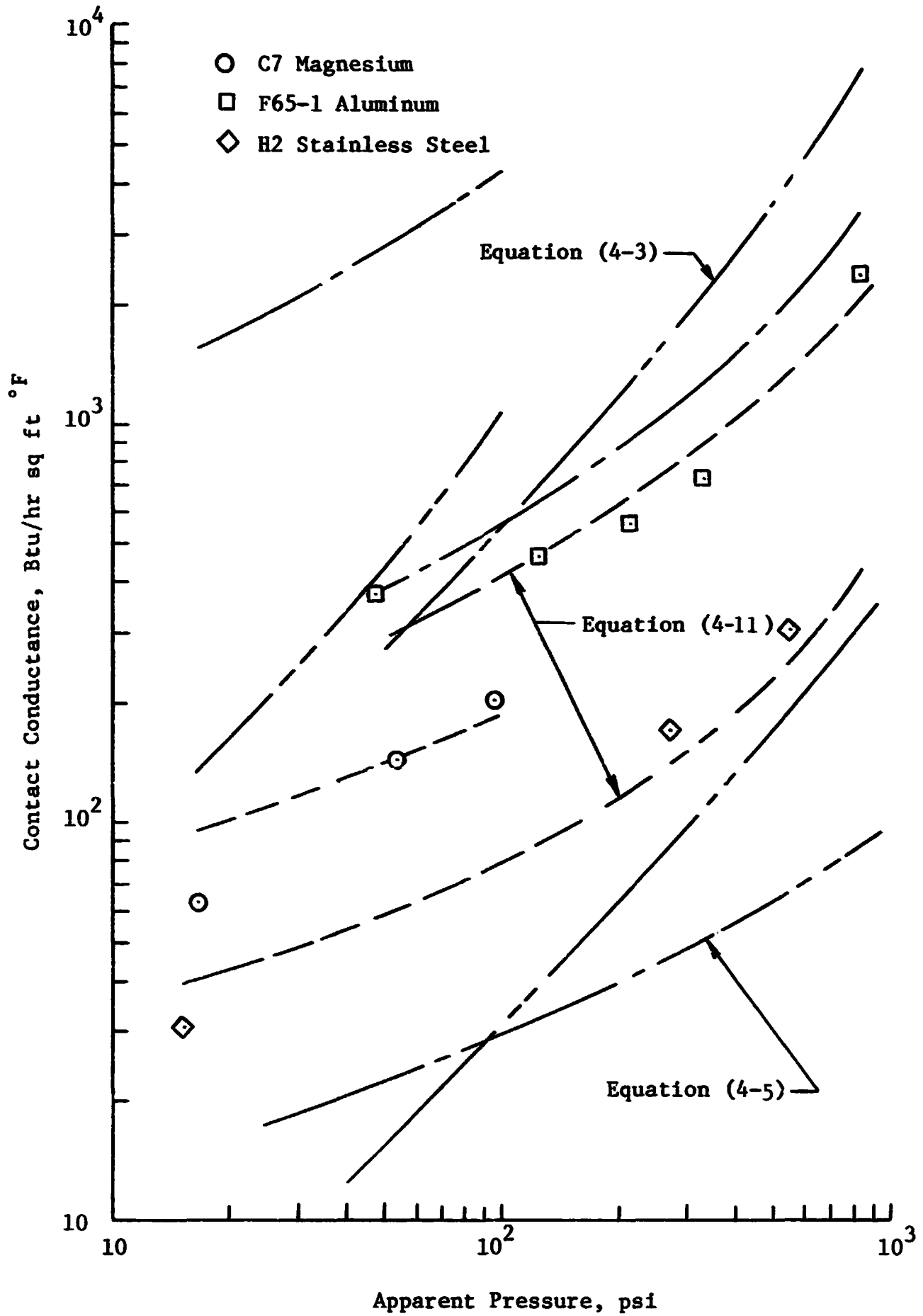
Figure 4-16. Comparisons of the Dimensionless Correlation, Clausing and Chao, and Modified Fenech Theories for Selected Published Data.

CHAPTER V

CONCLUSIONS AND RECOMMENDATIONS

A review of the published studies in thermal contact resistance
has shown that a large variation exists between theoretically predicted
and experimentally measured conductance values. Clearly, the magni-
tudes and trends exhibited by the experimental data have not been well
represented by the published theoretical studies. The purpose of the
present investigation, then, was to develop an equation for the pre-
diction of contact conductance which would be suitable for engineering
applications.

Conclusions

Based on the dimensionless correlation presented in this work,
an expression for the prediction of contact conductance was found to
predict published experimental data, as well as data of the present
investigation. This equation may be written in dimensionless form as:

$$\psi = (5.22 \times 10^{-6} \, \delta_o^* + 0.036 \, P^*T^*)^{0.56} \qquad (4\text{-}11)$$

The most important elements in this prediction equation are the
apparent interface pressure, mean junction temperature, and surface
parameter.

This expression, developed by semi-empirical techniques, predicts
contact conductance within an average overall error of 29 percent for

the data of this investigation. An average overall error of 24 percent

results when several of the data points for the oxidized magnesium sur-

faces are deleted. The average overall error for all experimental data

used, both present and published, is 24 percent.

It has been shown that the resistance due to surface oxidation

is small at normal operating pressures; however, it can become a dominant

factor for very smooth surfaces and at extremely large pressures. The

surface parameter, δ_o, may be adjusted for such oxidation, thus permit-

ting more accurate correlation of contact conductance values for

oxidized surfaces.

Recommendations

As a result of this investigation, it would seem appropriate to

make some recommendations for further study.

1) Although very few experimental tests are conducted with oxide-

free surfaces, little specific work has been done to determine the

actual contribution of such oxide films to the resistance of a contact.

Further, the variation of the surface film thickness with load pressure

should be investigated.

2) Most of the experimental contact conductance data obtained

to date has been for moderate to high load pressures. Those data

obtained at load pressures below fifteen psi exhibit extremely large

variations. Further study of contact conductance at low pressures would supplement existing data.

3) The results of this study might be fruitfully applied to electrical contact situations, such as low-voltage microswitches. By use of the expressions developed in this work, both the area of contact and junction resistivity might be predicted.

4) The techniques of this study might be used to establish a prediction equation for dissimilar metal contacts. Because of limit-ations of the model used in the present analysis, it was not possible to accurately predict conductance values for dissimilar metal contacts using the expression developed herein. Further, the sparsity of pub-lished dissimilar metal experimental data suggests that an experimental investigation should be undertaken to implement any analytical study.

5) There is a considerable amount of published experimental data obtained at atmospheric conditions. The procedures of this study might also be applied to these data.

An expression has been developed for the correlation of thermal contact conductance data. This expression may be used to predict conductance values for any similar metals in terms of the sur-face parameter, mean junction temperature, and interface pressure. The equation is simpler to use and results in more accurate prediction of conductance magnitudes and trends than any such expression pre-viously published, and known to the authors.

BIBLIOGRAPHY

1. Abbott, Rudolph Edward. "Experimental Facilities for Investigating Thermal Contact Conductance in a Vacuum Environment." Unpublished Master's report, Arizona State University (Department of Mechanical Engineering), Tempe, 1967.

2. Alcoa Structural Handbook. Pittsburgh: Aluminum Company of America, 1960.

3. Aluminum Company of America, Alcoa Research Laboratories. Through personal correspondence with C. R. Coppersmith, Manager of the Phoenix Office, June, 1968.

4. American Standards Association. "Surface Texture: Surface Roughness, Waviness and Lay." ASA B-46.1-1962. New York: ASME, 1962.

5. Anaconda American Brass Company, Research Center in Waterbury, Connecticut. Through personal correspondence with W. S. Stempfle, Los Angeles Division, June, 1968.

6. Archard, J.F. "Contact and Rubbing of Flat Surfaces," Journal of Applied Physics, 24:981-988, August, 1953.

7. _____. "Elastic Deformation and the Laws of Friction," Proceedings of the Royal Society (Great Britain), A 243:190-205, 1957.

8. Ascoli, A. and E. Germagnoli. "Measurement of the Thermal Resistance of Uranium and Aluminum Flat Surfaces in Contact," trans. from Energia Nucleare, 3:23-31, 1961, by Redstone Scientific Information Center, RSIC-99, November, 1963.

9. Atkins, Harry. "Bibliography on Thermal Metallic Contact Conductance," NASA TM X-53227, April, 1965.

10. Baker, H. Dean, E. A. Ryder, and N. H. Baker. Temperature Measurement in Engineering, Vol. 1. New York: John Wiley & Sons, 1953.

11. Barrington, Alfred E. High Vacuum Engineering. Englewood Cliffs, New Jersey: Prentice-Hall, Inc., 1963.

12. Birdsall,G.W. (ed.). The Aluminum Data Book. Richmond, Virginia: Reynolds Metal Company, 1965.

13. Bloom, M.F. "Thermal Contact Conductance in a Vacuum Environment," Douglas Aircraft Company Report SM-47700, December, 1964.

14. Blum, Harold A. "Heat Transfer Across Surfaces in Contact: Practical Effects of Transient Temperature and Pressure Environments," NASA CR 69696, October, 1965.

15. Boeschoten, F. and E.F.M. Van der Held. "The Thermal Conductance of Contacts Between Aluminum and Other Metals," Physica, 23:37-44, 1957.

16. Bowden, F.P. and D. Tabor, The Friction and Lubrication of Solids. London: Clarendon Press, 1950.

17. Cetinkale, T.N. and Margaret Fishenden. "Thermal Conductance of Metal Surfaces in Contact," General Discussions on Heat Transfer, Conference of the Institution of Mechanical Engineers and ASME. London: Institution of Mechanical Engineers, 1951.

18. Clark, W.T. and R.W. Powell. "Measurement of Thermal Conduction by the Thermal Comparator," Journal of Scientific Instruments (Great Britain), 39:545-551, 1962.

19. Clausing, A.M. and B.T. Chao. "Thermal Contact Resistance in a Vacuum Environment," ASME Paper No. 64-HT-15, August, 1964.

20. _____. "Thermal Contact Resistance in a Vacuum Environment," University of Illinois Experimental Station Report, ME-TN-242-1, August, 1963.

21. Cocks, M. "The Effect of Compressive and Shearing Forces on the Surface Films Present in Metallic Contacts," Proceedings of the Physical Society (Great Britain), B67:238-248, 1954.

22. Cunnington, G.R., Jr. "Thermal Conductance of Filled Aluminum and Magnesium Joints in a Vacuum Environment," ASME Paper No. 64-WA/HT-40, November, 1964.

23. Dahl, A.I. Temperature: Its Measurement and Control in Science and Industry, Vol. 3. New York: John Wiley & Sons, Inc., 1963.

24. Diels, K. and R. Jaeckel. Leybold Vacuum Handbook. Trans. H. Adam and J. Edwards. Oxford: Pergamon Press, 1966.

25. The Dow Chemical Company, Metal Products Department. Through personal correspondence and enclosures from A.A. Moore, Chief Standards Engineer, Metal Products Department, June, 1968.

26. _____. "Physical Properties of Magnesium and Magnesium Alloys," Revised, April, 1967. (Mimeographed.)

27. Dushman, Saul. Scientific Foundations of Vacuum Technique, Second Edition. New York: John Wiley & Sons, Inc., 1962.

28. D'yachenko, P.E., N.N. Tolkacheva, G.A. Andreev, and T.M. Karpova. "The Actual Contact Area Between Touching Surfaces," Trans. Consultants Bureau. New York: Consultants Bureau, 1964.

29. Dyson, J. and W. Hirst. "The True Contact Area Between Solids," Proceedings of the Physical Society (Great Britain), B 67: 309-312, 1954.

30. Eldridge, E.A. and H.W. Deem (eds.). "Report on Physical Properties of Metals and Alloys from Cryogenic to Elevated Temperatures," ASTM Special Technical Publication No. 296, April, 1961.

31. Fenech, H. and W.M. Rohsenow. "Prediction of Thermal Conductance of Metallic Surfaces in Contact," Journal of Heat Transfer, 85:15-24, February, 1963.

32. _____. "Thermal Conductance of Metallic Surfaces in Contact," United States Atomic Energy Commission Report NY)-2136, May, 1959.

33. Fletcher, Leroy S., Paul A. Smuda, and Donald A. Gyorog. "Thermal Contact Resistance of Selected Low Conductance Interstitial Materials," AIAA Paper No. 68-31, January, 1968.

34. Fried, Erwin. "Thermal Joint Conductance in a Vacuum," ASME Paper 63-AHGT-18, March, 1963.

35. _____. "Study of Interface Thermal Contact Conductance, Summary Report," General Electric Company Document No. 64SD652, 1965.

36. _____. "Study of Interface Thermal Contact Conductance, Summary Report," General Electric Company Document No. 65SE4395, 1964

37. _____. "Study of Interface Thermal Contact Conductance, Summary Report," General Electric Company Document No. 66SD4471, 1966.

38. Fried, Erwin, and Frederick A. Costello. "Interface Thermal Contact Resistance Problem in Space Vehicles," ARS Journal, 32:237-243, February, 1962.

39. Garofalo, F., P.R. Malenock, and G.V. Smith. "Influence of Temperature on the Elastic Constants of Some Commerical Steels," ASTM Special Technical Publication No. 129, 1952.

40. Gex, Roberc C. "Thermal Resistance of Metal-to-Metal Contacts: An Annotated Bibliograrhy," Lockheed Missiles and Space Division SB-61-39, July, 1961.

41. Goldsmith, A., T.E. Waterman, and H.G. Hirschkorn. Handbook of Thermophysical Properties of Solid Materials, Vol. 2 New York: Pergamon Press, 1961.

42. Graff, W.J. "Thermal Conductance across Metal Joints," Machine Design, 32:166-172, September, 1960.

43. Hargadon, Joseph M., Jr. "Thermal Interfa. Conductance of Thermoelectric Generator Hardware," ASME Paper No. 66-WA/NE-2, November, 1966.

44. Held, Wolfgang. "Heat Transfer Between Worked Surfaces," trans. from Algemine Warmetecknik, 8:1-8, 1957, by Redstone Scientific Information Center, RSIC-76, October, 1963.

45. Henry, J.J. and H. Fenech. "The Use of Analog Computers for Determining Surface Parameters Required for Prediction of Thermal Contact Conductance," Journal of Heat Transfer, 86:543-551, November, 1964.

46. Holm, Ragnar. Electric Contacts: The and Application, Fourth Edition. New York: Springer-Verlag, 1967

47. Hudack, Larry J. "An Engineering Analysis of Heat Transfer Through Metallic Surfaces in Contact." Unpublished Master's report, Arizona State University (Department of Mechanical Engineering), Tempe, 1965.

48. Jacobs, R.B. and C Starr. "Thermal Conductance of Metallic Contacts," Review of Scientific Instrumerrs, 10:140-141, April, 1939.

49. Jakob, Max. Heat Trnsfer, Vol. II. New York: John Wiley & Sons, Inc., 195/.

50. Jansson, Richard M. "The Heat Transfer Properties of Structural Elements for Space Instruments," M.I.T. Instrumentation Lab Report E-1173, June, 1962.

51. eng, D.R. "Thermal Contact Resistance in Vacuum," Journal of Heat Transfer, 89:275-276, August, 1967.

52. Kottler, F. "Elektrostatik der Leiter," Handbuch der Physik, Vol. 12. Berlin: Springer-Verlag, 1927. Pp. 472-473.

53. Kouwenhoven, W.B. and J.H. Potter. "Thermal Resistance of Metal Contacts," Journal of American Welding Society, 27:515-520, October, 1948.

54. Lafferty, J.M. "Techniques of High Vacuum," General Electric Company Report No. 64-Rl-3791 G, November, 1964.

55. Laming, L.C. "Thermal Conductance of Machined Metal Contacts," International Developments in Heat Transfer, Proceedings of the 1961-62 Heat Transfer Conference. New York: ASME, 1962. Pp. 65-76.

56. McAdams, W.H. heat Transmission, Third Fdition. New York: McGraw-Hill Book Company, 1954.

57. Miller, V.S. "Results of Experimental Investigation of Contact Heat Exchange Between Flat Metal Surfaces," trans. from Teploobmin ta Hidrodynamika, 20:44-53, 1960, by Redstone Scientific Information Center, RSIC-272, September, 1964.

58. Minges, Merrill L. "Thermal Contact R .stance: Volume 1— A Keview of the Literature," Air Force Materials Laboratory, AFML-TR-65-375, April, 1966.

59. Murphy, Glenn. Similitude in Engineering. New York: The Ronald Press Company, 1950.

60. Oberg, Erik and F.D. Jones. Machinery's Handbook: A Reference Book for the Mechanical Engineer, Draftsman, Toolmaker, and Machinist, Seventeenth Edition. New York: The Industrial Press, 1964.

61. Ozisik, M. Necati and Daniel Hughes. "Thermal Contact Conductance of Smooth-to-Rough Contact Joints," ASME Paper No. 66-WA/HT-54, November, 1966.

62. Pfahl, R.C. and D. Dropkin. "Thermocouple Temperature Perturbations in Low-Conductivity Materials," ASME Paper No. 66-WA/HT-8, November, 1966.

63. Pirani, M. and J. Yarwood. Principles of Vacuum Engineering. New York: Reinhold Publishing Corporation, 1961.

64. Roess, L.C. "Theory of Spreading Conductance," Appendix A, Unpublished Report, Beacon Laboratories of Texas Company, Beacon, New York, 1949.

65. Schenck, Hilbert, Jr. Theories of Engineering Experimentation. New York: McGraw-Hill Book Company, 1961.

66. Shenker, Henry, et al. Reference Tables for Thermocouples. National Bureau of Standards, United States Department of Commerce, Circular 561. Washington: Government Printing Office, 1955.

67. Shlykov, Yu P. and E. A. Ganin. "Experimental Study of Contact Heat Exchange," trans. from Teploenergetika, 8:73-76, 1961, by Redstone Scientific Information Center, RSIC-128, January, 1964.

68. Shlykov, Yu P., E. A. Ganin, and N. B. Demkin. "Analysis of Contact Heat Exchange," trans. from Teploenergetika, 7:72-76, 1960, by Redstone Scientific Information Center, RSIC-117, January, 1964.

69. Smuda, P. A., L. S. Fletcher, and D. A. Gyorog. "Heat Transfer between Surfaces in Contact: The Effect of Low Conductance Interstitial Materials; Part I: Experimental Verification of NASA Test Apparatus," NASA CR 73122, June, 1967.

70. Smuda, P. A. and D. A. Gyorog. "Heat Transfer between Surfaces in Contact: The Effect of Low Conductance Interstitial Materials: Part III: Comparison of the Effective Thermal Insulation for Interstitial Materials Under Compressive Loads. Arizona State University, Mechanical Engineering Department, ME-TR-033-3, August, 1968.

71. Sonokama, Konomo. "Contact Thermal Resistance," trans. from Journal of the Japan Society of Mechanical Engineers, 64:240-250, 1961, by Redstone Scientific Information Center, RSIC-215, July, 1964.

72. Stubstad, W. R. "Measurements of Thermal Contact Conductance in Vacuum," ASME Paper No. 63-WA-150, November, 1963.

73. _____. "Thermal Contact Resistance between Thin Plates in Vacuum," ASME Paper No. 65-HT-16, August, 1965.

74. Tachibana, F. "Study on Thermal Resistance of Contact Surface," trans. from Nihon Kikai Gakukai Shi, 55:102-107, 1952, by Redstone Scientific Information Center, RSIC-29, June, 1963.

75. Tarasov, L. P. "Relation of Surface-Roughness Readings to Actual Surface Profile," Transactions of the ASME, 67:189-196, April, 1945.

76. Thomas, T. R. and S. D. Probert. "Thermal Contact of Solids," Chemical and Process Engineering, 47:51-60, November, 1966.

77. Timoshenko, S. and J. N. Goodier. Theory of Elasticity. New York: McGraw-Hill Book Company, 1951.

78. Touloukian, Y. S. (ed.). Metallic Elements and Their Alloys, Vol. I. Lafayette, Indiana: Thermophysical Properties Research Center, Purdue University, 1966.

79. United States Steel. "Steels for Elevated Temperature Service." Pittsburgh: United States Steel, 1965.

80. Vidoni, Carlotta M. "Thermal Resistance of Contacting Surfaces: Heat Transfer Bibliography," Lawrence Radiation Laboratory, UCRL-14264, June, 1965.

81. Weills, N. D. and E. A. Ryder. "Thermal Resistance Measurements of Joints Formed between Stationary Metal Surfaces," Transactions of the ASME, 71:259-267, April, 1949.

82. Wilson, R. W. "The Contact Resistance and Mechanical Properties of Surface Films on Metals," Proceedings of the Physical Society (Great Britain), B 68:625-641, 1955.

83. Wong, H. T. "Thermal Conductance of Metallic Contacts - A Survey," paper presented at the International Symposium on Thermal Conductivity, National Physical Laboratory, England, July, 1964.

84. Yovanovich, M. Michael. "Thermal Contact Conductance in a Vacuum," M.I.T. Engineering Projects Laboratory, DSR Project No. 4542, November, 1965.

85. Yovanovich, M. Michael and H. Fenech. "Thermal Contact Conductance of Nominally-Flat, Rough Surfaces in a Vacuum Environment," AIAA Paper No. 66-42, January, 1966.

APPENDIXES

APPENDIX A

PUBLISHED EXPERIMENTAL DATA

The experimental data in the literature were analyzed thoroughly
in order to determine which data were accurate and would be useful for
the present analysis. The resulting data were considered satisfactory
for use in determining the trends of the experimental data, as well as
for comparison with the predicted values of contact conductance. These
data are listed here as given by the investigators, except as indicated.
The dimensions of the variables presented are as follows:

P_a	psi
h_c	Btu/hr sq ft°F
ΔT	°F
T_m	°F
FD	microinches
RD	microinches
k_h	Btu/hr ft°F
E	psi
β	in/in°F

TABLE A-1

PUBLISHED ALUMINUM DATA

P_a	h_c	ΔT	T_m		
280	465	22.7	-241	Run:	B 5-1 [13]
458	647	16.3	-256		AL 7075-T6
646	815	12.9	-262	FD =	100-200
834	954	10.9	-268	RD =	3-5
920	987	10.5	-270	k_m =	46.5*
309	461	25.1	-232	E =	$1.18 \times 10^{7*}$
312	488	23.7	-227		
512	741	16.9	-242	β =	$12 \times 10^{-6*}$
713	953	14.6	-244		
802	1080	13.9	-244		
73	382	42.9	-127	Run:	B 5-2 [13]
267	1260	13.2	-221		AL 7075-T6
662	233u	7.2	-247	FD =	200
856	2475	6.6	-251	RD =	15-17
929	2515	6.6	-253	k_m =	49.0*
				E =	$1.17 \times 10^{-7*}$
				β =	$12 \times 10^{-6*}$
166	202	51.6	-145	Run:	B 5-4 [13]
213	269	47.2	-232		AL 7075-T6
554	540	28.4	-230	FD =	150-500
719	741	24.4	-229	RD =	10-45
968	927	20.6	-231	k_m =	49*
118	190	44.9	-223	E =	$1.17 \times 10^{7*}$
309	320	40.2	-222		
493	421	34.6	-227	β =	$12 \times 10^{-6*}$
707	638	27.0	-230		
891	786	24.5	-238		
474	859	18.9	-236	Run:	B 5-5 [13]
672	1180	13.8	-243		AL 7075-T6
822	1490	11.2	-245	FD =	200-300
936	1600	10.5	-248	RD =	7-60
251	678	24.3	-231	k_m =	42*
439	910	17.7	-237	E =	$1.17 \times 10^{7*}$
668	1250	13.5	-245		
866	1410	11.7	-251	β =	$12 \times 10^{-6*}$
945	1460	11.3	-253		

* Selected from the literature for purposes of the present analysis.

TABLE A-1 (Cont'd)

P_a	h_c	ΔT	T_m			
51	520	9.9	243	Run:		B 5-7 [13]
242	1390	4.7	295			AL 7075-T6
446	1900	3.4	299	FD	=	200-500
600	2200			RD	=	10-25
800	2400			k_m	=	91*
				E	=	$1.01 \times 10^{7*}$
				β	=	$12 \times 10^{-6*}$
10.4	88	164	220	Run:		CC 1A [20]
28.4	191	109				AL 2024-T4
44.0	365	71.5		FD	=	115
86.2	660	46.7		RD	=	12
157	1330	30.9		k_h	=	79.0
310	2300	19.4		E	=	1×10^{7}
518	4520	10.6				
759	5670	8.8		β	=	$12 \times 10^{-6*}$
986	7940	6.4				
10.4	219	113	238	Run:		CC 2A [20]
44.0	513	65.8				AL 2024-T4
86.2	821	44.9		FD	=	115
157	1330	30.9		RD	=	12
310	2300	19.4		k_h	=	82.0
518	4520	10.6		E	=	1×10^{7}
759	5670	8.8				
986	7940	6.4		β	=	$12 \times 10^{-6*}$
10.4	38.2	253	240	Run:		CC 5A [20]
28.4	133	161				AL 2024-T4
67	476	69.3		FD	=	60
157	1220	32.5		RD	=	3
310	2450	17.6		k_h	=	82.0
518	4160	10.7		E	=	1×10^{7}
759	6500	6.9				
986	9500	5.0		β	=	$12 \times 10^{-6*}$
10.4	54	238	235	Run:		CC 6A [20]
28.4	213	128				AL 2024-T4
67	440	78.8		FD	=	110
157	762	52.5		RD	=	3
310	1270	34.5		k_h	=	82.0
518	1970	23.4		E	=	1×10^{7}
759	2780	17.0				
986	3740	12.9		β	=	$12 \times 10^{-6*}$

TABLE A-1 (Cont'd)

P_a	h_c	ΔT	T_m			
10.4	212	90	235	Run:		CC 7A [20]
28.4	452	63				AL 2024-T4
67	632	51.4		FD	=	110
157	1120	33.3		RD	=	45-80
310	1880	22.0		k_h	=	85.0
518	2640	16.6				
759	3380	13.6		E	=	1×10^7
986	4280	11.0		β	=	12×10^{-6}*
16.9	220		155*	Run:		CN 5 [22]
35	370					AL 6061-T4
54	495			FD	=	35
72	590			RD	=	12-18
92	680			k_m	=	109*
				E	=	1×10^{7}*
				β	=	12×10^{-6}*
16.9	210		200*	Run:		CN 6 [22]
54	620					AL 6061-T4
93	830			FD	=	25
				RD	=	46-50
				k_m	=	111*
				E	=	1×10^{7}*
				β	=	12×10^{-6}*
192	1642	29.3	286	Run:		FL A2 [33]
287	3821	13.8	297			AL 2024-T4
187	1665	29.0	288	FD	=	25-40
105	749	52.6	278	FD	=	3-5
104	896	47.9	277	k_m	=	108.9
186	1522	31.2	289			
277	3421	15.9	291	E	=	1.01×10^{7}*
277	3219	17.2	294	β	=	12×10^{-6}*
105	925	54.1	278			
239	2607	23.0	287			
385	3515	18.0	289			

TABLE A-1 (Cont'd)

P_a	h_c	ΔT	T_m			
102	487	86.4	-42	Run:		FL A4 [33]
305	1242	45.8	-53			AL 2024-T4
102	537	78.1	-33	FD	=	25-40
305	1353	40.5	-28	RD	=	3-5
				k_m	=	98.2
				E	=	$1.12 \times 10^{7*}$
				β	=	$12 \times 10^{-6*}$
101	578	62.5	-13	Run:		FL A6 [33]
297	1888	28.5	-25			AL 2024-T4
102	512	69.4	-20	FD	=	25-40
298	1665	31.8	-23	RD	=	3-5
				k_m	=	99.2
				E	=	$1.11 \times 10^{7*}$
				β	=	$12 \times 10^{-6*}$
99	1389	27.6	281	Run:		FL A8 [33]
306	2910	16.3	264			AL 2024-T4
98	770	43.8	267	FD	=	25-40
99	857	44.4	274	RD	=	3-5
305	3042	15.4	265	k_m	=	108.6
				E	=	$1.02 \times 10^{7*}$
				β	=	$12 \times 10^{-6*}$
47	367		~98*	Run:		FR 65:1-6 [36]
121	457					AL 2024-T4
214	560			FD	=	100-150
326	713			RD	=	40-50
805	2382			k_m	=	69.5
1120	3814			E	=	$1.07 \times 10^{7*}$
				β	=	$12 \times 10^{-6*}$
48	237		~98*	Run:		FR 65:11-17 [36]
83	333					AL 2024-T4
119	424			FD	=	100-150
226	621			RD	=	40-50
341	813			k_m	=	69.5
818	2414			E	=	$1.07 \times 10^{7*}$
1132	3781			β	=	$12 \times 10^{-6*}$

TABLE A-1 (Cont'd)

P_a	h_c	ΔT	T_m			
560	1500		~180*	Run:		FR 66:31-6 [37]
1050	3415					AL 7075-T6
1814	6761			FD	=	210-240
2021	7849			RD	=	160-170
2419**	42111**			k_m	=	75.5*
3024	8644			E	=	$1.04 \times 10^{7*}$
				β	=	$12 \times 10^{-6*}$
535	1244		~220*	Run:		FR 66:88-92 [37]
764	2308					AL 7075-T6
1311	4783			FD	=	6
1853	10249			RD	=	4
2476	23679			k_m	=	82.6*
				E	=	$1.03 \times 10^{7*}$
				β	=	$12 \times 10^{-6*}$
118	792	35.9	215	Run:		S2 [69]
251	2720	13.3	232			AL 2024-T4
384	4710	7.9	233	FD	=	23-35
539	7900	5.0	240	RD	=	3-5
702	9440	4.1	232	k_m	=	82.6
834	12120	3.2	236	E	=	$1.06 \times 10^{7*}$
1009	14200	2.6	229	β	=	$12 \times 10^{-6*}$
114	1270	34.5	280	Run:		S3 [69]
268	2190	22.3	289			AL 2024-T4
418	3550	14.3	291	FD	=	35-55
567	5240	10.0	293	RD	=	3-5
732	6190	8.6	294	k_m	=	88.8
881	7190	7.5	295	E	=	$1.06 \times 10^{7*}$
1038	8680	6.3	296	β	=	$12 \times 10^{-6*}$

** Data deleted in analysis

TABLE A-1 (Cont'd)

P_a	h_c	ΔT	T_m		
260	2340	20.0	285	Run:	S4 [69]
406	3400	109.0	281		AL 2024-T4
554	4370	71.5	292	FD =	35-55
722	5400	46.7	293	RD =	3-5
860	7520	33.8	293	k_m =	88.8
				E =	$1.06 \times 10^{7*}$
				β =	$12 \times 10^{-6*}$
106	148	45.8	-236	Run·	S A2 [70]
203	212	35.7	-250		AL 2024-T4
300	371	23.0	-257	FD =	30-50
303	703	41.6	-159	RD =	3-5
304	1011	58.7	-33	k_m =	89.5
				E =	$1.15 \times 10^{7*}$
				β =	$12 \times 10^{-6*}$

TABLE A-2

PUBLISHED STAINLESS STEEL DATA

P_a	h_c	ΔT	T_m	
29.2	38.4	122	245	Run: CC 3S [20]
67.7	71.7	77.2		SS 303
157	120	51.2		FD = 75
311	168	37.9		RD = 3
519	244	27.9		k_h = 9.53
760	321	21.2		$E = 2.8 \times 10^7$
987	396	19.4		$\beta = 9.5 \times 10^{-6}$*
236	70		⁓390*	Run: FR 66: 4-12 [37]
681	102			SS 304
⁓ 8	120			FD = 760-1000
1558	211			k_D = 300-325
1814	230			γ_m = 10.4*
2476	340			$E = 2.64 \times 10^{7}$*
2884	48⁄			
3591	775			$\beta = 9.5 \times 10^{-6}$*
3909	1047			
15	30		255	Run: H2 [43]
260	170			SS 340
545	300			FD = 500
810	415			RD = 50-70
				k_m = 9.82*
				$E = 2.8 \times 10^{7}$*
				$\beta = 9.5 \times 10^{-6}$*

---

*Selected from the literature for purposes of the present analysis.

TABLE A-3

PUBLISHED BRASS DATA

P_a	h_c	ΔT	T_m	
11.1	172	65	340	Run: CC 1B [20]
29.2	245	64		Br Alloy 271
44.6	259	64		FD = 410
87	346	57		RD = 12-14
157	465	50		k_h = 69
311	652	41		E = 13.1 x 10^6
519	918	33		
760	1126	29		β = 11.8 x 10^{-6}*
954	1327	26		
11.1	126	86	265	Run: CC 2B [20]
29.2	220	70		Br Alloy 271
44.6	257	63		FD = 390
87	334	58		RD = 14
157	432	53		k_h = 66.5
311	5?	44.5		E = 13.35 x 10^6
519	8??	36		
750	1045	30.9		β = 11.8 x 10^{-6}*
954	1260	27		
11.1	93.5	118	160	Run: CC 3B [20]
29.2	148	103		Br Alloy 271
44.6	174	92.5		FD = 475
87	238	81		RD = 14-18
157	316	72		k_h = 62.5
311	422	62		E = 13.7 x 10^6
519	579	51.5		
760	706	45.5		β = 11.8 x 10^{-6}*
954	849	40		
11.1	158	134	260	Run: CC 4B [20]
29.2	253	98.0		Br Alloy 271
44.6	289	91.8		FD = 390
86.9	370	78.1		RD = 14
157	472	67.8		k_h = 66.5
311	647	54.1		E = 13.4 x 10^6
519	881	42.5		
760	1182	33.2		β = 11.8 x 10^{-6}*
954	1390	28.9		

*Selected from the literature for purposes of the present analysis.

TABLE A-4

PUBLISHED MAGNESIUM DATA

P_a	h_c	ΔT	T_m	
10.2	35.0	201	215	Run: CC 1M [20]
28.4	85.3	142		MG AZ 31B
67	152	105		FD = 22.꞉
157	344	61.4		RD = 3
310	816	31.7		R_h = 50.8
518	1540	18.0		
759	2270	12.6		$E = 6.1 \times 10^6$
986	3200	9.0		$\beta = 14.4 \times 10^{-6*}$
10.2	283	68.7	210	Run: CC 2M [20]
28.4	687	33.6		MG AZ 31B
67	1450	17.4		FD = 53
157	3570	7.5		RD = 3
311	9100	3.0		k_m = 49.6
				$E = 6.1 \times 10^6$
				$\beta = 14.4 \; \div \; 10^{-6*}$
10.2	61	170	210	Run: CC 3M [20]
28.4	145	107		MG AZ 31B
67	511	43		FD = 130
157	1250	20		RD = 3
310	2320	11		k_m = 49.3
518	5050	5.4		$E = 6.1 \times 10^6$
759	8700	3.2		$\beta = 14.4 \times 10^{-6*}$
16.9	62		150	Run: CN 7 [22]
54	150			MG AZ 31B
93	200			FD = 25
				RD = 100-125
				k_m = 48.3*
				$E = 6.1 \times 10^{6*}$
				$\beta = 14.4 \times 10^{-6*}$

* Selected from the literature for purposes of the present analysis.

TABLE A-4 (Cont'd)

P_a	h_c	ΔT	T_m	
143	335	~103*	Rr : FR 65: 134-41 [36]	
179	263		MG AZ 31B	
218	279		FD = 23	
433	697		RD = 5-7	
552	1785		k_m = 46.5*	
796**	14969**		$E = 6.1 \times 10^{6*}$	
917**	7985**			
1257	5755		$\beta = 14.4 \times 10^{-6*}$	
471	957	~75*	Run: FR 66: 57-66 [37]	
764	1444		MG AZ 31B	
974	2375		FD = 6	
1331	3872		RD = 4	
1515	4975		k_m = 44.9*	
1993	12309		$E = 6.5 \times 10^{6*}$	
2470**	89590**			
2674	21293		$\beta = 14.4 \times 10^{-6*}$	
3043	31380			
3266	94543			

APPENDIX B

PRESENT EXPERIMENTAL DATA

The full scope of an experimental investigation is not suffi-
ciently represented merely by presenting the contact conductance
data obtained. Material properties and surface conditions of the
test materials are as important as the conductance data. The signi-
ficant material properties useful in data analysis, including those
essential to this investigation, are presented in this section. The
specimen configuration, surface finish, surface hardness, thermal
conductivity, coefficient of thermal expansion and modulus of elas-
ticity are discussed briefly in terms of the property values used,
with the appropriate references cited. The thermal contact conduct-
ance data for this investigation are also presented in tabular form.

Specimen Configuration

Detailed drawings of the specimens are shown in Figures B-1 and
B-2, with the test surfaces noted. Identical specimen sets were
machined from aluminum 2024-T4, brass alloy 271, stainless steel 304,
and magnesium AZ31B. Each specimen set consisted of five pieces;
one source end, and two each of the center slug and sink or threaded
end. The contacting surfaces were numbered one through seven. Sur-
faces one and two were lapped and polished; three and four were
sanded; and five, six, and seven were peened.

Note 1

Drill and tap 2 holes,
4-40 thread, 1/2 inch
deep.

Note 2

Drill 3 holes, #56
drill, 17/32 inch
deep. All positions
±0.001 from each
other.

Note 3

Drill 1 hole, #56
drill, 3/32 inch
deep, 180° opposite
center hole.

Note 4

All dimensions in
inches.
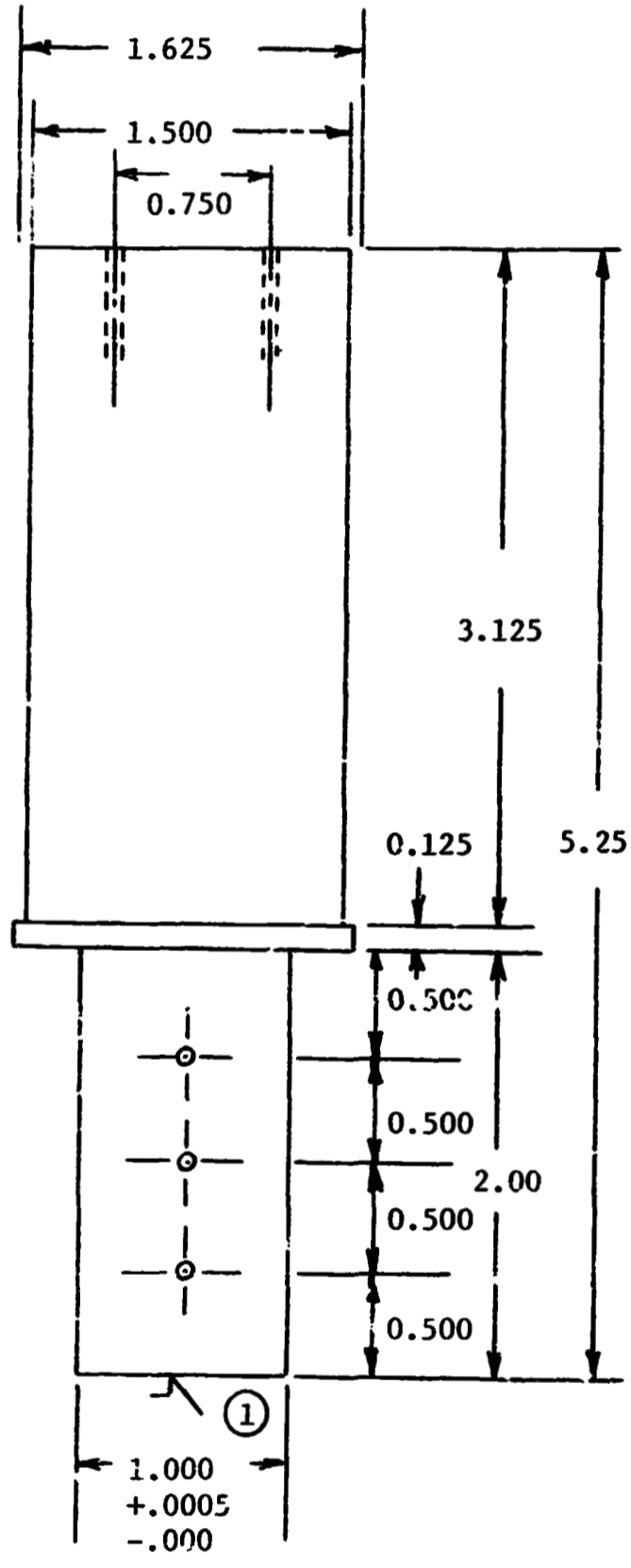
Figure B-1. Detailed Drawing of the Source Specimen.

Note 1

Drill 3 holes, #56
  drill, 17/32 inch
  deep. All positions
  ±0.001 from each
  other.

Note 2

Drill 1 hole, #56
  drill, 3/32 inch
  deep, 180° opposite
  center hole.

Note 3

All dimensions in
  inches.
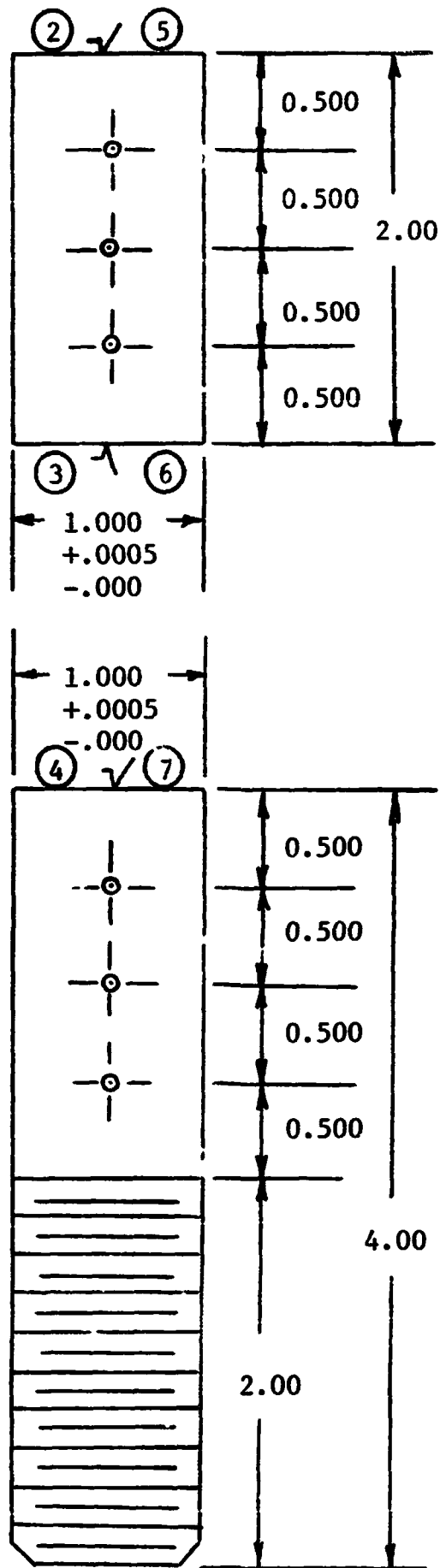
8 threads/inch

Detailed Drawing of the Center and Sink Specimens.

Surface Finish Measurements

The condition of each specimen surface used in this investigation was measured with a Bendix Micrometrical Proficorder and Profilometer. Both the proficorder and profilometer were set for 0.030-inch cutoff. The stylus diameter on the proficorder was 0.0001 inches; however, a 0.005-inch diameter stylus was used on the profilometer. Several traces were made on two specimens to assure that any random trace would adequately represent the surface condition. The remainder of the surfaces were then measured with one trace across the sample. The resulting values for flatness and roughness deviations are listed in Table B-1.

Hardness

Although hardness data are not essential in determining the experimental values of thermal contact conductance, hardness is one of the factors considered in many analyses of contact conductance. The hardness values were obtained for each type of surface with a Wilson Rockwell Hardness Tester, Model 3-QR. A Kendent Diamond Cone indentor was used for the harder surfaces, and a one-sixteenth-inch diameter ball indentor was used for the remaining surfaces. A series of indentations was made on each surface and the resulting hardness ˙ ₃dings were averaged. These values of hardness were then converted to a Vickers hardness number by means of a Comparative Hardness Chart published by the Riehle division of Ametek Corpor-tion. The final hardness values are presented in Table B-1.

TABLE B-1

SURFACF CHARACTERISTICS

Material	Surface	Flatness (μ in)	Roughness (μ in)	Hardness (Vickers)
Aluminum	1	15	2	131
2024-T4	2	20	3	131
	3	400	55	133
	4	530	63	133
	5	3100	5	137
	6	2800	8	137
	7	3400	6	137
Stainless	1	20	2	203
Steel 304	2	25	2	203
	3	150	36	206
	4	180	30	206
	5	4300	2	285
	6	4300	3	285
	7	3600	3	285
Magnesium	1	30	4	57
	2	40	4	57
	3	350	110	60
	4	200	125	60
	5	3900	5	79
	6	4200	7	79
	7	4500	6	79
Brass Alloy	1	60	2	108
271	2	50	2	108
	3	700	60	113
	4	540	63	113
	5	4500	7	160
	6	4100	6	160
	7	4700	7	160

Thermal Conductivity

Accurate knowledge of the specimen material thermal conductivity is essential since it is used to calculate the heat flux across the contacting interface. These conductivity values are generally available in the literature; however, some materials experience property changes with annealing and must be individually determined. Since aluminum is one of these materials with changeable properties, the aluminum 2024-T4 specimens were annealed at 575°F for twenty-four hours before use, to assure knowledge of specific conditions. An apparatus was built to measure the thermal conductivity of solid metallic materials [69]. Tests of the annealed aluminum were found to agree very favorably with the published values presented by Eldridge and Deem [30] and Goldsmith, et al [41]. The thermal conductivity values for the remainder of the materials were selected from the literature since heat treatment does not affect the thermal material properties appreciably. The thermal conductivity for brass alloy type 271* was obtained from data presented by Goldsmith, et al [41] and by the Anaconda American Brass Company [5]. Thermal conductivity data for magnesium AZ31B were obtained from Eldridge and Deem [30] and the Dow Chemical Company [25, 26]. The thermal conductivity values for stainless steel 304 were taken from Touloukian [78], Goldsmith, et al [41], McAdams [56], and the United States Steel Company [79]. The thermal conductivities for materials used in this investigation are shown as a function of temperature in Figure B-3.

---

*The new Copper Development Association designation for this alloy is the number 360.
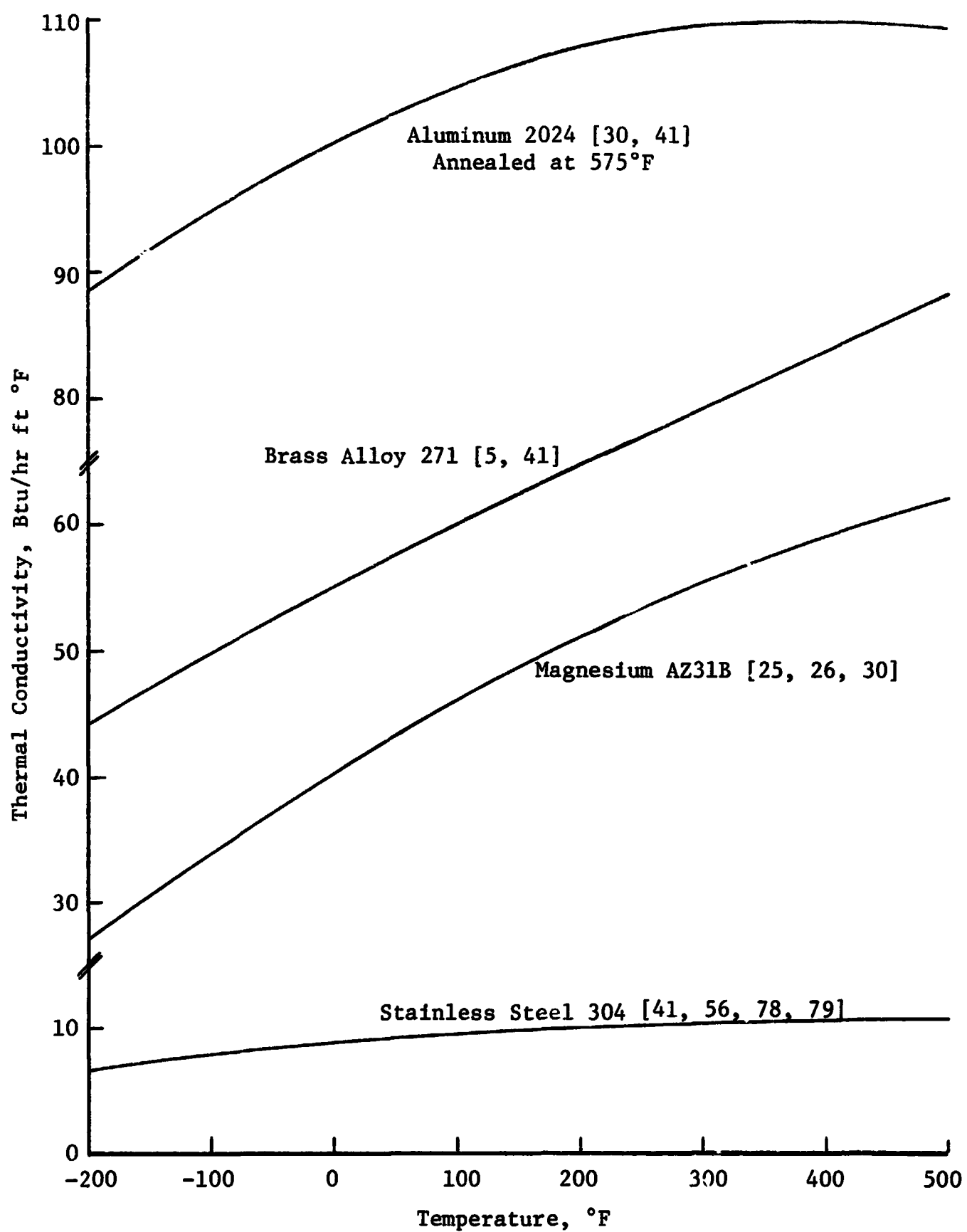
Figure B-3. Variation of Thermal Conductivity with Temperature for Aluminum, Stainless Steel, Brass, and Magnesium.

Coefficient of Thermal Expansion

The coefficient of thermal expansion was used in the formulation
of the dimensionless parameters used in this investigation. These
coefficients were obtained from published data for aluminum [2, 3, 12],
stainless steel [39, 79], brass [5], and magnesium [25, 26]. Since
the values of these coefficients are not highly temperature dependent
over the range of temperatures used in this investigation, constant
values were selected as:

$$\text{aluminum 2024} \quad \beta = 0.0000122 \text{ inch/inch } °F$$

$$\text{stainless steel 304} \quad \beta = 0.0000095 \text{ inch/inch } °F$$

$$\text{brass alloy 271} \quad \beta = 0.000118 \text{ inch/inch } °F$$

$$\text{magnesium AZ31B} \quad \beta = 0.0000144 \text{ inch/inch } °F$$

Modulus of Elasticity

Knowledge of the modulus of elasticity, like hardness, is not
essential for determination of experimental values of contact con-
ductance; however, it is used in many empirical analyses. hence,
appropriate modulus values have been determined for materials used
in this investigation and are presented as a function of temperature
in Figure B-4. The modulus of elasticity of metals is generally a
function of temperature, and this effect should not be neglected.
The modulus of elasticity for brass alloy 2.1 was determined through
information provided by the Anaconda American Brass Company [5] and
Clausing [20]. Modulus data for aluminum 2024-T4 were calculated
from information given by the Aluminum Company of America [3], the
Alcoa Handbook [2], and Birdsall [12]. Stainless steel modulus data
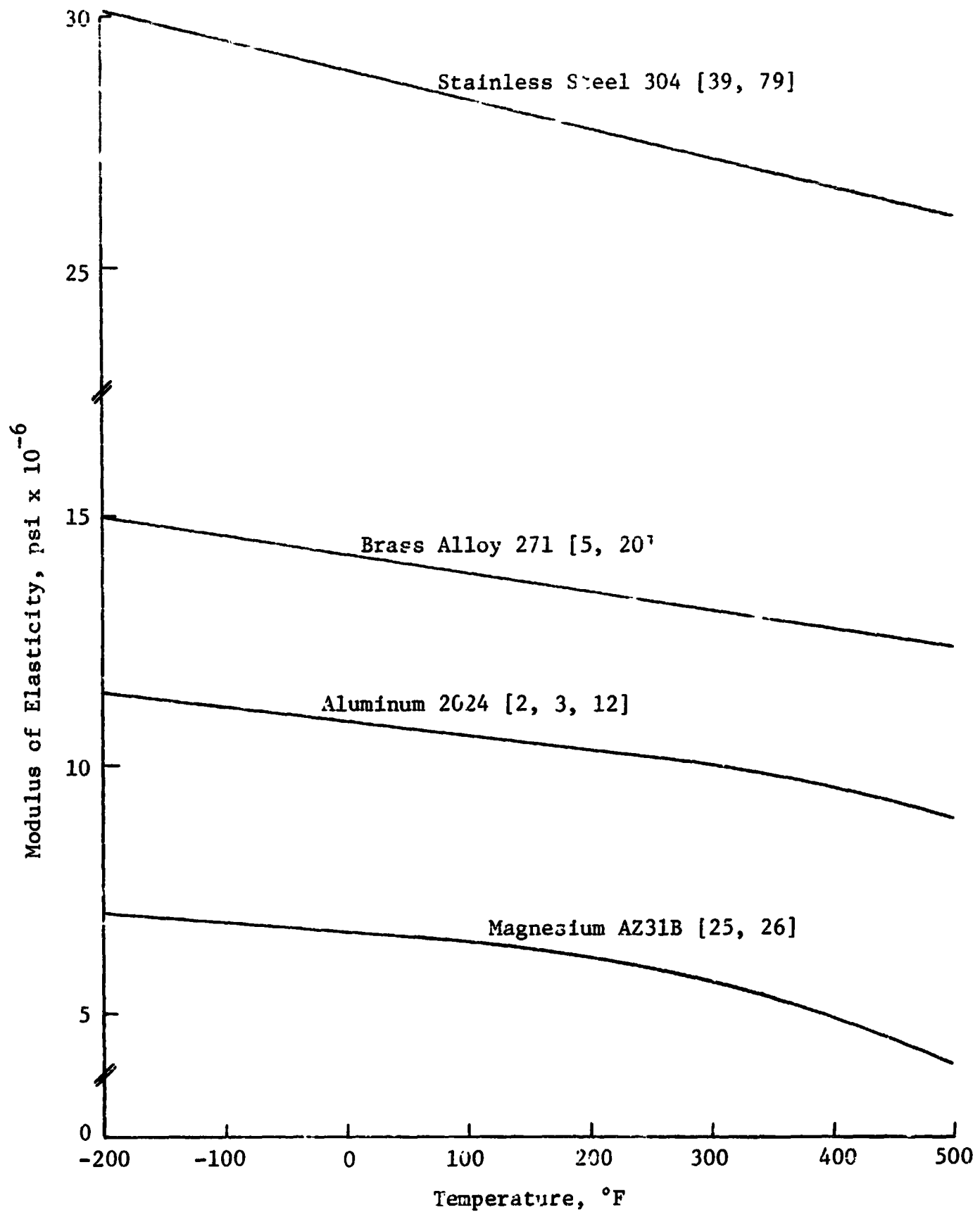
Figure B-4. Variation of Modulus of Elasticity with Temperature
for Aluminum, Stainless Steel, Brass, and
Magnesium.

were taken from the United States Steel Handbook [79] and Garofalo, et
al [39]. The curve for magnesium AZ31B was obtained from material
provided by the Dow Chemical Company [26].

Contact Conductance Data

Thermal contact conductance was defined in Chapter I by the
relationship:

$$h_c = \frac{q/A}{\Delta T}$$

where ΔT is the temperature difference at the contact interface. The
axial temperatures were plotted versus the distance from the interface,
and graphically extrapolated to the interface. In addition, a linear
least squares fit of the data was made for each test run to find the
temperatures at the interface. The difference between the interface
temperatures provided the ΔT across the contact. The heat flux, q/A,
in the specimen was found from the calculated temperature gradients
in the specimen and the thermal conductivity (Figure B-3), both of
which were determined from the temperatures measured along the speci-
men center-line. As a check, the heat flux was also determined by
subtracting the estimated heat losses from the measured heat input
and was then compared with the heat flux calculated by use of the
thermal conductivity and temperature gradient. The average differ-
ence between these heat fluxes was approximately 10 percent. The
experimental results of thermal contact conductance obtained in this
investigation are listed in Table B-2 through Table B-6.

The repeatability of the experimental data was checked by con-
ducting a second series of runs for the aluminum specimens at similar

TABLE B-2

CONTACT CONDUCTANCE DATA -- ALUMINUM 2024-T4

Coolant	Q/A	P_a		SURFACES 1 & 2			SURFACES 3 & 4	
			ΔT	h_c	T_m - S	ΔT	h_c	T_m - M
Water	18,140	2	57.3	317	287	82.6	220	189
	33,810	98	18.4	1,838	290	42.1	803	208
	41,510	305	5.0	8,302	284	23.9	1,737	206
	47,520	795	1.3	36,554	287	14.2	3,346	206

Coolant	Q/A	P_a		SURFACES 6 & 7			SURFACES 5 & 1	
			ΔT	h_c	T_m - R	ΔT	h_c	T_m - SR
Water	16,870	20	96.5	175	320	107.7	157	192
	(18,760)*	(26)	(102.5)	(183)	(329)	(107.2)	(175)	(195)
	24,200	96	65.8	368	304	79.6	304	194
	31,660	315	41.7	759	293	60.1	527	194
	(32,030)	(319)	(38.7)	(828)	(290)	58.5	(548)	(192)
	39,200	794	30.3	1,294	300	44.3	885	202
	(38,540)	(804)	(29.9)	(1,289)	(297)	(45.9)	(840)	(200)

Coolant	Q/A	P_a		SURFACES 1 & 2			SURFACES 3 & 4	
			ΔT	h_c	T_m - S	ΔT	h_c	T_m - M
Liquid Nitrogen	14,700	2	72.0	204	129	199.5	74	-30
	(33,950)	(36)	(59.3)	(573)	(138)	(142.3)	(239)	(-17)
	50,420	92	52.3	964	149	97.3	518	-7
	71,340	288	17.3	4,124	150	57.5	1,242	-3
	74,260	802	5.9	12,586	127	30.0	2,475	-12

Coolant	Q/A	P_a		SURFACES 6 & 7			SURFACES 5 & 1	
			ΔT	h_c	T_m - R	ΔT	h_c	T_m - SR
Liquid Nitrogen	19,020	25	96.6	197	144	207.8	92	-33
	35,000	105	93.5	374	155	175.8	199	-36
	51,350	266	82.4	623	161	127.7	402	-27
	68,040	809	58.4	1,165	167	96.2	707	-20

* Repeatability Data

TABLE B-3

CONTACT CONDUCTANCE DATA -- STAINLESS STEEL 304

Coolant	Q/A	P_a	SURFACES 1 & 2 - S			SURFACES 3 & 4 - M		
			ΔT	h_c	T_m	ΔT	h_c	T_m^*
Water	3,320	30	56.0	59	307	77.9	43	184
	3,970	102	34.0	117	298	52.2	76	188
	4,800	302	18.1	265	303	31.6	152	196
	5,430	813	7.8	696	307	19.4	280	201

Coolant	Q/A	P_a	SURFACES 6 & 7 - R			SURFACES 5 & 1 - SR		
			ΔT	h_c	T_m	ΔT	h_c	T_m^*
Water	960	29	136.7	7.1	328	156.2	6.1	165
	1,480	104	122.7	12	334	145.1	10	175
	2,090	307	83.5	25	316	119.9	17	178
	2,480	790	56.5	44	301	102.2	24	180

Coolant	Q/A	P_a	SURFACES 1 & 2 - S			SURFACES 3 & 4 - M		
			ΔT	h_c	T_m	ΔT	h_c	T_m^*
Liquid Nitrogen	3,490	27	83.0	43	163	197.3	18	-44
	5,600	105	47.2	119	154	116.3	48	-34
	7,000	315	25.9	270	161	61.3	114	-15
	7,560	813	13.5	560	154	38.4	197	-15

Coolant	Q/A	P_a	SURFACES 6 & 7 - R			SURFACES 5 & 1 - SR		
			ΔT	h_c	T_m	ΔT	h_c	T_m^*
Liquid Nitrogen	1,300	29	174.5	7.4	183	307.9	4.2	-83
	1,660	99	129.9	13	166	290.6	5.7	-75
	2,400	307	100.9	24	153	249.7	9.6	-67
	3,720	806	86.3	43	153	187.8	20	-54

TABLE B-4

CONTACT CONDUCTANCE DATA -- BRASS ALLOY 271

Coolant	Q/A	P_a	ΔT	h_c	T_m	ΔT	h_c	T_m
			SURFACES 1 & 2 - S			SURFACES 3 & 4 - M		
Water	18,760	26	22.6	830	282	62.1	302	193
	24,400	102	11.5	2,122	297	48.7	501	207
	25,960	305	3.8	6,832	284	34.9	744	201
	28,040	804	-	-	282	24.6	1,141	200
			SURFACES 6 & 7 - R			SURFACES 5 & 1 - SR		
Water	8,486	28	51.5	163	295	139.6	60	179
	10,960	102	43.2	254	276	104.8	105	175
	14,340	305	38.6	372	279	85.6	168	181
	19,210	804	35.5	541	292	64.9	296	194
			SURFACES 1 & 2 - S			SURFACES 3 & 4 - M		
Liquid Nitrogen	16,060	29	31.8	505	119	79.1	203	18
	18,220	96	18.6	980	121	45.7	399	38
	35,560	300	13.8	2,577	136	57.5	618	-0.1
	39,850	789	3.6	11,069	134	42.8	931	-2.5
			SURFACES 6 & 7 - R			SURFACES 5 & 1 - SR		
Liquid Nitrogen	8,990	26	86.0	105	135	248.4	36	-57
	11,820	100	58.9	201	129	225.1	53	-46
	20,150	302	62.4	323	141	159.0	127	-27
	27,100	787	56.1	483	157	114.5	236	-4.9

164

TABLE B-5

CONTACT CONDUCTANCE DATA -- MAGNESIUM AZ31B

Coolant	Q/A	P_a	ΔT	h_c	T_m	ΔT	h_c	T_m
				SURFACES 1 & 2 – S			SURFACES 3 & 4 – M	
Water	17,310	25	25.3	684	284	38.8	446	197
	22,120	100	4.6	4,793	283	13.7	1,609	204
	23,770	295	3.2	7,428	289	11.6	2,049	207
	24,370	798	1.4	17,407	284	9.0	2,708	202
				SURFACES 6 & 7 – R			SURFACES 5 & 1 – SR	
Water	10,410	25	43.9	237	298	105.0	99	192
	13,830	101	34.9	396	296	76.0	182	197
	15,310	300	26.1	587	278	49.9	307	191
	18,580	797	17.6	1,056	282	35.1	529	197
				SURFACES 1 & 2 – S			SURFACES 3 & 4 – M	
Liquid Nitrogen	12,920	23	70.0	185	148	118.4	109	5.8
	21,710	101	30.2	719	135	42.7	508	17
	28,530	301	15.8	1,806	146	28.1	1,015	18
	32,710	787	7.3	4,481	140	17.4	1,880	4.7
				SURFACES 6 & 7 – R			SURFACES 5 & 1 – SR	
Liquid Nitrogen	10,880	23	92.9	117	154	169.9	64	-17
	16,660	100	61.9	269	146	123.3	135	-8.0
	23,440	296	47.0	499	153	88.5	265	-1.8
	28,810	771	33.8	852	150	70.0	412	-9.3

TABLE B-6

CONTACT CONDUCTANCE DATA -- DISSIMILAR JUNCTIONS
(Aluminum 2024 and Stainless Steel 304)

Coolant	Q/A	P_a	ΔT	h_c	T_m	ΔT	h_c	T_m
				SURFACES 6 & 7 -- R			SURFACES 5 & 1 -- SR	
Water	2750	34	123.0	22.4	198	85.8	32.1	307
	3330	108	103.3	32.2	206	62.1	53.6	294
	4100	311	77.0	53.2	215	36.9	111.1	278
	4910	813	48.0	102.3	217	24.4	201.2	260

test conditions. Before these check runs, the test specimens were separated and the system was shut down for several hours. The experimental procedure was the same as that used for the initial tests. The energy input to the source heater and the contact pressure were reproduced as closely as possible. The data for these repeatability tests are shown in Table B-2. Further substantiation of the repeatability of data using this apparatus has been given by Smuda, et al [69].

An uncertainty analysis was performed to estimate the range of error in the heat flux and thermal contact conductance. Uncertainty for the heat flux was approximately 7 percent. Uncertainty for the thermal contact conductance data is given as a function of apparent pressure in Appendix C.

APPENDIX C

UNCERTAINTY ANALYSIS

An experimental investigation is not complete without an estima-
tion of the uncertainties in the measured quantities. The uncertainty
in a particular result may be given as a percent of the calculated
value, R, by the expansion [65]:

$$\frac{\delta R}{R} = \{(\frac{\delta X}{X})^2 + (\frac{\delta Y}{Y})^2 + (\frac{\delta Z}{Z})^2\}^{1/2}$$

The delta terms are the uncertainties associated with their respective
measured quantities such as temperature or length. Thus, it was nec-
essary to determine the uncertainty in each of the variables measured
in this investigation.

The temperatures were measured with copper-constantan thermo-
couples and a Leeds and Northrup 8686 millivolt potentiometer. One-
half of the smallest scale division on the potentiometer was 2.5
microvolts, which corresponds to 0.1°F for the conditions used. As a
result of a thermocouple calibration [69], the thermocouples were
found to be accurate to ± 0.5°F over the temperature range used.
Thus, the uncertainty in the temperature was estimated to be 0.5°F.

The temperature gradient for determination of the heat flux was
found by taking the difference, ΔT, in the adjacent temperatures
recorded along the specimen and dividing it by the distance, Δx,
between the thermocouples used to measure the temperatures. According

to the estimated error in the temperatures, ΔT could deviate by as much as 1°F. Several of the runs were plotted on an expanded scale of temperature versus distance along the specimen. Analysis of the temperature gradients indicated that the temperature differences were seldom in error by more than 0.5°F.

Thermocouples were mounted in holes 0.047 inches in diameter placed 0.500 inches apart. The loc.tion of the holes was specified to be within ±0.001 inches; however, differences of ±0.01 inches occurred. Thus, the uncertainty in Δx was selected as 0.01 inches.

The thermal conductivity, k, was obtained from a graph of thermal conductivity versus temperature where the smallest scale division of k was 0.5 Btu/hr sq ft °F (Figure B-3). The graph was plotted from the values of thermal conductivity given in the reference material cited in Appendix B. Considering the effects of graphical interpolation and the experimental uncertainty in k, the uncertainty associated with thermal conductivity for all materials was estimated to be 5 percent for the range of temperatures used.

The heat transfer rate was defined as:

$$q = - A k \frac{\Delta T}{\Delta x}$$

and the uncertainty in the heat transfer rate was determined as follows:

$$\frac{\delta q}{q} = [(\frac{\delta k}{k})^2 + (\frac{\delta \Delta T}{\Delta T})^2 + (\frac{\delta \Delta x}{\Delta x})^2 + (\frac{2 \delta D}{D})^2]^{1/2}$$

Results of this expression varied from 2.1 to 6.4 percent for the range of heat transfer rates used in this investigation.

The temperature difference, ΔT_j, in the thermal conductance equation was determined graphically as described in Appendix B. Two graphs, representative of the data, were plotted on an expanded scale where the smallest scale division for temperature was 0.5°F. Points 0.5°F above and below each data point were included to reflect the probable error in the temperature measurements. The variations in thermocouple location were included to reflect error in location. A line of maximum and a line of minimum feasible slope were then drawn through each of the two arrays of points. These four lines were extrapolated to the interface to establish the maximum and minimum probable temperatures for each side of the interface. The maximum temperature difference, ΔT_{max}, was established by taking the average of the difference between the minimum upper and lower interface surface difference; ΔT_{min} was determined in a similar manner using the maximum upper and lower interface surface temperatures.

The contact conductance for each maximum and minimum junction temperature difference was calculated using the average heat flux. The uncertainty in the contact conductance was then determined as the magnitude of the deviation from the mean value presented ir Tables B-2 through B-6. The uncertainty may be found for the dt by locating the junction temperature difference for a given apparent pressure in Figure C-1, and reading the magnitude deviation in Figure C-2.

The uncertainty in the apparent interface pressure is determined from the expression:
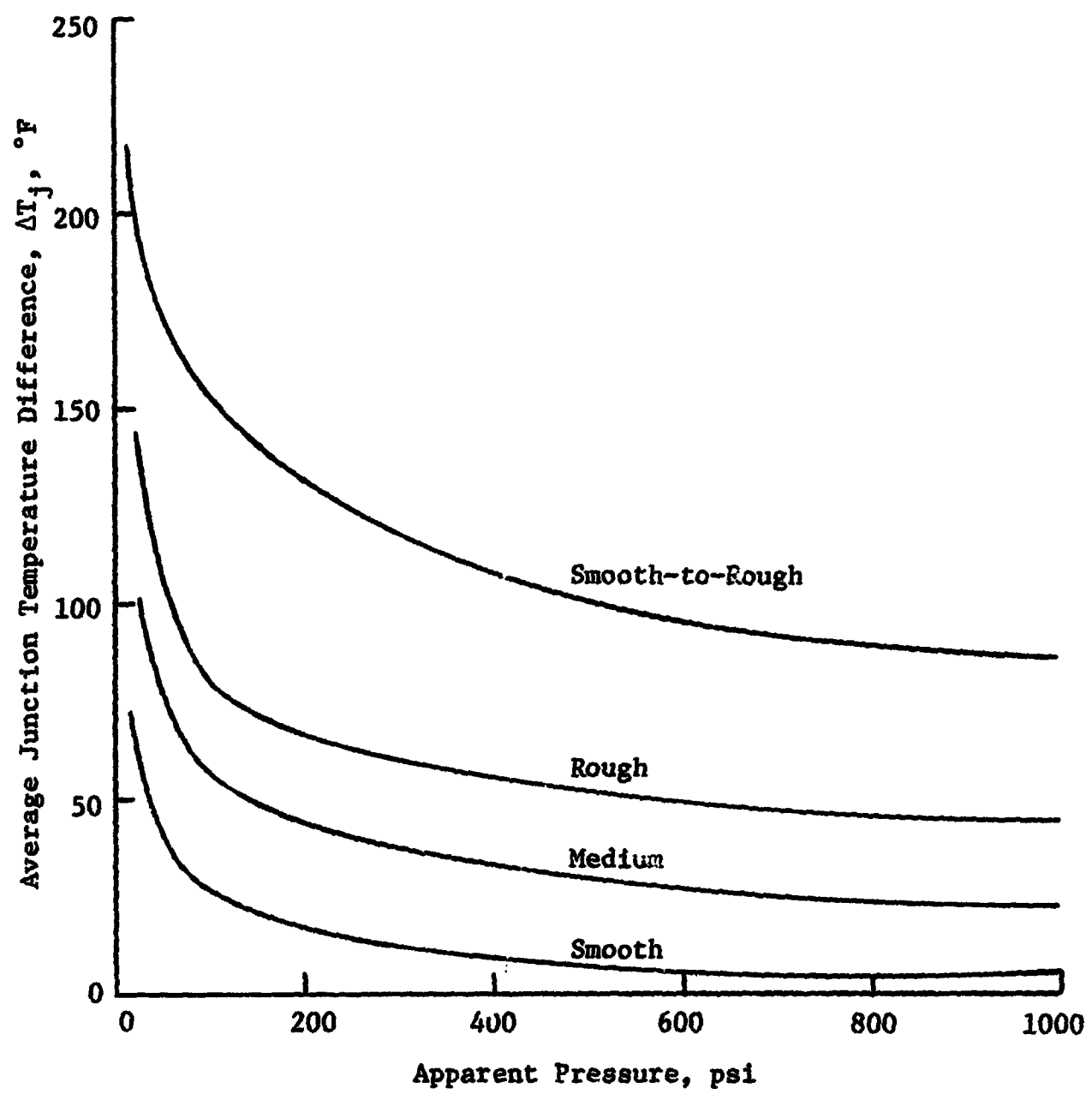
Figure C-1. Variation of Junction Temperature Difference
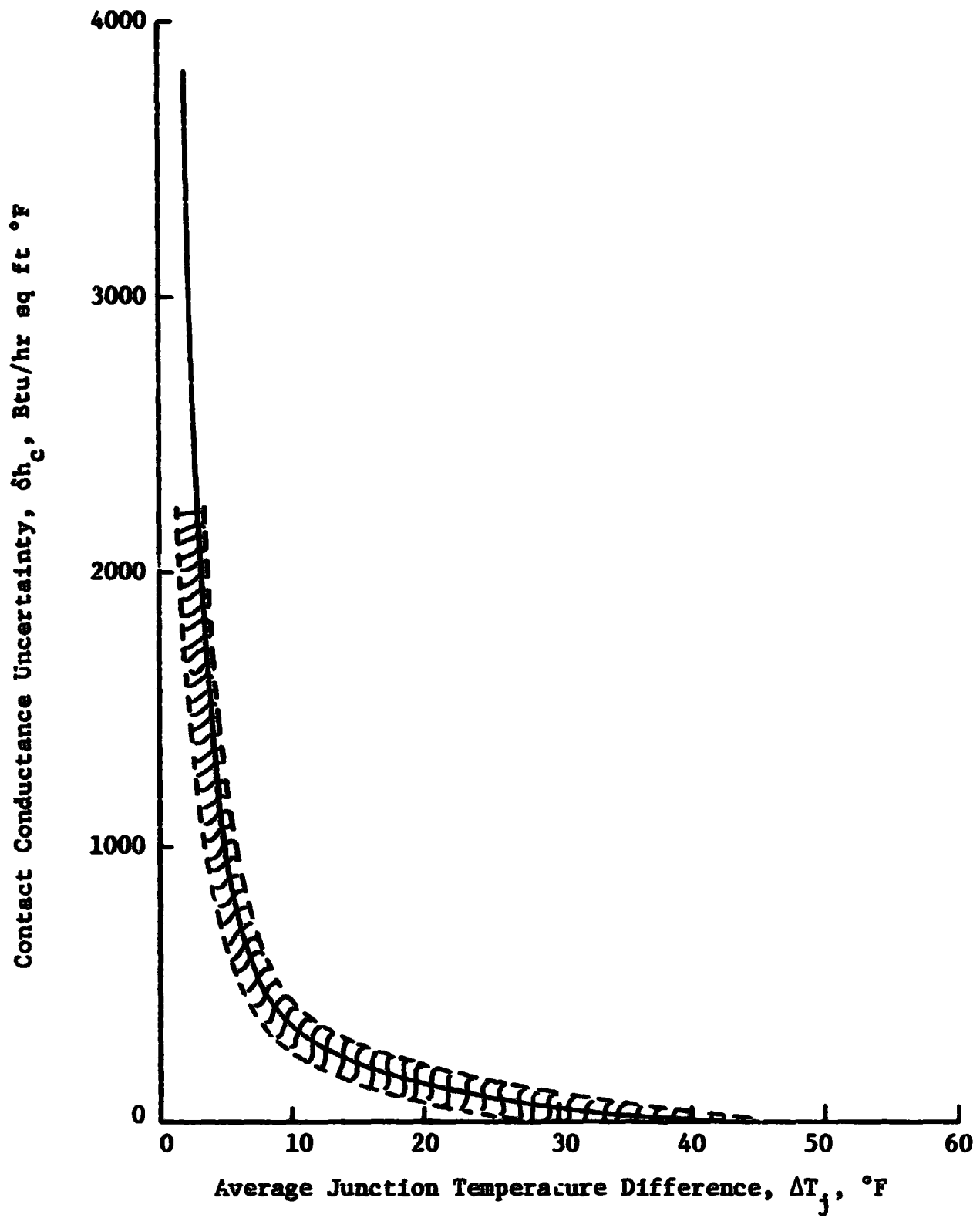with Interface Pressure.

Figure C-2. Variation of Uncertainty in Contact
Conductance with Junction Temperature
Difference.

$$\frac{\delta P_a}{P_a} = \{(\frac{\delta L}{L})^2 + (\frac{\delta A}{A})^2\}^{1/2}$$

The uncertainty in the load is five pounds, and the uncertainty in the area results from a 0.001-inch uncertainty in the specimen diameter. Results of this expression vary from 0.7 to 4.8 percent for the range of loads used in this investigation.